Robust dimensioning of wireless optical networks with multiple partial link failures

Marinela Shehaj

Par **Marinela SHEHAJ**

Robust dimensioning of wireless optical networks with multiple partial link failures

Thèse présentée
pour l'obtention du grade
de Docteur de l'UTC

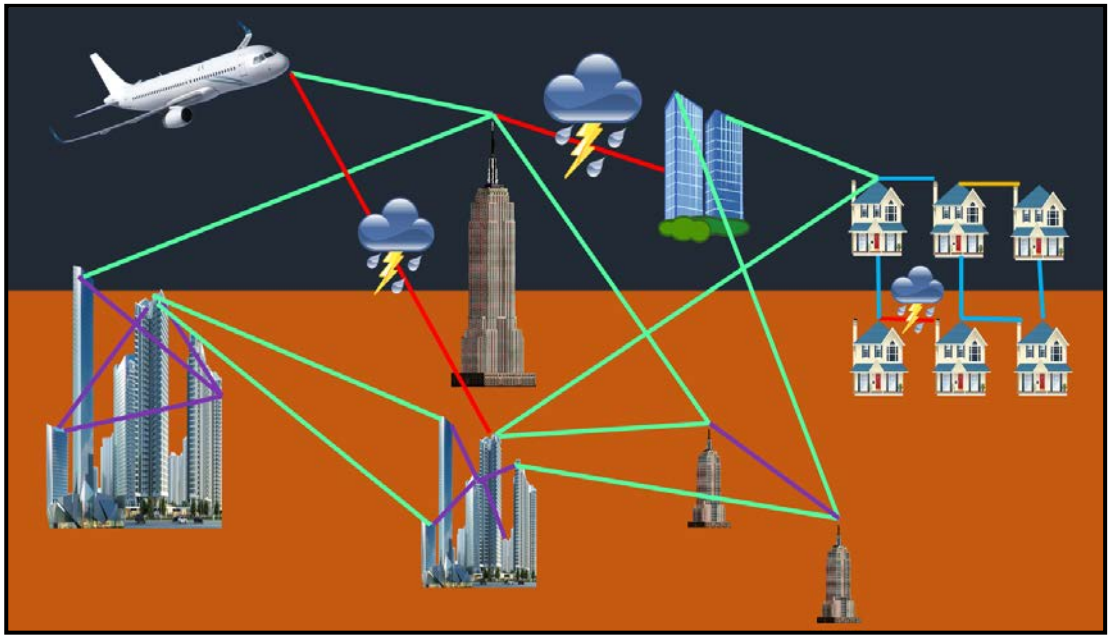

Soutenue le 3 février 2020
Spécialité : Sciences et Technologies de l'Information et des Systèmes : Unité de recherche Heudyasic (UMR-7253)
D2540

A thesis presented for the degree of Doctor

UNIVERSITÉ DE TECHNOLOGIE DE COMPIÈGNE

Laboratoire Heudiasyc UTC UMR CNRS 7253
Technologie de l'Information et des Systèmes

Marinela SHEHAJ

Robust dimensioning of wireless optical networks with multiple partial link failures

Defended on February 3rd, 2020
Thesis Committee:

Reviewers:

Walid BEN-AMEUR
Professor
UMR CNRS 5157, TELECOM SudParis

Jacek RAK
Professor
Gdansk University of Technology

Examiners:

Corinne LUCET-VASSEUR
Associate Professor (HDR)
Université de Amiens Picardie Jules Verne

Ghada JABER
Associate Professor
Université de Technologie de Compiègne

Supervisors:

Dritan NACE
Professor
Université de Technologie de Compiègne

Michał PIÓRO
Professor
Warsaw University of Technology

Guest:

Michael POSS
Researcher
UMR CNRS 5506 LIRMM, Université de Montpellier

Acknowledgment

The research work done in this thesis took place in Heudiasyc Laboratory, Université de technologie de Compiègne from December 2016 to December 2019. It was carried out in the framework of the Labex MS2T funded by the French National Education and Research Ministry through the program "Investments for the future" managed by the National Agency for Research [Reference ANR-11-IDEX-0004-02].

At the end of this thesis, I would like to express my sincere gratitude to my supervisor Prof. Dritan Nace, who gave me the honor of leading this work under the best conditions. I am truly grateful for his precious guidance, his constructive advises and his availability during all this time. I would like to underline and appreciate his passion for research and immense knowledge and especially his human qualities, his optimism, enthusiasm and generosity which will always be an example for me. I am deeply grateful for the trust he has placed in me and cared about my future in every minutes during my thesis.

I would like to express my gratitude to my co-supervisor Prof. Michał Pióro, for his valuable advices, constructive assistance and precious help. His persistence for perfection and honesty in research and life, have a great influence in my first steps in research and it will be helpful in my future carrier.

Besides my supervisors, I want to thank all my co-authors, Dr. Michael Poss, PhD student Ilya Kalesnikau and Dr. Fabio D'Andreagiovanni for their participation in this work and for their assistance.

I want to thank all the members of the jury for agreeing to participate to my thesis committee and for their constructive comments. A special thanks goes to Prof. BEN-AMEUR and Prof. RAK for agreeing to be reviewers of my dissertation.

A sincere thanks goes to all the members and colleagues of Heudiasyc laboratory and specially the SCOP team for their friendly support during this period. I can't let apart the Labex MS2T, Control of Technological System of Systems, for its financial support during this research.

Finally, and most importantly, my warmest ans deepest thanks go to my family and friends, for their love, patience and their unconditional and constant support.

List of Publications

International journal

- Marinela Shehaj, Ilya Kalesnikau, Dritan Nace and Michał Pióro, "Link dimensioning of hybrid FSO/fiber networks resilient to adverse weather conditions", Computer Networks, 161 : 1-13, (2019).
- Dritan Nace, Michał Pióro, Michael Poss, Fabio D'Andreagiovani, Ilya Kalesnikau, Marinela Shehaj and Artur Tomaszewski, "An optimization model for robust FSO network dimensioning", Optical Switching and Networking, 32 : 25-40, (2019).

International conference

- Marinela Shehaj, Ilya Ktalesnikau, Dritan Nace, Michał Pióro, and Ermioni Qafzezi, "Modeling transmission degradation on FSO links coused by weather phenomena in WMN", In Proceedings of the 11th International Workshop on Resilient Networks Design and Modeling (RNDM 2019), Cyprus, October 2019.
- Marinela Shehaj, Dritan Nace, Ilya Kalesnikau and Michał Pióro, "Dimensioning of hybrid FSO/ïňĄber networks", In Proceedings of the 2nd International Balkan Conference on Communications and Networking,BalkanCom 2018. Podgorica, Montenegro, June 2018.
- Fabio D'Andreagiovani, Dritan Nace, Michał Pióro, Michael Poss, Marinela Shehaj, and Artur Tomaszewski, "On robust FSO network dimensioning", In Proceedings of the 9th International Workshop on Resilient Networks Design and Modeling (RNDM 2017), September 2017.

National conferences

- Marinela Shehaj, Dritan Nace,Michał Pióro, and Ilya Kalesnikau, "Modeling transmission degradation on FSO links caused by weather phenomena in WMN", PGMO Days 2019, Paris, France.
- Marinela Shehaj, Dritan Nace, and Michał Pióro, "Issues in robust network dimensioning - the case of FSO networks", ROADEF 2019, Le Havre, France.

- Marinela Shehaj, Dritan Nace, Michał Pióro, Michael Poss, Fabio D'Andreagiovani, Ilya Kalesnikau, and Aertur Tomaszewski„ "Robust network dimensioning - the case of FSO networks", PGMO Days 2018, Paris, France.

Journal article under preparation

- Ilya Kalesnikau, Marinela Shehaj, Dritan Nace, and Michał Pióro, "Modeling transmission degradation on FSO links coused by weather phenomena in WMN", Invited for publication in a special issue of the Optical Switching and Networking (Elsevier) journal, 2020.

Contents

List of figures

List of tables

Acronyms

FSO:	Free Space Optics
OFC:	Optical Fiber Cable
LED:	Light Emitting Diodes
VCSEL:	Vertical Cavity Surface Emitting Lasers
WMN:	Wireless Mesh Networks
ICT:	Information and Communication Technology
NDP:	Network Design Problems
LP:	Linear Programming
MIP:	Mixed-Integer Programming
IP:	Integer Programming
BB:	Branch-and-Bound
BC:	Branch-and-Cut
LS:	Local Search
SAN:	Simulated Annealing
EA:	Evolutionary Algorithm
MCS:	Modulation and Coding Scheme
QAM:	Quadrature Amplitude Modulatio
BPSK:	Binary Phase-Shift Keying

Abstract

This thesis summaries the work we have done in optimization of wireless optical networks. More specifically, the main goal of this work is to propose appropriate network dimensioning algorithms for managing the demand and ensuring traffic satisfaction in a network under partial link failures (i.e. when some links and/or nodes are operational with reduced capacity) caused mostly by weather conditions. The primary criterion in deciding the efficiency of the proposed algorithms for the network is the dimensioning cost of the network while keeping the traffic satisfaction at high reasonable levels.

The main application area we have in mind are the networks that apply Free Space Optics (FSO) - a well established broadband wireless optical transmission technology where the communication links are provided by means of a laser beam sent from the transmitter to the receiver placed in the line of sight. FSO networks exhibit several important advantages but the biggest disadvantage is vulnerability of the FSO links to weather conditions, causing substantial loss of the transmission power over optical channel. This makes the problem of network dimensioning important, and, as a matter of fact, difficult. Therefore, a proper approach to FSO network dimensioning should take such losses into account so that the level of carried traffic is satisfactory under all observed weather conditions.
In this thesis, we firstly describe such an approach. In the first part of the thesis, we introduce a relevant dimensioning problem and present a robust optimization algorithm for such enhanced dimensioning. To construct our approach we start with building a reference failure set which uses a set of weather data records for a given time period against which the network must be protected. Next, a mathematical model formulation of the robust network dimensioning problem uses the above failure set. Yet, such obtained reference set will most likely contain an excessive number of states and at the same time will not contain all the states that will appear in the reality. Hence, we propose to approximate the reference failure set with a special kind of virtual failure set called K-set parameterized by an integer value K, where K is less than or equal to the number of all links in the network. For a given K, the K-set contains all states corresponding to all combinations of K, or less, simultaneously affected links. Sometimes, there are situations where the weather is extremely bad and what we propose is to build a hybrid network model composed of FSO and fiber links.

The second part of this thesis is devoted to the improvement of the so-called uncertainty sets (or uncertainty polytopes). In the first part we have introduced the idea of link K-sets. Now we extend this by considering simultaneous degradations of K nodes (meaning degradation of all adjacent links). Finally, inspired by the hitting set problem a new idea was to find a large number of subsets of two or three affected links and to use all possible combinations (composed of 2 or at most 3 of this subsets) to build a new virtual failure set that covers as much as possible the reference failure set that we got from the study of real weather data records. Next, this new failure set will serve as input for our cut-generation

algorithm so that we can dimension the network at a minimum cost and for a satisfactory demand realization. A substantial part of the work is devoted to present numerical study for different network instances that illustrates the effectiveness of the proposed approach. A dedicated space is given to the construction of a realistic network instance called Paris Metropolitan Area Network (PMAN).

Keywords: Resilient and survivable networks, operational research, free space optics, variable link capacity, linear and mixed-integer programming, robust optimization.

Résumé

Cette thèse résume le travail que nous avons fait dans l'optimisation des réseaux optiques sans fil. Plus spécifiquement, l'objectif principal de ce travail est de proposer des algorithmes efficaces de dimensionnement de réseau pour assurer la satisfaction du trafic dans un réseau qui subit des pannes partielles de liens (par exemple lorsque certains liens et/ou noeuds sont opérationnels avec une capacité réduite) causés principalement par les conditions météorologiques.

Le critère principal pour déterminer l'efficacité des algorithmes proposés est le coût de dimensionnement du réseau tout en maintenant la satisfaction du trafic à des niveaux élevés. Les domaines d'application principal que nous avons à l'esprit sont les réseaux qui utilisent le *Free Space Optics* (FSO) - une technologie de transmission optique sans fil à large bande où les liens de communication sont assurés au moyen d'un faisceau laser envoyé de l'émetteur au récepteur placé en ligne droite. Les réseaux FSO présentent plusieurs avantages (comme le coût peu elevé, la facilité d'installation, la grande capacité de transmission, etc.), mais le plus grand inconvénient est la vulnérabilité des liens FSO aux conditions météorologiques, causant une perte substantielle de la puissance de transmission sur le canal optique. Cela rend le problème de dimensionnement du réseau important et difficile. Par conséquent, une approche appropriée du dimensionnement du réseau FSO devrait tenir compte de ces pertes afin que le niveau du trafic transporté soit satisfaisant dans toutes les conditions météorologiques observées. Dans cette thèse, nous décrivons une telle approche.

Dans la première partie de la thèse, nous introduisons un premier problème de dimensionnement, qui a pour objectif d'être le plus général possible et inclue les constraintes les plus importantes. Nous présentons ensuite un algorithme d'optimisation robuste pour ce problème de dimensionnement. Pour construire notre approche, nous commençons par définir un ensemble de défaillances des liens, dit de référence, qui utilise les données météorologiques d'une période donnée pour laquelle le réseau doit être protégé. Ensuite, nous formulons mathématiquement le problème de dimensionnement robuste de réseau qui utilise l'ensemble des pannes de liens ci-dessus. Pourtant, cet ensemble des pannes de référence obtenu contiendra, très probablement, un nombre excessif d'états et en même temps ne contiendra pas tous les états qui apparaîtront dans le futur. Par conséquent, nous proposons d'approximer cet ensemble par un type spécial d'ensemble de defaillances des liens virtuel (dite ensemble d'incertitude), appelé K-set et paramétré par une valeur entière K, où K est inférieur ou égal au nombre de tous les liens du réseau. Pour un K donné, le K-set contient tous les états correspondant à toutes les combinaisons d'au plus K liens affectés simultanément. Dans certains cas, il y a des situations où la météo est

extrêmement mauvaise et pour lequel nous proposons de construire un modèle de réseau hybride composé de liens FSO et de liens de fibre optique terrestre.

La deuxième partie de cette thèse est consacrée à l'amélioration des ensembles de d'incertitude (ou polytopes d'incertitude). Dans la première partie, nous avons présenté l'idée de K-sets des liens. Maintenant, nous étendons cela en considérant les dégradations simultanées de K noeuds (ce qui signifie la dégradation de tous les liens adjacents). Enfin, inspiré par le problème de couverture, dit l'hitting set, une nouvelle idée a été de construire un ensemble de sous-ensembles de deux ou trois liens affectés et d'utiliser toutes les combinaisons possibles (composé de 2 ou au plus 3 de ces sous-ensembles) pour créer un nouvel ensemble de pannes virtuelles qui couvre autant que possible l'ensemble des pannes de référence que nous avons obtenu de l'étude de conversion des données météorologiques réelles. Ensuite, ce nouvel ensemble de pannes servira d'entrée pour notre algorithme de génération de coupe afin que nous puissions dimensionner le réseau à un coût minimum et pour une réalisation satisfaisante de la demande. Une partie importante du travail est consacrée à la présentation d'une étude numérique pour différentes instances de réseau qui illustre l'efficacité de l'approche proposée. Une place importante est consacrée à la construction d'une instance de réseau réaliste appelée *Paris Metropolitan Area Network* (PMAN).

Mots clés: Réseaux résilients et fiables, recherche opérationnelle, free space optics, capacité variable de lien, programmation linéaire et mixte, optimisation robuste.

Part 1

The first part includes an introduction chapter, together with a literature review of state of art on partial link failures and optical networks. In Chapter 1, we present the context of our work, our contribution, and the outline of the thesis. In Chapter 2 we discuss the issues of modeling weather conditions based on meteorological records for a given time period, and the associated link capacity degradation. The review of the literature presented in Chapter 3 is followed by a mathematical formulation of the robust network dimensioning problem that is central to our investigations together with a solution approach to the problem based on a cut generation algorithm. Further we discuss modifications and enhancements of the introduced approach. Finally, the chapter is concluded by introducing and studying a particular optimization model for hybrid networks. These networks composed of FSO links supported by terrestrial optical fiber connections in order to increase resilience to adverse weather conditions. In this thesis work we will define resilience as the ability of the network to provide and maintain an acceptable level of service in the face of various faults and challenges to normal operation [1].

Introduction

The research work done in this thesis took place in Heudiasyc Laboratory, Université de technologie de Compiègne. It was carried out in the framework of the Labex MS2T funded by the French Government through the program "Investments for the future" managed by the National Agency for Research [Reference ANR-11-IDEX-0004-02]. The focus of this thesis are the network dimensioning problems, and more specifically the dimensioning that takes into account multiple partial link failures/degradation[1] in the case of Free Space Optics systems.

Part of the work has been done in collaboration with Polish authors from Institute of Telecommunications, Warsaw University of Technology, Warsaw, Poland. Their work was supported by the National Science Centre, Poland, grant number 2015/17/B/ST7/03910 "Logical tunnel capacity control - a traffic routing and protection strategy for communication networks with variable link capacity".

CONTEXT AND MOTIVATION

Free Space Optics

The considerations of this thesis are devoted to dimensioning communication networks resilient with respect to multiple partial link failures. The main application area we have in mind are networks that apply Free Space Optics (FSO) – a well established broadband wireless optical transmission technology where the communication links are provided by means of a laser beam sent from the transmitter to the receiver placed in the line of sight. FSO links are considered as an alternative to radio links for example in metropolitan Wireless Mesh Networks (WMN). Examples of networks that use this new technology can be founded in United Kingdom (provider Wireless Excellence LTD [2]), in San Diego, California, and France (provider LightPointe [3]), etc. FSO networks exhibit several important advantages: transmission range of several kilometers, high transmission bandwidth, secure communication, quick and easy deployment, lower cost (as compared with the fiber optical technology), immunity to electromagnetic interference, license-free long-range operation (contrary to radio communications). Despite the numerous advantages, a major disadvantage of FSO links (with respect to fiber links) is their sensitivity to weather conditions (such as fog, rain, snow, and pollution), causing substantial loss of the transmission power over optical channel, mostly due to absorption and scattering. This makes the problem of network dimensioning important, and difficult.

[1] In the continuation of this thesis we will use interchangeably the terms "failure" and "degradation" to express the loss of a portion (fraction) of link's nominal capacity due to bad weather conditions (i.e., compared with the bit-rate realized when weather is fine)

Thus, although FSO technology allows fast and low-cost deployment of broadband networks, its operation will be affected by this sensitivity, manifested by substantial losses in links' transmission capacity with respect to the nominal capacity. Therefore, a proper approach to FSO network dimensioning should take such losses into account. All this motivates the network optimization problem we study: how to dimension the network links at the lowest cost, and at the same time assure the traffic demand satisfaction at an acceptable level for all observed/predicted weather conditions. This is not a simple task, as it requires to take into account the uncertainty due to weather conditions resulting in a very large number of possible scenarios.

CONTRIBUTION Of THE THESIS

The contribution of this work consists in studying a network dimensioning problem taking into account resilience with respect to multiple partial link failures. In contrast to the previous investigations, this thesis deal with the problem involving a very large number of failure/degradation states, described by the so called uncertainty set (an instance of the budgeted uncertainty set formally described in [4] and [5]) for which we propose an optimization model together with a cut generation solution algorithm, and use it for a numerical study on robust dimensioning of a specific FSO network. The results of this work, among other issues, shows to what extent the network dimensioned with our algorithms can handle real weather conditions. These extensions are original and constitute a novelty in resilient network modeling and optimization.

OUTLINE OF THE THESIS

This thesis is composed of two main parts. We have included in the first part all mathematical models and solutions methods proposed for FSO link dimensioning. After that, in the second part we will continue with a study of enhancements of the model (especially on the robustness) together with an abundant numerical study. We have put all numerical results in the same chapter and not after each chapter, with the aim to provide a better comparison between the different models given in this thesis.

The first part includes three chapters. We start with a general overview of this thesis followed by a literature review. The impact of weather conditions on the wireless networks transmission capacity has been studied to some extent, but the majority of works has considered failure modeling for a single region failure and the problem of multiple partial link failures is something new. Then we give a wide presentation of FSO technology and a mathematical model to convert weather data into link traffic transmission ratios with respect to nominal capacity. Finally, we present a mathematical formulation for the network optimization problem we study, together with a cut-generation algorithm to solve it.

Chapter 1 provides a general background for the problems we investigate in this thesis. We begin with a short introduction of this new and promising technology known as Free Space Optics. Despite the numerous advantages that FSO systems owns, the biggest disadvantage of this technology is vulnerability of FSO links to weather conditions. This causes substantial loss of the transmission power over the optical channel, as a result

loss of capacity. We present two resilience mechanisms to deal with this problem. The first one is based on the notion of link margin and, the modulation and coding schemes applied at the transmitters of the affected FSO links. The second resilience mechanism we propose for some cases, extremely bad weather scenarios when the network can become disconnected, is a hybrid network configuration. It consists in installing a limited number of optical fibers combined with the FSO links. We study both mechanisms together with appropriate link dimensioning. We continue with a literature review on weather disasters, single and multiple partial link degradation. In this thesis we introduce a new optimization model for robust dimensioning of FSO networks in order to achieve resilience with respect to multiple partial link degradation. Furthermore, we discuss the complexity class of our problem. We and this first chapter presenting the solution methods that we have used for the robust dimensioning problem we study.

Chapter 2 goes deeper on Free Space Optical systems and the way it works and operates. It presents some technical information about FSO technologies and an analysis of advantages and disadvantages when implementing such a technology. Here we discuss a very important concept, the link margin. We can think of the link margin as the extra-power available at the receiver, compared to the minimum requirement of keeping the link active. It is important to understand that the link margin of a particular FSO link is a direct function of atmospheric conditions as well as the distance between terminals. In this chapter we discuss and present a mathematical formulation of the problem of converting the weather data to an explicit list of link degradation states (availability states may be immediately obtained). Typically, a given weather condition affects a subset of network links, and each affected link loses a portion (fraction) of its nominal capacity. Typical values of link capacity degradation ratios are $0.50, 0.75$ and 1, and each particular weather condition that may occur defines a network state referred to as link degradation state. We start with converting the weather conditions into link margin and then convert it into availability ratio for the FSO link. An important part of the chapter is the discussion of the modulation and coding scheme for the FSO system. Despite the numerous advantages, as said before, a major disadvantage of FSO links (with respect to fiber links) is their sensitivity to weather conditions (such as fog, rain, and snow) causing loss of the transmission power over the optical channel. Thus, although FSO technology allows fast and low-cost deployment of broadband networks, its operation will be affected by this sensitivity, manifested by substantial losses in links' transmission capacity with respect to the nominal capacity. Therefore, a proper approach to FSO network dimensioning should take such losses into account.

In Chapter 3 we present an introduction to the robust network dimensioning problem that is central to our investigations followed by a mathematical formulation. This problem is formulated as a mixed-integer program (MIP) in the node-arc notation and we assume that in any failure state, each demand can be routed in a bifurcated way along all possible paths from origin to the destination, and the resulting traffic flows in particular states are independent to each other. This means the network applies the so called *Global Rerouting or Unrestricted Reconfiguration* mechanism. Furthermore we develop a solution approach to the problem based on a cut generation algorithm. This is followed by some modifications and enhancements of the introduced approach. Because of modular links, our primarily problem denoted $\mathrm{P}(\mathcal{S})$ is $\mathcal{NP}$-hard even for a polynomial number of states in set $\mathcal{S}$ (see [6] and [7]). Moreover, the direct approach to $\mathrm{P}(\mathcal{S})$ requires solving linear programs involving

a large number of arc-flow variables during the branch-and-bound process performed by the MIP solver. For this reason, we have developed a more efficient approach to $\mathrm{P}(\mathcal{S})$. This approach is based on Benders' decomposition [8] and is presented in the continuation of this chapter.

As already mentioned, the problem we study is motivated by the necessity of dealing with the degradation of the FSO data transmission caused by weather conditions. A solution is to control the current signal MCS applied at the transmitter of the affected FSO link to secure correct data transmission. This, however, results in decreasing effective transmission data rates. As discussed in [9], weather conditions may have a significant impact on link capacity, in particular they may even cause network disconnection. This may occur in severe cases approximately in $10-15\%$ of hourly states during a one year period. One way to reduce this impact is to install a (limited) number of terrestrial fibers to assure connectivity. In fact, optimizing hybrid networks combining the use of FSO with terrestrial fibers is the main issue underlying the studies of second part of Chapter 3. The network optimization problem studied in this part is as follows: how to dimension the network links at the lowest cost, so that each link is equipped either with a set of several FSO modules or a fiber, and at the same time assure an acceptable level of the demand traffic satisfaction for all observed/predicted weather conditions. The problem is formulated as a mixed integer program (MIP) using the node-arc formulation. In such a hybrid network, a link is composed of either a set of parallel FSO transmission systems, or a high capacity optical transmission system (for example a DWDM system of capacity of the order of 10 Tbps in each direction) installed on a fiber. In both cases the transmission systems are of the full duplex type. An FSO transmission system is established by means of two parallel oppositely directed light beams connecting a pair of nodes placed in the line of sight, each equipped with an appropriate transceiver. Each such light beam carries the data with a given nominal bit-rate of 1–20 Gbps [3]. The solution approach we have chosen for this problem falls into the category of cut generation algorithms and is based on successive iterations, each consisting of solving a *master problem* and a set of *feasibility tests*. The master problem contains a set of capacity constraints that are successively extended with new cuts found by means of feasibility tests performed on the current optimal capacity solution of the master.

The second part of the thesis is composed of Chapters 4, 5, 6 and the Conclusion Chapter. In this part we will focus more on the improvements and the generalization of our approach. Chapter 4 tackles the problem of the so-called uncertainty sets (or uncertainty polytopes). As we have mentioned above, an important part of our optimization approach is related to weather states which are expressed as network states using the so called link degradation ratios. Certainly, the set of such states used in optimization, called the reference set of (link degradation) states, needs to be somehow predicted. Such a prediction can be made using historical weather records for the network area observed in the past, and possibly long term weather forecasts. Yet, such obtained reference set will most likely contain an excessive number of states and at the same time will not contain all the states that will appear in the reality. Thus, in our optimization approach we use a different characterization of the reference set of states, called uncertainty sets (or uncertainty polytopes). A certain type of such sets were studied in [9]. Hence, we have proposed to approximate the reference failure set with a special kind of virtual failure set called K-set, parameterized by an integer value K, where K is less than or equal

to the number of all links in the network. For a given K, the K-set contains all states corresponding to all combinations of K, or less, simultaneously affected links. We have extended this by considering simultaneous degradations of K nodes (meaning degradation of all adjacent links). Finally, inspired by the "hitting set" problem a new idea was to find a large number of subsets of two or three affected links and to use all possible combinations (composed of 2 or at most 3 of this subsets) to build a new virtual failure set that covers as much as possible the reference failure set that we got from the study of real weather data records. Next, this new failure set will serve as input for our cut-generation algorithm so that we can dimension the network at a minimum cost and for a satisfactory demand realization. As it will be shown in the numerical section, this allows achieving more cost-efficient link dimensioning with the same or even higher traffic satisfaction, as compared to the previous characterization. Numerical results are presented to show the effectiveness of our solution.

For our numerical studies in Chapter 5 we have used two network instances corresponding to *polska* and $nobel - germany$ that can be found in SNDlib (available at *sndlib.zib.de*). The original instance for *polska* from SNDlib connects $V = 12$ nodes (metropolitan areas) and is composed of $E = 18$ undirected links and $D = 66$ undirected traffic demands. The second instance we use to apply our robust optimization approach is a moderate-size network example derived from the instance called *nobel-germany* that can be found in SNDlib [10]. The instance is composed of 17 nodes and 26 undirected links, and there are 120 undirected traffic demands. We have used three different weather scenarios constructed for the purpose of this study. The way we construct these weather scenarios is explained in details in this chapter.

A realistic FSO network instance is presented in Chapter 6. We call this instance PMAN (Paris Metropolitan Area network) since it was created using the real data for the Paris metropolitan area. However, although all the data used to design the PMAN instance are real, the instance itself is not real, and has been elaborated only for the purpose of this thesis. The network is composed of $V = 12$ (core) nodes and covers an area of around 250 km^2. Two nodes (Paris1 and Paris2) are located in the inner Paris area, and the remaining 10 nodes represent autonomous cities around it. The set of links is composed of $E = 21$ links in total and the traffic matrix for PMAN includes all $D = V(V-1) = 132$ directed traffic demands (expressed in [Gbps]). The steps we followed and the way we designed this realistic network are presented in details in the first sections of this chapter. The last part of the chapter presents an extensive numerical study for PMAN network that illustrate the effectiveness of the proposed methodology.

Finally, the conclusion of this thesis summarize the work we have done and the contribution given to the literature about the problem of multiple partial link failures in the case of FSO networks. To conclude, future perspectives and possible works are presented.

General context and literature review

Nowadays, Free Space Optics communication system is one of major hot topics in the world of optical and wireless network communication. FSO is a well established broadband wireless optical transmission technology where the communication links are provided by means of a laser beam sent from the transmitter to the receiver placed in the line of sight. FSO links are considered as an alternative to radio links for example in metropolitan Wireless Mesh Networks (WMN). Inspired from the importance of this topic and the difficulties that it presents, the main focus of this thesis is devoted to dimensioning communication networks resilient with respect to multiple partial link failures in FSO networks.

Because of several important advantages that FSO networks exhibit, it becomes appealing to research community. We can mention here its huge bandwidth, transmission range of several kilometers, higher bit-rate and lower BER, licence free operation and its easy deployment, lower cost (as compared with the fiber optical technology), immunity to electromagnetic interference, license-free long-range operation (contrary to radio communications). These features of FSO communications are very attractive for applications in free web browsing, electronic commerce, data library access, enterprise networking, work-sharing capabilities, real time medical imaging transfer and high speed interplanetary links [11].

However, a disadvantage of this technology is vulnerability of the FSO links to weather conditions such as fog, rain, and snow (and pollution, for that matter), causing substantial loss of the transmission power over optical channel, mostly due to absorption and scattering. As a result the need for research on predictable models of optical attenuation and impairments due weather conditions is steadily increasing.

One of the two resilience mechanisms considered in our work is based on the notion of link margin, the quantity representing the additional amount of attenuation that can be accepted on an FSO link without losses in the transmitted data [12]. The use of this notion makes it possible to determine proper modulation and coding schemes (MCS) applied at the transmitters of the affected FSO links for a given weather condition [11, 13]. The fraction of the maximally attainable (i.e., nominal) link capacity that is lost due to a change of its MCS is referred to as link degradation ratio. Typical values of link capacity degradation ratios are $0.5, 0.75$ and 1, and each particular weather condition that may occur defines a network state referred to as link degradation state. Certainly, the set of such states used in optimization, called the reference set of (link degradation) states, needs to be somehow predicted. Such a prediction can be made using historical weather records

for the network area observed in the past, and possibly long term weather forecasts. Yet, such obtained reference set will most likely contain an excessive number of states and at the same time may certainly not contain all the states that will appear in the reality. Thus, in our optimization approach we use a different characterization of the reference set of states, called uncertainty sets (or uncertainty polytopes). These new uncertainty sets are discussed in details in the next chapters.

Moreover, in some extreme cases link degradation ratio on some links may become equal to 1 leading to network disconnection (such disconnections can be observed for $10-15\%$ of the weather states during a one year period). To deal with such unacceptable disconnections we consider another resilience mechanism. It consists in installing, instead of FSO systems, a limited number of (weather insensitive) optical fibers on the key links in order to secure connectivity of the so obtained (hybrid FSO/fiber) network in all the foreseen weather conditions.

In the present study we focus on specific features of the FSO networks such as full-duplex links, realistic link failure scenarios, etc. Finally, we concentrate on estimating the reference failure set by means of an approximate compact set of failure states, which opens a way to a considerable reduction of computation time.

1 Weather disasters

Natural disasters are extreme, sudden events caused by environmental factors that injure people and damage property. Dangerous hurricanes, tornadoes, floods, fires, blizzards and severe storms, all strike anywhere on earth, often without warning. Do you know the book "One Second After"? It is a 2009 novel by the American writer William R. Forstchen. The novel deals with an unexpected electromagnetic pulse attack on the United States that affects the people living in and around the small American town of Black Mountain, North Carolina. Disaster events can happen frequently worldwide with catastrophic consequences. Although by definition they are considered rare, their occurrence is inevitable, and their risk is rising. Another important observation is that their negative effects, always considered significant, cannot be precisely evaluated in advance [14]. Despite this, they can helped us understand that organising and maintaining effective communication, during and after the disaster, are vital for the execution of rescue operations. As communication resources are often entirely or partially damaged by disasters, the demand for information and communication technology (ICT) services explosively increases just after the events [15].

Communication networks operate in unpredictable environments, and are based on devices and media that are likely to fail due to many causes including various disasters. These disasters instigate serious network traffic congestions and physical damage of ICT equipments and emergency ICT networks. Thus, it is impossible to predict and eliminate all factors that can affect connectivity in the network. The consequences of network failures can become critical, especially when they are related to backbone networks. Therefore, network resilience is an indispensable part of analyzing existing and designing new networks [14] and [16]. In [15], the authors present a protection mechanism based on the

idea of designing a network architecture by integrating the existing network infrastructure with the reinforcement of layers based techniques and cloud processing concepts. This resilient network architecture allows the ICT services to be launched within a reasonable short period of time of development.

Every year, we observe tens of hurricanes worldwide, often leading to power outages disrupting communications on a massive scale for a relatively long time (i.e., 10 days on average). From the 18th-century, the hurricane that ravaged the Caribbean, to the devastating blow issued by Sandy in 2012, history is replete with stories of the wreckage and ruin that come from weather disasters. Examples include Hurricane Katrina, which caused severe losses in Louisiana and Mississippi in in the southeastern United States in August 2005. Another one, Hurricane Harvey, after traveling through the Gulf of Mexico in late August 2017, arrived in the United States as a Category 4 storm. It was the first major hurricane to make landfall in the continental United States in a decade, after 2005's Hurricane Katrina. But hurricanes are not the only challenge. Earthquakes can bring about even greater destruction to communication networks due to the long time of manual repair actions. We can mention here the earthquake of December 2006 in southern Taiwan. With a magnitude of 7.1, this weather disaster resulted in simultaneous failures of seven submarine links providing Internet connectivity between Asia and North America, which visibly affected the international communications to China, Taiwan, Hong Kong, Korea, and Japan. Another example is the Greatest Japan Earthquake on March 11, 2011 (of 9.0 magnitude), which caused widespread damage to undersea cables, as well as completely or partially destroyed telecom switching offices [14].

While knowing that failure of communications systems may cause catastrophic damage to human life and economic activities as people are unable to communicate with each other in a timely manner and with a convenient quality of service, another reasons for disasters in communication networks are humans themselves. We can mention here intentional human activities, such as bombing or weapons of mass destruction attacks, malicious actions where electromagnetic pulse (EMP) attacks are used to intense energy fields, disrupting nodes and links in a specific geographic area. Also big industries pollution, smog and pollution from automobiles may couse problems sometimes. Finally, disasters may also occur as a result of technological issues (e.g., the Northeast Power Grid Blackout). It was a widespread power outage throughout parts of the Northeastern and Midwestern United States, and the Canadian province of Ontario on August 2003. The blackout's primary cause was a software bug in the alarm system at the control room of First Energy, an Akron, Ohio-based company, which rendered operators unaware of the need to redistribute load after overloaded transmission lines drooped into foliage. What should have been a manageable local blackout cascaded into the collapse of the entire Northeast region.

All of these disasters decrease the traffic handling capability of the network, sometimes causing a whole network subarea to be turned off. Vulnerability of network nodes/links to disaster-based failures can only be based on probability analysis depending on, for example, the distance of the network element from the event epicenter, the area topography, as well as the characteristics of a network element itself (also comprising its physical protection features, such as location of the element in the building) [14, 17].

Thus, it is impossible to predict and eliminate all factors that can affect connectivity in the network. Therefore, network resilience is an indispensable part of analyzing existing

and designing new networks [14].

2 Partial link degradation

The impact of weather conditions on the wireless networks transmission capacity has been studied to some extent, but the majority of works have considered failure modeling for a single region failure (some investigations for the case of weather perturbations occurring simultaneously in different regions can be found in [18]). In particular, paper [19] discusses three measures of the WMN survivability for a regional failure scenario assuming circular failure areas with random location of failure epicenters. As observed in [19], from the network topology viewpoint, networks with nodes covering a square area in a regular way have a better performance in terms of the total traffic surviving a regional failure. It is also shown that in the case of heavy rain storms, using information on forecasted attenuation of links based on radar measurements allows for periodic updates of the network topology in advance, and thus dealing efficiently with these phenomena. In [20], a mixed-integer programming (MIP) model for network reconfiguration in case of unfavorable weather conditions is presented. The model looks for alternative routes for rerouting some of the disturbed traffic, while reducing the interference between adjacent transmission links. Other studies, such as [21], have considered the relevance and impact of specific weather factors on the FSO links capacity. Another study that takes into account up to two link failures along a path is presented in [22]. In this work the authors develops novel mechanisms for recovering from failures in IP networks with proactive backup path calculations and Internet Protocol (IP) tunneling. Their scheme provides resilience for up to two link failures along a path. More general, the developed routing approach is that a node reroutes a packet around the failed link without the knowledge of the second link failure. The proposed technique requires three protection addresses for every node, in addition to the normal address. Associated with every protection address of a node is a protection graph. Each link connected to the node is removed in at least one of the protection graphs, and every protection graph is guaranteed to be two-edge-connected. The network recovers from the first failure by tunneling the packet to the next-hop node using one of the protection addresses of the next-hop node; the packet is routed over the protection graph corresponding to that protection address. The authors also do an extension to the basic scheme providing in this way recovery from single-node failures in the network [22].

Other examples are given in [14], [23] and [24], where major disasters are considered for wired network optimization. As for wireless mesh networks, new measures of survivability for a regional failure scenario, including the region failure survivability function and the expected percentage of total flow delivered after a failure as a function of the region radius are discussed in [25]. These measures are used from the authors to evaluate the vulnerability of example wireless mesh networks to region failures.

On the other hand, the “traditional” failure scenarios, aiming at covering the equipment failures, assume usually single total failures of links or nodes, and sometimes multiple simultaneous total link failures (the so called shared risk link groups). The main resilience mechanism considered in this case is, roughly speaking, flow rerouting taking advantage of

spare link capacity foreseen in network dimensioning. A lot of research has been devoted to this area, but almost exclusively for wired networks; for a summary see [6]. As far as wireless networks are concerned, there is some work on resilient network optimization but again typically taking into account isolated failure events, involving a (total) failure of one network link/node at a time (see [26]). Furthermore, in [27], the authors investigate wireless mesh networks and their sensitivity to weather conditions, in particular the heavy rainstorms that may lead to important signal attenuation. The contributions of that work include presentation of a MIP model of weather-resistant links formulation problem followed by an analysis of its computational complexity.

It happens, however, that the above characterized research is hardly relevant to the subject of this thesis, which is wireless network resilience to adverse weather conditions. In fact, we are not treating weather changes as a factor causing network (in particular link capacity) failures. Although sometimes very bad weather (like heavy snow) can cause reliable data transmission on a link impossible, we treat the changing weather condition as natural, always present, element of network operation (this is why we sometimes do not use the term "link failure" but rather "link degradation"). In any case, even if we treat the weather degradation as multiple but partial link capacity failures we observe that this case has been treated to a very small extent in the literature. In Chapter 3, we will present a short study on such an impact in terms of simultaneously affected FSO links.

3 Multiple partial link degradation

Failures in communication networks occur due to a variety of both external and internal reasons of different range and scale. For example, these can be natural disasters such as floods, earthquakes and fires, weather phenomena like tornadoes and snow storms, and technology-related disasters such as power blackouts or equipment (node or link) breakdowns. All of them decrease the traffic handling capability of the network, sometimes causing a whole network subarea to be turned off.

Large-scale failures caused by disasters are by far more dynamic and broader in terms of range than the failures traditionally considered in network optimization. The large-scale failures frequently result in the so-called region failures, i.e., simultaneous failures of network elements located in a specific geographical area. Examples of research in this area can be found in [28], where the authors propose to use spectral graph theory to characterize network survivability regarding geographically correlated failures. They present a network survivability evaluation model employing an optimization problem to find the most vulnerable geographic locations. In line with this, the authors of [29] present assessments on the vulnerability of optical networks and a comparative analysis of network robustness for different synthetic and real optical network topologies under various types of massive failures using the Girona Network Robustness Simulator (GNRS).

As already mentioned, this thesis introduces a (new) optimization model for robust dimensioning of FSO networks in order to achieve resilience with respect to multiple partial link failures. Similar problems have been widely investigated in the literature but for a given list of failure states, see for instance [6, 17] and the list of literature therein.

More recently, robust optimization approaches to resilient network dimensioning have been developed in [30], [31], and [32] (under traffic demand uncertainty), and in [33] (under signal propagation uncertainty in wireless networks). Yet, to the best of our knowledge, no models have been developed for uncertainty concerning available capacity on transmission links, i.e., for the case relevant to networks employing FSO. Also, as majority of work on traffic restoration and resilient network dimensioning has been done for wired networks, multiple partial link failures are virtually not considered despite common appearance of this phenomenon in modern wireless networks that cope with it by means of adjustable modulation and coding schemes (MCS). Multiple partial link failures were addressed in [6] (for the so called Unrestricted Reconfiguration mechanism, commonly called Global Rerouting [34]), and more recently in [35] (for the so called oblivious routing) and in [36]. An optimization approach, based on disjoint path routing, to FSO networks with multiple partial failures is presented in [37].

Paper [36], along with [38], are the starting point for this work. In those two papers the authors have studied a specific traffic protection mechanism, called *Flow Thinning* (FT). The main feature of FT is handling partial failures without any traffic rerouting at all. In FT, each traffic demand is equipped with a set of dedicated routing paths whose flows are thinned accordingly to the current availability of network link capacity (for more details on FT see [36]). Although the context of the present study and of [36] and [38] is the same, as we deal with cost-efficient dimensioning of communication networks resilient to multiple link failures, the following differences main can be observed. First, our work assumes the Global Rerouting mechanism instead of FT. (Recall that Global Rerouting allows for establishing path flows in an unrestricted way from scratch when a failure state occurs – this feature makes the cheapest possible mechanism traffic protection mechanism in terms of the cost of link capacity). Our alternative characterization of link degradation states captures the incidence of links and nodes for a given weather state. That is, we consider simultaneous degradations of subsets of links or nodes (degradation of a node implies degradation of all links incident to it). As shown in the numerical chapter, this allows achieving more cost-efficient link dimensioning with the same or even higher traffic satisfaction, as compared to the previous characterization.

Finally, we note that as far the hybrid feature is concerned, an optimization approach related to the FSO network link dimensioning problem was presented in [39], where disjoint path routing to ensure protection against link degradation in hybrid FSO/fiber networks was considered.

4 Our case, FSO systems

The FSO networks considered in this thesis are characterized by fluctuations of capacity currently available on the links caused by adverse weather conditions. For this reason, optimization of FSO becomes complex as it has to cope with degradation of data transmission on the FSO links at the network design stage. Here, an important element is the use of proper, channel condition-dependent, signal modulation and coding schemes (MCS) at the transmitters. This allows affected link transmissions to remain operational, assuring proper data decoding at the receivers at the expense of decreased data

transmission rate, i.e., link capacity. Thanks to that, the influence of degraded weather condition on link capacity (bit-rate) is kept under control but at some price that one needs to evaluate and optimize. In this study, the fraction of the maximum attainable (i.e., nominal) link capacity lost due to a change of its MCS is referred to as link degradation ratio. Typical values of such ratios are $0.50, 0.75$ and 1, and each particular weather condition that can occur defines a degradation state referred to as the link degradation state.

5 Complexity

Complexity theory is a central topic in today's theoretical computer science and it addresses problems and the algorithms that solve them. It studies the time and space complexity of computational problems and uses computation models such as Turing machines to help testing the complexity of different problems. In computer science, the time complexity is the computational complexity that describes the amount of time it takes to run an algorithm. Time complexity is commonly estimated by counting the number of elementary operations performed by the algorithm, supposing that each elementary operation takes a fixed amount of time to perform [40]. Thus, the amount of time taken and the number of elementary operations performed by the algorithm are taken to differ by at most a constant factor. In the same way, the space complexity of an algorithm or a computer program is the amount of memory space required to solve an instance of the computational problem as a function of the size of the input. It is the memory required by an algorithm to execute a program and produce output [6]. Similar to time complexity, space complexity is often expressed asymptotically in big O notation, such as $O(n)$, $O(n \log n)$, $O(n^{\alpha})$, $O(2^n)$, etc., where n is the input size in units of bits needed to represent the input.

Complexity theory helps computer scientists relate and group problems together into complexity classes. Informally, the problems to be considered fall into two categories: those for which there are algorithms that always solve the problem in reasonable time, and those for which there is no such guarantee. Sometimes, if one problem can be solved, it opens a way to solve other problems in its complexity class. In many cases, problems can be modeled as decision problems which are problems that can be answered with a "yes" or a "no". For example, "is this number prime?", "does this graph have a Hamiltonian path?" "is there an assignment of variables to the equation such that a set of constraints are satisfied?" Examples of decision problems include the traveling salesperson problem, 3SAT, and primality testing. Decision problems can be simulated on computational models such as Turing machines. This theory helps determine the difficulty of a problem, often measured by how much time and space (memory) it takes to solve a particular problem. For example, some problems can be solved in polynomial amounts of time and others take exponential amounts of time, with respect to the input size [6]. This may also include optimization problems while any optimization problem can always be transformed into a decision problem. Often, an optimization problem can be solved by solving a sequence of decision problems, such as:

begin
k:=1;
while *solveDecisionProblem(k)* **do**
k:=k+1;
end.

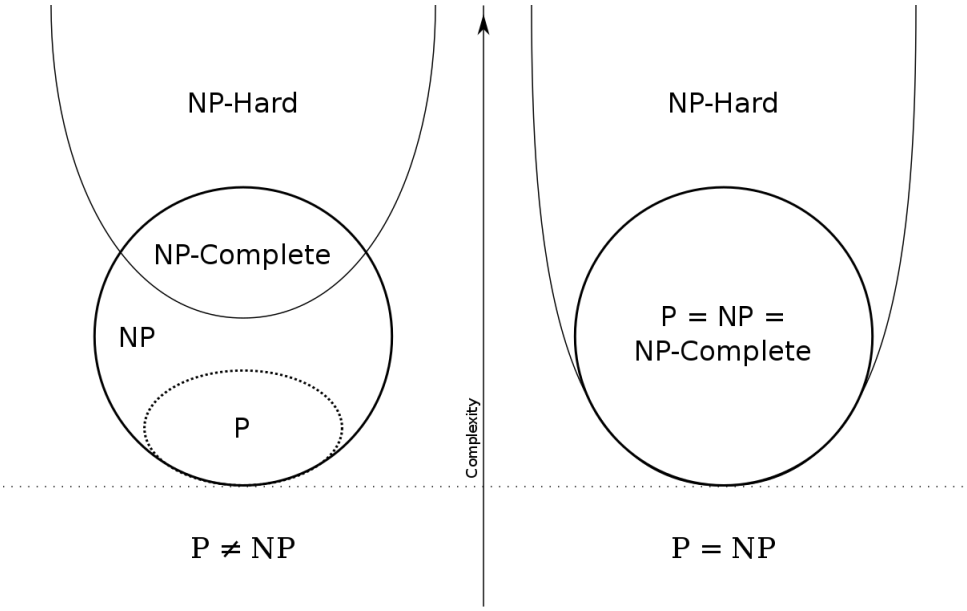

Figure 1.1 – Diagram of complexity classes [41].

Among the different classes of problems, the P, NP and $NP-Complete$ classes have a special role in the combinational optimization problems:

- P class (deterministic polynomial time): contains all the problems that can be solved by an algorithm of polynomial complexity.
- NP class (non-deterministic polynomial time): contains all the problems for which we can check if a given proposition is a solution with an algorithm of polynomial complexity.
- $NP-Complete$ class: a problem is $NP-complete$ when it can be solved by a restricted class of brute force search algorithms. A problem p in NP is $NP-complete$ if every other problem in NP can be transformed (or reduced) into p in polynomial time.

It is easy to see that $P \subseteq NP$. The reverse inclusion, $NP \subseteq P$, however, is yet an open question, the most famous open question in computer science. There are a few observations to be made.

Remark 1
If a problem p is in P, that means it can be solved on a deterministic machine in polynomial time. That also means, that it can be done on a non-deterministic machine in polynomial

time. This does not imply that it can be done faster on a non-deterministic machine, nor does it exclude this possibility. Consider, for example, the problems" is the sum of all n elements in a set equal to K?" and "is there an element x in this set?."

Remark 2
Similarly, if problem p is in NP, it can be solved on a non-deterministic machine in polynomial time. That also means that it can be done on a deterministic machine in exponential time by using a level-order traversal of the execution tree. This does not imply that a deterministic algorithm must take exponential time, because it just might be that there is also a deterministic algorithm that solves p in polynomial time. The same two problems can be used as examples here [6].

The NP class contains most of combinatorial optimization problems, including NP-Complete problems. The NP-Complete subclass contains the most difficult problems of NP. The notion of The NP-Complete can be introduce formally in the following. A problem p is said to be The NP-Complete if: 1) $p \in NP$, and 2) all other problems in NP reduce to the problem p, that is, for all $r \in NP$ it is true that $r \propto p$.

The problem we deal with in this thesis is a network flow/dimensioning problem and is most likely to be a NP-hard problem. Because of modular links, our primarily problem is NP-hard even for a polynomial number of states (see [6]). Moreover, the direct approach to our problem requires solving linear programs involving a large number of arc-flow variables during the branch-and-bound process performed by the MIP solver. For more detailed discussion the the complexity of the problem that is central to our investigations, the reader is pleased do se Chapter 3, Section Computational complexity of P($\mathcal{K}$).

6 Solution methods

The resilient network dimensioning problem has been one of the most investigated problems in these last decades. Different approaches for robust dimensioning of wireless mesh networks in order to achieve resilience with respect to partial link failures have been widely proposed in the literature, but for a given list of failures states. Yet, to the best of our knowledge, no models have been developed for uncertainty concerning available capacity on transmission links, i.e., for the case relevant to networks employing FSO. Also, as majority of work on traffic restoration and resilient network dimensioning has been done for wired networks, multiple partial link failures are virtually non considered. In the following we will discus some of the methods we used to solve the dimensioning problem in the case of FSO networks we study.

6.1 Exact methods

Here we will discuss basic optimization methods and algorithms applicable to the network design problems (NDPs). Most of these problems are multi-commodity flow NDPs, and as such they often either possess exact linear programming (LP) formulations or can be

reasonably approximated with LP formulations. This, and the fact that these are the mainly the LP problem formulations that can ne effectively solved in the exact way with a fair implementation effort, make the role of LP crucial for the network design. [6].

Exact methods guarantee to give an optimal solution. For NP problems, these methods have exponential complexity and they can solve in a reasonable time only instances of limited size by performing an exhaustive search of the solution space in order to guarantee optimality.

6.1.1 Linear Programming

LP gives an exact, effective, and easy accessible optimization approach, applicable on network dimensioning problems whenever they can be formulated as LP problems. LP solvers are available on both the commercial and freeware basis, and some of them are capable of solving really large linear programs with thousands of variables and constraints. Between the most popular solvers we can mention: CPLEX, GUROBI, AMPL, and MATLAB. For the numerical results in this work, we have used the CPLEX solver implemented in Java programming language.

In optimization theory, the duality is a powerful concept. In essence, using duality, an optimization problem given in a particular form, called *primal problem* in this context, can be transformed to a related problem, called its *dual problem*, so that the optimal solutions to both primal and dual are closely related. Sometimes this transformed problem can be easier solved. Furthermore, some efficient algorithms for solving primal problems can be developed using duality. More examples can be found in [6] and [4].

6.1.2 Mixed-Integer Programming

There are important design problems which are NP-Complete and involve such non-linear features as modular links/flows (which is the case os FSO networks that we study in this thesis) or non-bifurcated routing. Therefore, the LP formulations are in many cases too simplified bringing the necessity to use additional integral(binary) variables. This leads to mixed-integer programming (MIP) formulations and, sometimes, to integer programming (IP) formulations, with no continuous variables at all. Practically, the only general exact approach used in professional solvers for MIP and IP problems is the branch-and-bound (BB) technique together with its less known enhancement called branch-and-cut (BC) [6].

6.1.2.1 Branch-and-Bound method is based on the principle that the total set of feasible solution can be partitioned into smaller subsets of solutions. These smaller subsets can then be evaluated systematically until the best solution is found. In other words, the BB process consists of the three consecutive phases: 1) finding an initial yet feasible solution; 2) finding optimal feasible solution; and 3) proving that the solution is optimal. The application of this method to MIP problems is best illustrated for binary variables. It should be noted that the BB approach may fail to find the exact optimum for

large networks, as its execution time is in general exponential with the number of binary variables. In many cases it is able to find near-optimal solutions [6].

The enumeration of the solutions results in the exploration of a virtual tree where each node represents a partial solution. The efficiency of BB depends heavily on the quality of the lower bounds obtained by solving the BB tree node problems. If these bounds are close to the optimal integer solution than we can expect that the majority of the BB tree nodes will never be visited as most of the BB tree branches will not be entered. Therefore, it may happen that it is advantageous to spend more time on a node and try to find a better lower bound then the one resulting from simple relaxation [6].

6.1.2.2 Branch-and-Cut method is a very successful approach for solving a variety of integer programming problems, and it also can provide a guarantee of optimality. As we mentioned above, the idea is to find a better lower bound, and the application of these lower bound improvement techniques is the heart of the BC enhancement of BB. A basic way to achieve this is to construct valid inequalities in the BB tree nodes. Sometimes the generation of valid inequalities at the root of the BB tree might be interesting, as they may yield a tighter set of constraints than the standard relaxed formulation of the problem. These additional constraints will be used in the problems definition for all other nodes of BB tree. It can even happen that solving the the root problem will immediately yield a point, which, if an appropriate (feasible) rounding-off of the continuous variables can be found, provides a good near-point feasible integral solution [6]. We will make use of valid inequalities latter on, to speed up our algorithms.

6.1.3 Bender's decomposition

Benders decomposition's (BD) is a general method applicabel to LP and MIP problems that can be partitioned with respect to variables [42]. In the multi-commodity network design, BD has been used for restoration and/or modular design in [43, 44].

Roughly speaking, BD is applicable when we can distinguish a subset of *master variables* (e.g., link capacities) and decompose the original problem into *master problem* involving minimization of the original objective function using only the distinguished variables, and a set of auxiliary tests (called *feasibility tests*) which generate inequalities for the master problem. The Bender decomposition algorithm is iterative: the master problem minimizes the objective function, and then the resulting optimal master variables are tested for feasibility in the sense of the original problem. When a feasibility test fails, a new (linear) inequality is added to the master problem [6].

As we already mentioned, our problem is a NP-hard and the BB technique may be considered to find the exact optimal solution. To make BB more effective, we can use BD and apply BB only to the master problem which has less variables than the original MIP formulation. It can be proved ([45] and [46]) that the procedure will terminate after a finite number of steps. We discuss all this in details in Chapter 3 where we give the MIP formulation of our problem.

In fact, the Benders cutting plane approach may need a large number of Benders' inequalities to converge to optimum. This may pose an efficiency issue since test (3.8) (called also the separation problem) performed in Step 2 of our algorithm contains binary variables. One way to deal with this issue is to try to speed up the convergence of the algorithm by using additional valid inequalities on top of the Benders cuts in the master problem solved in Step 1 of the algorithm that we use.

6.1.4 Valid inequalities

Cutting planes, variously called cuts or valid inequalities, are linear inequalities that can be inferred from an integer or mixed integer constraint set. Such inequalities are generated and inserted to the problem $P(\Omega)$, on the top (and sometimes instead) of the existing constraints. The idea is to exploit the integrality of variables in order to produce inequalities that are valid for all feasible solutions and at the same time separate parts of the solution polyhedrom $P(\Omega)$ containing the non-feasible optimal solutions, leaving the integral(feasible) optimal solutions within the adjusted polyhedron. It is also desirable that such inequalities define the faces of the convex hull of the solution set of the non-relaxed version of $P(\Omega)$ (recall that such a convex hull is the smallest polyhedron containing all feasible solutions of the non-relaxed version of $P(\Omega)$).

A useful class of valid inequalities is the cutset inequalities class, first introduced in the robust context in [32]. Given a partition $\mathcal{V} = \mathcal{V}_1 \cup \mathcal{V}_2$ of the nodes, the cutset inequality associated with the partition states that the amount of capacity installed on the arcs going from $\mathcal{V}_1$ to $\mathcal{V}_2$ should not be less than the sum of the volumes of the demands from $\mathcal{V}_1$ to $\mathcal{V}_2$. Defining $\mathcal{E}(\mathcal{V}_1, \mathcal{V}_2) = \{a \in \mathcal{A} : o(a) \in \mathcal{V}_1 \wedge t(a) \in \mathcal{V}_2\}$ and $\mathcal{D}(\mathcal{V}_1, \mathcal{V}_2) = \{d \in \mathcal{D} : o(d) \in \mathcal{V}_1 \wedge t(d) \in \mathcal{V}_2\}$, the inequality is formally defined as:

$$\min_{s\in\mathcal{S}} \sum_{a\in\mathcal{E}(\mathcal{V}_1,\mathcal{V}_2)} \big(1 - \beta(e(a), s)\big)c(e(a)) \geq \sum_{d\in\mathcal{D}(\mathcal{V}_1,\mathcal{V}_2)} h(d) \tag{1.1}$$

In [?] the nodes are randomly partitioned into two subsets and then a local search is performed, picking up one node and moving it to the other subset until there is no more improvement in the violation. If no violated inequality has been found, another initial partition is considered up to a maximum of 5 iterations.

In this context, it is noteworthy that recent implementations of Benders' decomposition have witnessed improvements when interior points instead of extreme points are separated in the algorithm, see [47].

6.2 Heuristic methods

Integer programming problems are a special case of more general combinatorial optimization's problems i.e., problems with finite solution space. Although BB can be applicable in this more general case as well, for many problems, especially for large networks, a heuristic approach an be more efficient in obtaining close-to-optimal solutions. In recent

decades, a number of general heuristics methods (sometimes called meta-heuristics) have been developed, including simulated annealing, evolutionary algorithms, tabu search, and others. All of these methods involve some randomness and, therefore, are called stochastic meta-heuristics [6].

- **The local search** (LS) approach is probably the simplest and most commonly known heuristic for these class of problems [48]. Ls uses the notion of neighborhood. The algorithm starts by building the unique initial solution and then iteratively applies local changes to move to a better neighbor solution until reaching a certain stopping criterion.
- **Simulated Annealing** (SAN) is a heuristic method for solving unconstrained and bound-constrained optimization problems of the type **minimize** $F(x)$ for $\mathbf{x} \in S$. As local search method, SAN also uses the notion of a neighborhood. After selecting an initial point $x \in S$ and setting the initial temperature T^0 (initial temperature is a parameter, typically a large number), the algorithm proceeds. At each iteration of the simulated annealing algorithm, a new point is randomly generated. The distance of the new point from the current point, or the extent of the search, is based on a probability distribution with a scale proportional to the temperature. The algorithm accepts all new points that lower the objective, but also, with a certain probability, points that raise the objective. By accepting points that raise the objective, the algorithm avoids being trapped in local minima, and is able to explore globally for more possible solutions. An annealing schedule is selected to systematically decrease the temperature as the algorithm proceeds. As the temperature decreases, the algorithm reduces the extent of its search to converge to a minimum.
- **Evolutionary Algorithm** (EA) is another heuristic method of general purpose. The algorithm aims of solving optimization problems, with or without constraints, based on a natural selection process (process similar to that of biological evolution). In such an algorithm, a population of solutions is modified several times. Each time, the algorithm randomly selects individuals in the population and uses them to produce the next generation of solutions. Over successive generations, the population "evolves" towards an optimal solution. The stopping criterion can be reaching a certain iteration limit or, as in SAN, lack of improvement of the objective function or, reaching a solution exceeding a certain predefined lower bound.

Finally, when considering all these methods, we can say that most successful meta-heuristics are the result of combination of several methodologies, these depending of the particular problem we are trying to optimize.

7 Graph Theory

So many things in the world would have never come into existence if there had not been a problem that needed to be solved. "Fundamentally, computer science is a science of abstraction" (A. Aho and J. Ulman). Computer scientists must create abstractions of

real-world problems that can be represented and manipulated in a computer. For example, we use a logic to design a computer circuits. Another example - scheduling final exams. For successful scheduling we have to take into account associations between courses, students and rooms. Such set of connections between items is modeled by graphs. The basic idea of graphs were introduced in 18th century by the great Swiss mathematician Leonhard Euler. He used graphs to solve the famous Königsberg bridge problem. We can define a graph as a set of points (that we call vertices or nodes) connected by lines (edges or arcs). We can think of the entire Web as a graph, where items are documents and the references (links) are connections. The network is a graph itself. There are a lot of well known problems that can be modeled and solved using the graphs. We can mention here the coloring and partitioning problems, the traveling salesman problem,the knapsack problem etc,. A graph can be directed or undirected.

The network optimization problem studied in this thesis is as follows: how to dimension the network links at the lowest cost, so that each link is equipped with a set of several FSO modules, and at the same time assure an acceptable level of the demand traffic satisfaction for all observed/predicted weather conditions. To deal with this problem we have proposed a mathematical formulation together with a cut-generation algorithm to solve it.

For this, we consider a network that is modeled by means of a bi-directed (or undirected in some cases) graph. The problem is formulated as a mixed integer program (MIP) using the node-arc formulation (called node-link formulation in [6]). Capacity of links is modular and each module provides the bit-rate of M Gbps separately for each of the two oppositely directed arcs related to the link – this assumption corresponds to full duplex transmission of FSO systems. To each link there corresponds a non-negative cost for the FSO module. We have considered the network design problem corresponding to FSO networks resilient with respect to multiple partial link degradation. The failures we are dealing with are due to adverse weather conditions and we need to ensure robustness, which makes the problem more difficult. To construct our approach we start with building a reference failure set which uses weather data records. Still, this set does not necessarily covers all future failure states but gives a good idea of what the network should be protected.

Finally, inspired by the hitting set problem we explore a new idea that aims to find a large number of subsets of two or three affected links and to use all possible combinations (composed of 2 or at most 3 of this subsets) to build a new virtual failure set that covers as much as possible the reference failure set that we got from the study of real weather data records. This new failure set will serve as input for our cut-generation algorithm so that we can dimension the network at a minimum cost and for a satisfactory demand realization. A more detailed discussion of the problem is given in Chapter 3 and Chapter 4.

8 Conclusion

In this chapter we have presented a general overview of the main problem we dial with in this thesis together with a literature review. In the first part we do an analysis of weather based disasters and the impact they have in the network survivability. When the network

does not provide resilience mechanisms to ensure and maintain an acceptable level of service in the face of various challenges, the failures may lead to severe data losses in the network.

In contrast to the previous investigations, we deal with a problem involving a very large number of failure states, described by the so called uncertainty set for which we propose an optimization model together with a cut generation solution algorithm.

In the second part of this chapter we presented some basic optimization techniques which are described in numerous handbooks, monographs, and research papers in the optimization theory and operational research, including the works in communication and computer networks.

In the next chapter, we present a more detailed description of the network dimensioning problem that we study and our solution algorithms proposed for this class of problem.

FSO and mathematical model for weather conversion

Introduction

This chapter is dedicated to a general presentation of FSO and the impact of weather conditions in FSO performance. First, we will give a short history of wireless optical telecommunications and FSO, including the principles of this system and it's advantages and disavantages. Second, we describe the link margin concept and all the elements that we should consider when we have an FSO system. Further, we devote special attention to the problems associated with converting the link margin into availability ratio and the modulation schemes that better fit our system. Finally, we consider applications of FSO system, standards as well as safety and confidentiality issues.

1 Introduction to FSO

The history of modern telecommunications starts at the end of the 18^{th} century with the appearance, in France, of Claude Chappe's optical telegraph. The Chappe free-space optical telegraph was quickly and completely replaced by the electrical telegraph. For the optical communication network to be used again, it would need to adapt and find new applications. Information can be transmitted in various ways. Among the possibilities, one of the most powerful is the use of electromagnetic waves for the transfer of information.
Free Space Optics is an optical communication technology that offers a large bandwidth for data, voice and video transmissions in mostly short -to medium -link distances (the distance goes up to 15 km [3]). But free-space optics is not a new idea. It has roots that go back over 30 years to the era before fiber-optic cable became the preferred transport medium for high-speed communication. In those days, the notion that FSO systems could provide high-speed connectivity over short distances seemed futuristic, to say the least. But research done at that time has made possible today's free-space optical systems, which can carry full-duplex (simultaneous bidirectional) data at gigabit-per-second rates over metropolitan distances of a few city blocks to a few kilometers. In this technology the information is transmitted by propagation of light in free space allowing optical connectivity. There is no requirement of the optical fiber cable. FSO operates similar

to OFC (optical fiber cable) networks but the only difference is that the optical beams are sent through free air instead of OFC cores that is glass fiber. FSO is a LOS (Line Of Sight) technology that could be deployed as the primary, back-up and disaster recovery links.

1.1 How does FSO system work

Communication systems provide information transmission from a source point to a destination. The purpose of communication is therefore to transfer communication (e.g., data, voice, multimedia, etc). The most powerful aspect of FSO communication for either analog or digital communication system is the large bandwidth available at optical frequencies. A wavelength of $1\mu m$ corresponds to 3 x 10^{14} Hz (300GHz) and therefore a single 16 GHz channel corresponds to only 3.3 x 10^{-6} μm of wavelength spread. There are two types of communication, digital communication (data transmitted from a digital source) and analogous communication (data transmitted from analogous source). The FSO technology is based on the connection between the FSO units, using optical radiation as the carrier channel, consisting of an optical transceiver providing full duplex communication (bidirectional). A basic block diagram of FSO system communication is shown in Figure 2.1

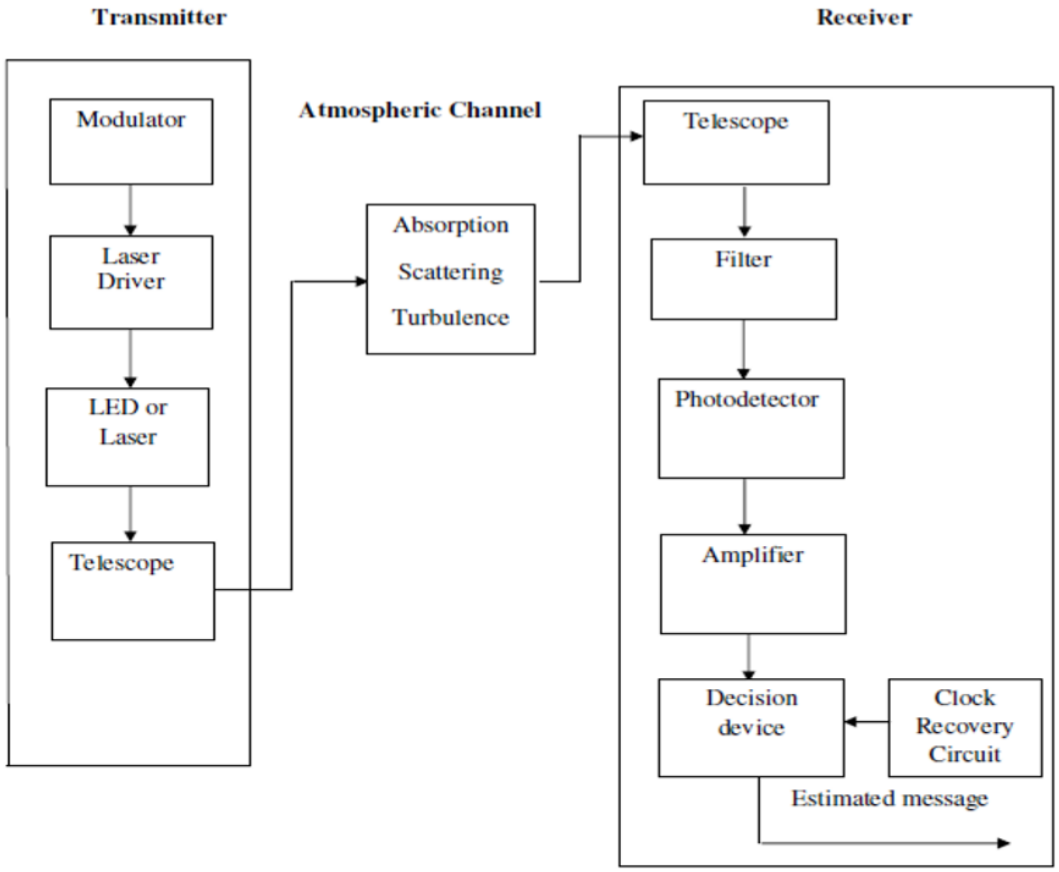

Figure 2.1 – Block diagram of FSO system [12].

The main elements are the transmitter unit, the medium and the receiver unit. At the transmitter, the modulator modulates the information signal using the Intensity Modulation and converts the electrical signal to optical. As a transmitter it can be used either light emitting diodes (LEDs) (single or multiple), usually 1mW, or lasers (single or multiple), usually 10-100mW (transmitter). Typically, laser is used for the transmitter, as a high power optical source, while a receiver uses optical diodes, capable of receiving information from the laser (Figure 2.1).

The medium where signal propagates is the air. At the receiver end, the telescope receives the incoming radiated signal and directs the signal towards optical filter. The optical filter allows passing only the wavelength of the signal and blocks other radiations from the atmosphere. The detector converts the optical signal back to the electrical signal which later is amplified by the amplifier. In order to recover the information, the receiver processing circuits include clock recovery circuit and decision device. As a receiver it can be used detector positive intrinsic-negative (PIN) diodes with -43 dBm or advanced photodiode (APD) with -53 dBm as minimum received power. In each FSO unit we also find lens that transmits light through the atmosphere to another lens that receives the information [49]. The receiving lens (optical diode) connects to a high sensitivity receiver via optical fibers.

The use of FSO does not require spectrum licensing. FSO is easy to mount (consists of several hours of installation) in various environment and its adaptive interfaces is supported by device from a variety of vendors, making this technology easy to use and upgrade-able. FSO systems use low powered invisible infrared laser light of wavelengths in the 750nm to 1550nm range. Generally speaking, anything that can be done in fiber, can be done in FSO too, safer and costless.

1.1.1 Optical Sources and Detectors

FSO communication systems operate mainly in the windows of 780-850 nm and 1520-1600 nm. Within the range of 700-10,000 nm wavelengths, several atmospheric transmission windows are available with an attenuation in the range of < 0.2 dB/km. At 850 nm wavelength, it is possible to use as a transmitter the Vertical Cavity Surface Emitting Lasers (VCSEL), and as a receiver the highly sensitive silicon Avalanche Photo Diode (APD). VCSEL are economic and have low power density (provide up to 10 Gbps).

In the 1300 nm to 1550 nm wavelength range, the lasers available are Febry Perot (FP) lasers and Distributed feedback (DFB) lasers which offer higher power density. They provide a data rate transmission up to 40 Gbps. Higher wavelengths are less affected by severe weather conditions (e.g., fog).

The 1550 nm band is mostly preferred by providers because it can provide wavelength division multiplexing technology and it reduces scattering effect. In addition, longer wavelengths find more usage because of their advantage of being safer to the human eye. About 50-65 times higher power can be transmitted at longer wavelength (1520-1600 nm) compared to 780-850 nm. Quantum cascade lasers and quantum well/quantum dot detectors are used for 10 μm wavelength, although they are not budget friendly [50].

1.2 Advantages of Free Space Optical communication networks

Compared to the conventional radio frequency wireless and wired technologies, the line of sight FSO links offer a number of advantages including:

- Easy Installation. It takes less than 30 minutes to install at normal locations.
- A wide unlicensed frequency spectrum capable of transmitting data in excess of hundreads of Gbit/s using the wavelength division multiplexing scheme.
- Secure communication and immunity to the electromagnetic interference [51, 52].
- A relatively lower power consumption and lower cost as compared to fiber optical networks.
- High transmission bandwidth.
- Long link transmission range up to 10 km.
- Transmission of optical beam is done through air, hence, the information is transmitted with light speed [53, 54].

1.3 Disadvantages of Free Space Optical communication networks

Nonetheless the big number of advantages that this technology presents, FSO links experience substantial optical signal losses due to weather conditions, which severely degrade the link performance and the achievable range. The loss is mainly due to atmospheric absorption, scattering and temperature dependent scintillations. As the medium of the transmission is the air and the light passes through it, some environmental challenges are unavoiadable for FSO systems. Some of these limitations are briefly described below.

- Scintillation can be thought of as changing intensities of light in both space and time at the receiver plane. The received optical signal level at the photodetector varies due to changes in the temperature and the pressure of the propagation medium. It can also be defined as the temperature variation among different air packets due to the heat rising from the earth and the man-made drives like heating ducts. These temperature variations can cause fluctuations in amplitude of the signal which causes image dancing at the FSO receiving end [12, 50, 55].
- Geometric attenuation (which can be called optical beam attenuation) causes light beam to diverge as it moves throughout its propagation path. As a result, not all of the light beam would hit the receiver, and some of the signal would be lost. The geometrical attenuation is a function of the beam divergence, the distance and the receiver capture area.

- Atmospheric turbulence happens due to weather and environment structure. It is caused by wind and convection which mixe the air parcels at different temperatures leading to fluctuations in the density of air. The scale size of turbulence cell can create different type of effects.

- Atmospheric attenuation is the resultant of fog and haze phenomena. It also depends upon dust and rain. Haze is wavelength dependent. Atmospheric attenuation at 1550nm is less than attenuation for other wavelengths in haze weather condition [53].

- The scattering phenomena happens when the optical beam and scatterer collide. It is a wavelength dependent phenomenon. During this phenomenon the directional redistribution of optical energy happens and this leads to the reduction in the intensity of beam for longer distance. The scattering phenomena is divided into three types:
  (a) Rayleigh scattering which is known as molecule scattering and is a result of the interaction of light with particles of size smaller than the wavelength.
  (b) Mie scattering which is known as aerosol[1] scattering and depends strongly on the size of the aerosol compared to the wavelength.
  (c) Non-selective scattering which is known as geometric scattering. [56]

Another element that causes loses in the FSO link includes the physical obstacles like flying birds, trees, and high buildings. These obstacles can temporary block a single beam, but their negative effect can be avoided by chossing the apropiate place to put the transmission channel for the FSO system. Figure 1 illustrates the impact of weather conditions on an FSO link.

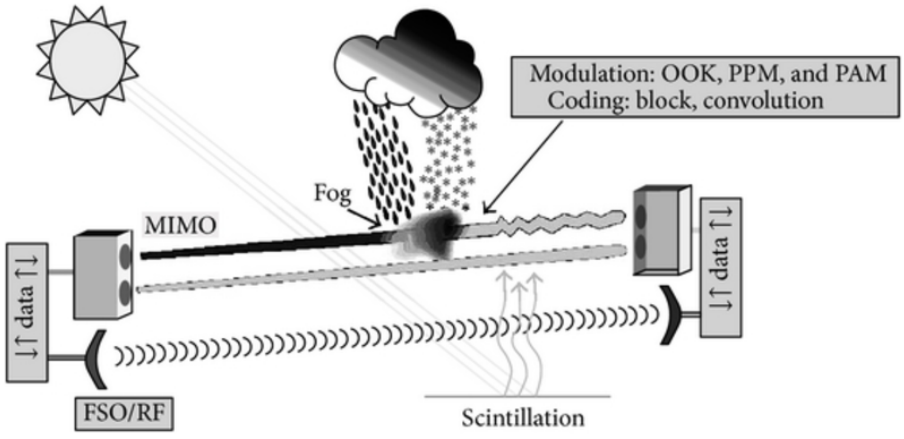

Figure 2.2 – Atmospheric effects on FSO system [12].

In addition, in the real world, the weather effects can be a combination of atmospheric elements like fog, rain, turbulence, smoke, dust, snow, etc. Therefore, carrying out a proper

[1] An aerosol is a suspension of fine solid particles or liquid droplets, in air or another gas. Aerosols can be natural or anthropogenic. Examples of natural aerosols are fog, dust, forest exudates and geyser steam. Examples of anthropogenic aerosols are haze, particulate air pollutants and smoke.

link assessement for specific weather conditions becomes a challenging task. FSO network exhibits capacity loss depending on weather conditions. All this raises the problem of how to represent the weather condition in a mathematical model in order to take into account the network robustness. The question that naturally all of us can have is how to convert these weather conditions into availability link ratio for our network.
All this process goes into different steps and the very first one consists in computing the link margin of the system: the amount of the light recieved by a terminal over and above what is required to keep the link active.

1.4 FSO Network Topologies

Many topology networks are possible for FSO. We can mention here point to point (PTP), star, ring, mesh topology. Each of the topologies offer their advantage depending on the application used. PTP topology is a good choice when we want to have only one path for data communication. Star topology is used on centralized applications. Ring topology provides a close loop with no single point of failure and is not affected by high traffic. This topology is beneficial when we have to ensure continues transmission with no interruption. In a mesh topology, devices are connected with many redundant interconnections between network nodes. Each node is connected to each node. Mesh topology is considered in two categories: partial mesh technology (in this topology only some nodes are connected to the others by following the rule of mesh technology) and full mesh technology. Mesh offers robust communication and easily fault diagnosis.

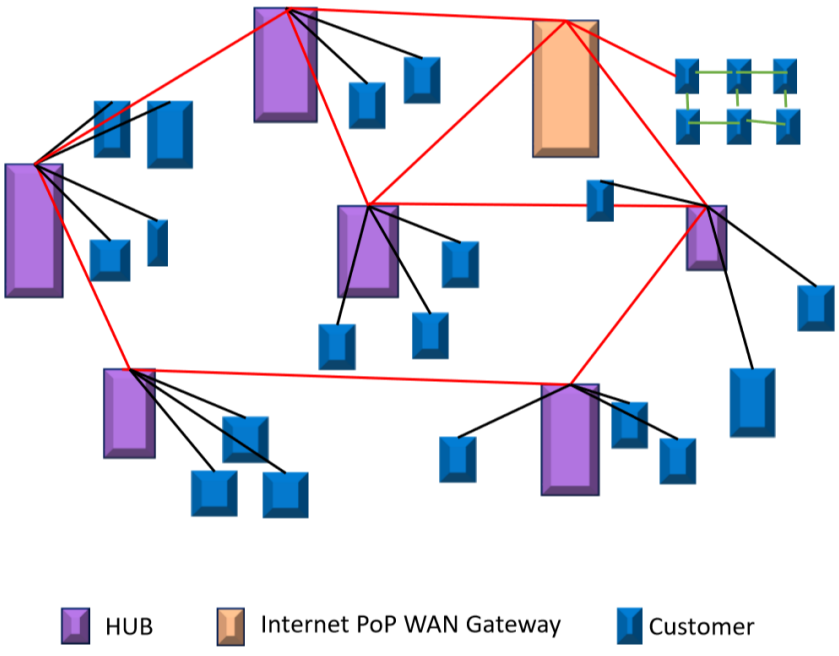

Figure 2.3 – The PTP, star, mesh and ring hybrid topologies for FSO (electronicsforu.com).

Hybrid topologies including ring, mesh, PTP and/or star interconnections for FSO systems are illustrated in Figure 2.3. In ring interconnections, customer nodes can be

ring nodes of more than one ring or one hop away from another ring. At the same time, PTP connections with nodes that do not belong to the ring can exist. On the other hand, in star interconnections, central nodes (hubs) are connected with other central nodes utilizing PTP links. The primary reason of extending the standard network topologies is the increase of reliability and coverage area whilst keeping the associated cost low. The choice of network topology significantly affects the performance, reliability, scalability, design complexity and overall cost of a free-space optics network

2 Link Margin

The link margin of a particular FSO link is a function of the atmospheric conditions, as well as of the distance between the terminals of the link, the power of the transmitter, and the sensitivity of the receiver. Another definition of link margin is to consider it as the extra-power P available at the receiver (measured in W (Watt)), compared to the minimum requirement P_{min} of keeping the link active [12]. This is shown in equation (2.1):

$$M_{Link}[dB] = 10 * log_{10}(\frac{P[W]}{P_{min}[W]}) \tag{2.1}$$

For example, suppose the receiver must receive minimum 2 milliWatts (mW) of power in order to keep the link active. If the transmitter sends out enough power so that the receiver actually receives 4 milliWatts, then the link margin is 3dB.

$$M_{Link}[dB] = 10 * log_{10}(P/P_{min}) = 10 * log_{10}(4/2) = 10 * 0.3 = 3dB$$

This means that up to half the power of the transmitted beam can be attenuated in the atmosphere before the link is down. It is important to understand that the link margin of a particular FSO link is a direct function of the atmospheric conditions as well as the distance between terminals. In order to compute the link margin, the following parameters are required:

- distance between terminals
- emitted power
- receiver sensitivity
- receiver aperture surface
- divergence of the emitted beam

Considering the technical data provided by the manufacturer and the weather conditions for a specific geographical zone, we can compute the link margin in order to obtain the availibility ratio of the links using the following formula [12]:

$$M_{Link} = P_e + |S_r| - Att_{Geo} - Att_{Fog} - Att_{Rain} - Att_{Snow} - P_{Syst} \tag{2.2}$$

where:
M_{Link} is the link margin,
P_e is the emitted power, expressed in decibels per milliWatt (in dBm)[2],
S_r is the receiver sensitivity in decibels per milliWatt (in dBm),
Att_{Geo} is the geometric attenuation (in dB)[3],
Att_{Fog} is the fog attenuation (in dB),
Att_{Rain} is the rain attenuation (in dB),
Att_{Snow} corresponds to the snow attenuation (in dB),
P_{Syst} is the system loss or the equipment loss (in dB) given by the manufacturer (possibly multiplied by 2).

Different studies have been done on different weather conditions in order to design new models based on the effectiveness of the system. The main focuses of these studies are fog, haze, rain and snow weather conditions. The following sections describe in details all components of equation (2.2) that impact the link margin.

2.1 Geometric Attenuation

As we have mentioned before, the geometric attenuation causes the light beam to diverge its propagation path. This results in a reduction of radiation quantity due to the effect only of the distance between the point of interest and the source. Therefore, by increasing receiver aperture surface, more light could be collected by the receiver and geometric loss would reduce. Geometric attenuation can be computed using the equation (2.3) [12, 55]:

$$Att_{Geo} = \frac{\frac{\pi}{4}(L\theta)^2}{S_{receiver}} \tag{2.3}$$

where L is the distance between the transmitter and the receiver (in m), $S_{receiver}$ is the receiver aperture surface (in m^2) and θ is the divergence of the emitted beam (in rad). Generally, θ stands between 1 and 3 mili-rad (mrad) depending on the system. This part of attenuation is not directly dependent on weather conditions, but it is very important when choosing how to build up the FSO link. The geometric attenuation in dB is computed as follows (2.4):

$$Att^*_{Geo}[dB] = 10log_{10}(Att_{Geo}) \tag{2.4}$$

[2]The unit dBm denotes an absolute power level measured in decibels and referenced to 1 milliwatt (mW). To convert from absolute power 'P' (in watts) to dBm, is used the formula $dBm = 10 * log_{10}(P/1mW)$. In most of cases these data are given for each equipment from the manufacturer.

[3]Decibels (dB) are used to express power ratios in a logarithmic way, so that very large and very small powers can be compared using comfortable numbers. A decibel is a dimensionless pseudo-unit because it's defined by the ratio of two powers, but since decibels are so handy, to express true power instead of just a dimensionless ratio, referenced decibels are very often used. Two different scales are used when expressing a ratio in decibels, depending on the nature of the quantities: power and field (root-power). When expressing a power ratio, the number of decibels is ten times its logarithm to base 10.

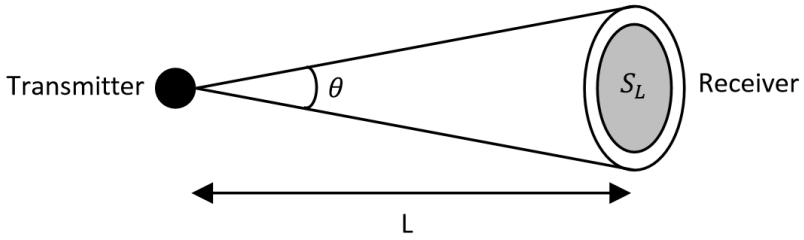

Figure 2.4 – Geometric attenuation due to beam divergence [12].

2.2 Atmospheric attenuation

Outdoor FSO links experience substantial optical signal losses due to adverse weather conditions. In a turbulence channel, the received optical signal level will fluctuate as a result of variation of the aerosols and gas molecules. Atmospheric attenuation is a combination of absorption and diffusion effects caused by aerosols and gas molecules (water vapor, dust, pollution) present in the atmosphere. Absorption is caused by the beams photons colliding with various finely dispersed liquid and solid particles in the air such as water vapor, dust, ice, and organic molecules. The aerosols that have the most absorption potential at infrared wavelengths include water, O2 and CO2. Absorption has the effect of reducing link margin, distance and the availability of the link [57]. The transmitted signal of an FSO system is function of the range and is defined by the Beer-Lambert law (2.5).

$$\tau(L) = e^{-\gamma(\lambda)L} \tag{2.5}$$

where $\tau(L)$ is the transmission coefficient, L is the distance between transmitter and receiver (in km) and $\gamma(\lambda)$ is the total molecular attenuation coefficient.
Molecular attenuation represents absorption and diffusion phenomenon. In the case of fog, it occurs since the water vapors in the air begins to condense into the liquid state and is the most degrading component for optical transmission. In the case of haze, it is traditionally an atmospheric phenomenon in which dust, smoke, and other dry particulates obscure the clarity of the sky. This phenomenon often occurs when dust and smoke particles accumulate in relatively dry air. When weather conditions block the dispersal of smoke and other pollutants they concentrate and form a usually low-hanging layer that impairs visibility and may become a respiratory health threat.
Widely accepted models to evaluate fog attenuation, are the Kim model [56] and the Kruse model [58]. These models are based solely on the wavelength of the signal and on the visibility range which can be estimate empirically:

$$\gamma(\lambda) = \frac{3.91}{V}\left(\frac{\lambda}{550}\right)^{-q} \tag{2.6}$$

where:
$\gamma(\lambda)$ is the molecular attenuation (in dB/km);
V : is the visibility (visual range in km);
λ : is the incident laser beam wavelength (in nm);
q : is the size distribution coefficient of scattering related to the size distribution of the droplets particles which tipically varies from 0.7 to 1.6 corresponding to visibility conditions from poor to excellent.

Thus, atmosphere causes signal degradation and attenuation in an FSO system link in several ways, including absorption, scattering and scintillation. All these effects are varying with time and depend on the current local conditions and weather. Kim's model gives the same results as Kruse's model when the visibility is greater than 6 km. For lower visibilities the Kim's model is more accurate.
Due to the fact that the visibility is an easily obtainable parameter, the value of q depends on the model. For example, the Kim et al. model [56] uses the following values of q:

$$q = \begin{cases} 1.6 & \text{for } V > 50km \\ 1.3 & \text{for } 6km < V \leq 50km \\ 0.16V + 0.34 & \text{for } 1km < V \leq 6km \\ V - 0.5 & \text{for } 0.5km < V \leq 1km \\ 0 & \text{for } V \leq 0.5km \end{cases}$$

Considering the optical depth obtained by the Kim et al. model [56], fog attenuation, expressed in dB can be computed by the following equation:

$$Att_{Fog} = 10log_{10}(\frac{1}{\tau(L)}) \tag{2.7}$$

where $\tau(L)$ is the transmittance[1] of the signal at a distance L (in km) of the transmitter.

2.3 Rain Attenuation

Rain attenuation is due to beam distortion while passing through rain drops. Typical raindrops range from 500 nm to 4000 nm but their size is irregular. During rainfall, the beam will pass through drops of different size, sometimes smaller (FSO system wavelength: 690-1550 nm) sometimes much bigger. Hence, experimental results in [59] demonstrate that rain attenuation is independent from the beam wavelength. Rain attenuation only depends on the rain intensity (precipitation rate) and it is computed as follows (2.8):

$$Att_{Rain} = 1.076R^{0.67} \tag{2.8}$$

where Att_{Rain} is the attenuation of rain in dB/km and R is the rainfall rate (precipitation

[1]Transmittance of signal is the amount of light energy that passes through the sample. For example, there is a signal which transmittance is 80%. That means that 80% of light passes (is transmitted) through the sample and 20% of the light is absorbed from the environment

intensity in mm/h).
If we take a simple example and we have a precipitation of 1.6 mm of rain for a period of 1 hour and the distance between the transmitter and receiver is 2 km (D=2 km), we can calculate the rain attenuation:

Att_{Rain}=1.076(1.6$^{0.67}$)=1.47 dB/km

To obtain the result in dB we have:
$At^*_{Rain} = Att_{Rain} * D$
Att^*_{Rain}=1.47 (dB/km)*2 (km)
Att^*_{Rain}=2.94 dB

2.4 Snow Attenuation

Snowfall intensity (precipitation rate) is a fundamental parameter used to describe snow. Attenuation of snow depends on the wavelength λ nm and the snowfall intensity. It can be computed by the the following equation (2.9):

$$Att_{Snow} = (0.0001023\lambda + 3.7855476)S^{0.72} \tag{2.9}$$

where Att_{Snow} is the specific attenuation due to snow precipitation (in dB/km), λ is the wavelength of the signal and S represents the snowfall rate (precipitation intensity in mm/h) [12]. For example if we have a S=1.6 mm/h for a period of one hour and the distance between the transmitter and receiver is 2 km (D=2 km), we can calculate the snow attenuation for a 1550 nm wavelength signal as follow:
$Att_{Snow} = (0.0001023 * 1550 + 3.7855476) * 1.6^{0.72}$
Att_{Snow}=5.53 dB/Km
To obtain the attenuation in dB we have:
$Att^*_{Snow} = Att_{Snow} * D$
Att^*_{Snow}=5.53 (dB/km)*2(km)
Att^*_{Snow}=11.06 dB

Hence, from the calculations and the evaluation of the attenuation depending on the rainfall and snowfall intensity for an FSO system, we can deduce that snow will be more problematic comparing to rain. This is graphically illustrated below.

Figure 2.5 represents the evolution of the attenuation depending on the rainfall and the snowfall intensity for an FSO system with a wavelength of 690 nm. Notice that the rainfall is classified according to the rate of precipitation: light rain (<2.5mm/h), moderate rain (2.5-10 mm/h), heavy rain (10-50 mm/h) and violent rain (>50 mm/h). In a similar way, snowfall is defined as light snow (when the precipitation rate is <1 mm/h), moderate (1-5 mm/h), and heavy snowfall (> 5 mm/h) [59].
In order to better understand the elements that determine the link margin, we have considered the following example. We take in observation an FSO system with a distance

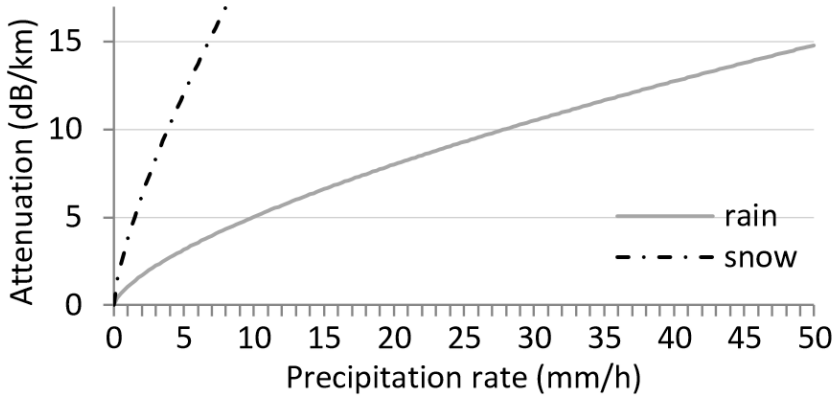

Figure 2.5 – Rain and snow attenuation depending on the precipitation rate for an FSO system [21].

of 7 km between the transmitter and receiver using a wavelength of 1550 nm to transmit the data. Table 1 illustrates the link margin and the modulation scheme applied to this system. We have observed 5 different weather conditions: sunny day, moderate rainfall, heavy rainfall, light snowfall and heavy snowfall.

Table 2.1 – Link margin for 5 typical weather conditions.

	Sunny day	Moderate rain [4 mm/h]	Heavy rain [15 mm/h]	Moderate snow [2.2 mm/h]	Heavy snow [10 mm/h]
Emitted power [dBm]	51	51	51	51	51
Visibility [km]	15	8.7	4.0	3.0	0.2
Receiver sensitivity [dBm]	-38.23	-38.23	-38.23	-38.23	-38.23
Beam divergence [mrad]	2.5	2.5	2.5	2.5	2.5
Aperture surface [m$\hat{2}$]	0.025	0.025	0.025	0.025	0.025
Att_{Geo} [dB]	39.83	39.83	39.83	39.83	39.83
Att_{Fog} [dB]	0.00026	0.00045	0.012	0.059	594.33
Att_{Rain} [dB]	0	19.07	46.22	0	0
Att_{Snow} [dB]	0	0	0	47.10	144.89
System losses [dB]	0	0	0	0	0
Link margin [dB]	16.94	14.82	4.98	3.48	NaN

2.5 Wavelength and modulation schemes for FSO system

2.5.1 Electromagnetic spectrum wavelengths for FSO system

Low-power infrared beams, which do not harm the eyes, are the means by which free-space optics technology transmits data through the air between transceivers, or link heads, mounted on rooftops or behind windows. It works over distances of several hundred meters to a few kilometers, depending upon atmospheric conditions. Unlike most of the lower-frequency portion of the electromagnetic spectrum, the part above 300 GHz (which

includes infrared) is unlicensed worldwide and does not require spectrum fees [54].

In [56] the results of a laboratory-based set-up have shown that the terahertz (THz is a range of the electromagnetic spectrum waves that is founded at the far end of the infrared band, just before microwaves) signal displays significantly lower attenuation due to fog when compared to the FSO link operating at 1550 nm. A real-time measurement of fog-induced attenuation showed that the FIR (far infrared waves that lie in the spectral region between wavelengths of 10 and 2000μm) at 10 μm offers higher transmission range in the presence of fog. Despite the advantages of FSO links, operating them at the THz and FIR wavelength bands can be very costly at the present time, thus, almost all commercially avaiable FSO systems operate in the wavelength range of 600-1550 nm.

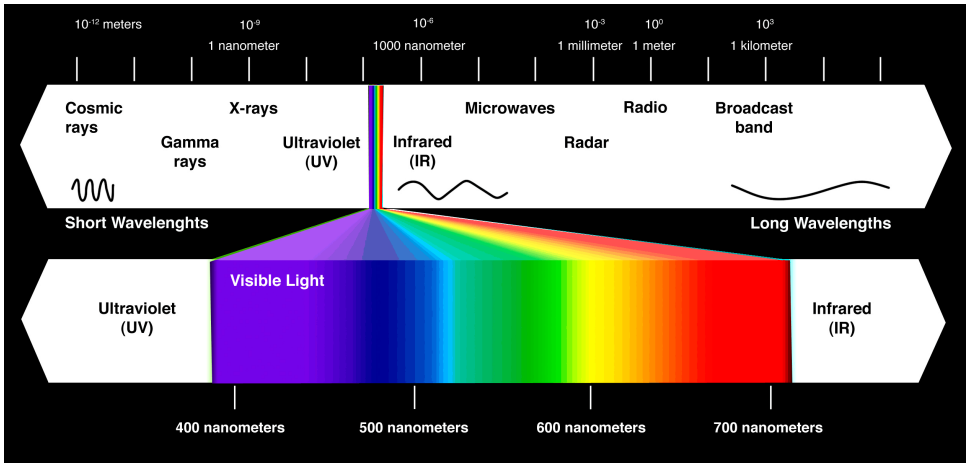

Figure 2.6 – The electromagnetic spectrum with respect to the wavelength with the usual names for the various frequency bands [50].

Given all this, we can ask why would a 1550-nm laser ever be chosen? The advantages offered by this wavelength include a better ocular safety, greater availability of industrial components, the emission of photons at 1.5 μm using semiconductors or rare earth erbium, the possibility of communication systems operating in the continuation of other communication systems based on fibers (and therefore operating at 1.5 μm), and less sensitivity to disturbances induced by the ambient light (sun, different illumination conditions, remote controls, etc.) [12]. Regulations accordingly allow these longer-wavelength beams to operate at higher power than the 850-nm beams, by about two orders of magnitude. That power increase can boost link lengths by a factor of at least five while maintaining adequate signal strength for proper link operation. Alternatively, it can boost data rate considerably over the same length of link. So for high data rates, long distances, poor propagation conditions (like fog), or combinations of those conditions, 1550 nm can become quite attractive [60].

2.5.2 Different modulation schemes for FSO

Bad weather conditions deteriorate the FSO link, and in severe cases the transmission capacity of a link can be lost even entirely. In order to keep the link active, the data

rates of the affected links can be increased by changing the signal modulation scheme, depending on the receiver sensitivity. Yet, the range of such a control is bounded by the equipment limitations.

Modulation is the process by which a carrier wave is able to carry the message or digital signal (series of ones and zeroes). There are three basic methods to this: amplitude, frequency and phase shift keying. Higher orders of modulation allow us to encode more bits per symbol or period (time). Techniques described in this section include amplitude shift keying (ASK), quadrature phase shift keying (QPSK), quadrature amplitude modulation (QAM) and how these techniques can be used to increase the capacity and speed of a wireless network.

2.5.2.1 Amplitude Shift Keying (ASK) in the context of digital communications, is a form of amplitude modulation that represents digital data as variations in the amplitude of a carrier wave. This modulation process relates to a sinusoid two or more discrete amplitude levels. These are related to the number of levels adopted by the digital message. For a binary message sequence there are two levels, one of which is typically zero. In the binary ASK system, the binary symbol 1 is represented by transmitting a fixed-amplitude carrier wave and fixed frequency for a bit duration of T seconds. If the signal value is 1 then the carrier signal will be transmitted; otherwise, a signal value of 0 will be transmitted. Figure 2.7 illustrates a binary ASK signal, together with the binary sequence which initiated it. Neither signal has been bandlimited.

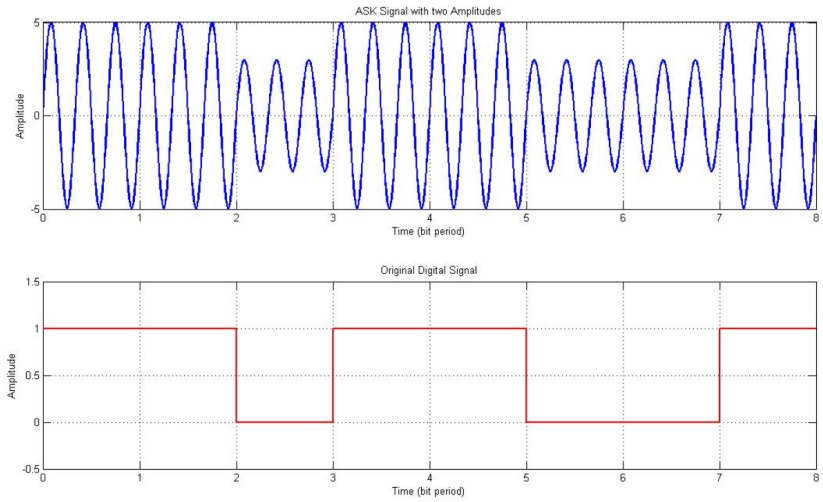

Figure 2.7 – Binary ASK signal (above) and the message (below) [50].

One of the disadvantages of ASK is that it offers lower power efficiency. Also, ASK modulation is very susceptible to noise interference. This is due to the fact that noise affects the amplitude. Hence another alternative modulation technique such as BPSK (binary phase shift keying) which is less susceptible to error than ASK is used.

2.5.2.2 Phase Shift Keying (PSK) is a digital modulation process which conveys data by changing (modulating) the phase of a constant frequency reference signal (the

carrier wave). The modulation is accomplished by varying the sine and cosine inputs at a precise time. It is widely used for wireless LANs, RFID and Bluetooth communication. There are several methods that can be used to accomplish PSK. The simplest PSK technique is called binary phase-shift keying (BPSK). It uses two opposite signal phases (0 and 180 degrees). The digital signal is broken up timewise into individual bits (binary digits). The state of each bit is determined according to the state of the preceding bit. If the phase of the wave does not change, then the signal state stays the same (0 or 1). If the phase of the wave changes by 180 degrees – that is, if the phase reverses – then the signal state changes (from 0 to 1, or from 1 to 0). Because there are two possible wave phases, BPSK is sometimes called biphase modulation. In Figure 2.8 is presented a simple example of BPSK modulation. The first wave shows the normal state and the second wave is shifted by half a period or 180 degrees. The receiver can than recognize this shift indicating either a digital 1 or 0.

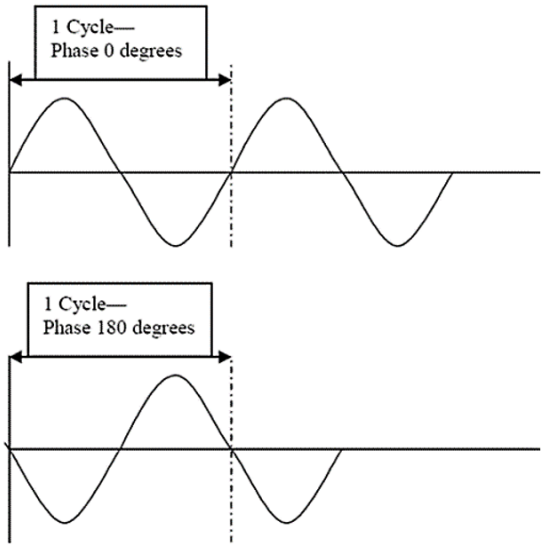

Figure 2.8 – Binary Phase Shift Keying (BPSK) [50].

BPSK is a power efficient modulation technique as less power is needed to transmit the carrier with less number of bits. But, despite this, in BPSK modulation, one bit is carried by one single analog carrier. Hence data rate in bits per second is same as the symbol rate. This is half in comparison to the QPSK modulation technique and many times less compare to other higher modulation techniques such as 16QAM, 64QAM, ect. Due to the above reason, BPSK is not bandwidth efficient modulation technique compared to other modulation types.

An important factor on the selection of modulation technique for FSO systems is the receiver sensitivity as there is always a trade off between the receiver sensitivity and complexity. Though amplitude shift keying (ASK) is the simplest and widely reported, it does not offer immunity to the turbulence induced. Differential phase shift keying (DPSK) with coherent phase diversity system offers better sensitivity in optical fiber systems. However, there is an additional power penalty caused by the frequency offset because of delayed and not delayed bits not being in phase. Further more, there is an extra power

penalty due to the phase noise of the semiconductor lasers sources [13].
Towards of the end of the 1950's there was a big interest in digital phase modulation transmission schemes[2] as an alternative to digital amplitude modulation. It was a natural extension of this trend to consider the simultaneous use of both amplitude and phase modulation. Hence, ASK and PSK can be combined to create QAM where both the phase and amplitude are changed. Many data transmission systems migrate between the different orders of M-QAM(i.e. 4-QAM, 16-QAM, 32-QAM, etc.), dependent upon the link conditions. If there is a good link margin, higher orders of QAM can be used to gain a faster data rate, but if the link margin deteriorates, lower orders are used to preserve the noise margin and ensure that a low bit error rate is preserved.

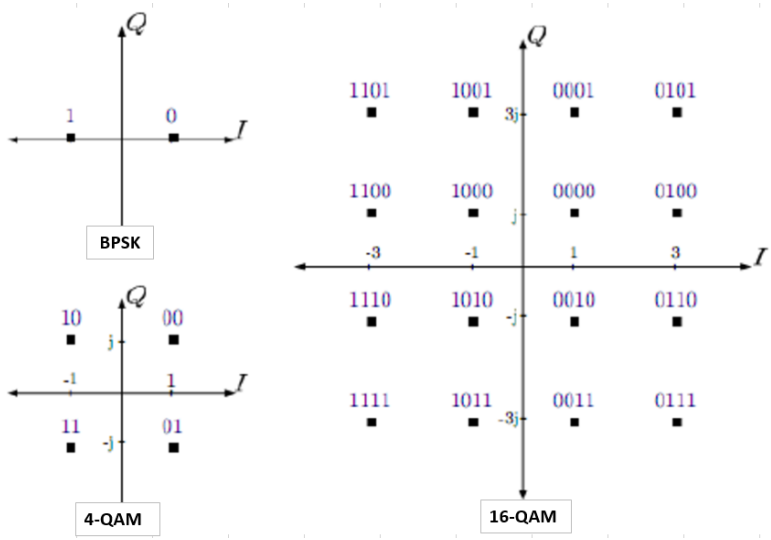

Figure 2.9 – Quadrature Amplitude Modulation (BPSK, 4-QAM and 16-QAM) [50].

The constellation diagrams (Figure 2.9) show the different positions for the states within different forms of QAM. It can be seen from these QAM constellation diagrams, that as the modulation order increases, so the distance between the points on the constellation decreases. Accordingly small amounts of noise can cause greater issues. It is also found that the higher the order of modulation for the QAM signal, the greater the amount of amplitude variation.
The advantage of using QAM is that it is a higher order form of modulation and as a result it is able to carry more bits of information per symbol. By selecting a higher order format of QAM, the data rate of a link can be increased. While higher order modulation rates are able to offer much faster data rates and higher levels of spectral efficiency for the radio communications system, this comes at a price. The higher order modulation schemes are considerably less resilient to noise and interference. As a result of this, many radio communications systems now use dynamic adaptive modulation techniques. They sense the channel conditions and adapt the modulation scheme to obtain the highest data rate for the given conditions. As signal to noise ratios decrease errors will increase along with re-sends of the data, thereby slowing throughput. By reverting to a lower order modulation scheme the link can be made more reliable with fewer data errors and re-sends. Selecting

[2]Digital phase modulation schemes are those whereby the amplitude of the transmitted carrier is held constant but the phase changes in response to the modulation signal.

the right order of QAM modulation for any given situation, and having the ability to dynamically adapt it can enable the optimum throughput to be obtained for the link conditions for that moment. Reducing the order of the QAM modulation enables lower bit error rates to be achieved and this reduces the amount of error correction required. In this way the throughput can be maximised for the prevailing link quality [13], [61] and [62].

Accordingly there is a balance to be made between the data rate and QAM modulation order, power and the acceptable bit error rate. Whilst further error correction can be introduced to mitigate any deterioration in link quality, this will also decrease the data throughput. Different order modulations allow you to send more bits per symbol and thus achieve higher throughput or better spectral efficiency. However, it must also be noted that when using a modulation technique such as 16-QAM, better signal-to-noise ratios (SNRs) are needed to overcome any interference and maintain a certain bit error ratio (BER). The use of adaptive modulation allows a wireless optical system to choose the highest order modulation depending on the channel conditions.

2.6 Converting link margin into availability ratio

The link margin represents the additional amount of attenuation that can be managed without loss of transmission. As presented in (2), the link margin depends on several elements, where we can distinguish two variable parameters: the emitted power P_e and the receiver sensitivity S_r. Hence, increasing power or sensitivity allows for stronger attenuation management, but those increases are limited by the equipment limitation. However, data rates can be increased by changing the signal modulation, which depends on the receiver sensitivity. Kahn [**?**] demonstrates the correlation between M-modulation scheme and S_r. Hence, whatever the modulation, the link margin must be positive to not suffer from total link failure. We consider that in nominal condition (good visibility and no precipitation) we can use the modulation 16-QAM. However, lower visibility will require to decrease the modulation to 4-QAM. If we note $L_m = 10log_{10}(M_{link_i})$ the link margin of link i in dB and $M^*_{link_{max}} = 10log_{10}(M_{link})$ the *maximum* link margin of our system in the best conditions in dB, in general we can do the following correspondence between link margin of an FSO system and the modulation scheme that we apply.

Table 2.2 – Link margin and corresponding modulation schemes.

Link Margin	Modulation scheme	Failure ratio
$L_m > 0.5M^*_{link_{max}}$	16-QAM	0%
$0.25M^*_{link_{max}} < L_m \leq 0.5M^*_{link_{max}}$	4-QAM	50%
$1 < L_m \leq 0.25M^*_{link_{max}}$	BPSK	75%
otherwise	Loss of communication	100%

Table 2.2 shows a general estimation of the channel conditions needed for different modulation schemes. In our considerations we assume four operation modes for each link. The first mode realizes the nominal link capacity (maximal link margin value) and

is applied in good weather conditions using the 16-QAM (failure ratio 0). The second mode corresponds to weather conditions worse than normal when the scheme is switched to 4-QAM. In this case we have lost up to 50% of maximal link margin (failure ratio 0.5). When the weather conditions are even more degraded, the third mode is applied by switching to the BPSK scheme, losing approximately 75% of maximal link margin (failure ratio 0.75). The last case is when the link margin is zero or negative. In this case we have lost the link (failure ratio 1).

If we go back to our example, we will have the following Table 2.3 that shows the modulation scheme for each weather condition that we took in observation.

Table 2.3 – Link margin and modulation scheme.

	Sunny day	Moderate rain [4 mm/h]	Heavy rain [15 mm/h]	Moderate snow [2.2 mm/h]	Heavy snow [10 mm/h]
Link margin [dB]	16.94	14.82	4.98	3.48	NaN
Modulation scheme	16-QAM	16-QAM	4-QAM	BPSK	Loss of communication

If we take in consideration the FSO system in the previous example (table 1), when we have a sunny day and the link margin is equal to 16.94 dB, the modulation scheme we use is the 16-QAM. When the weather conditions change and we have moderate rainfall situation, the link margin goes to 14.82 dB. In this case, we have lost less than 50% of the link margin, that's why we can still use the 16-QAM modulation scheme. If the weather conditions are more degraded, i.e. Heavy rainfall, the link margin is equal to 4.98 dB. The 4-QAM modulation scheme is applied because we have lost more than 50% of our link margin. If we lose more than 75% of the link margin, which is the case of heavy rainfall in our example, the modulation scheme applied is the BPSK (the case of moderate snowfall where the link margin is equal to 3.48 dB). All this is shown in Figure 2.10.

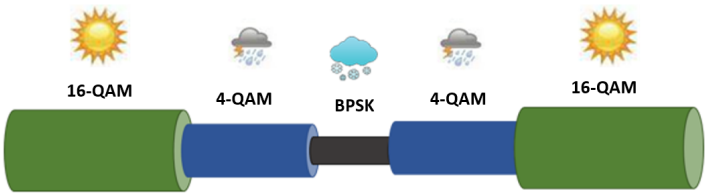

Figure 2.10 – Amplitude Modulation.

The last case is when the link is totaly lost and the link margin has a negative value. This happens in the case of heavy or storm snowfall. In our example, we have a snow precipitation of 10 mm/h and the visibility is les than 0.2 km. The value of link margin for this case is -689.83 dB and we can not transmit any data from the transmitter to the receiver.

Based on this information and [12], we have developed a method which computes, for a given meteorological state, a given transmission range and given characteristics of the FSO equipment, the modulation scheme that can be applied. This is shown in Figure 2.11.

Figure 2.11 – General scheme.

2.7 Applications, safety and confidentiality of Free Space Optical communication networks

2.7.1 Applications of Free Space Optical communication networks

Until recently, the technology was used primarily for internal company connectivity. It shows up mainly in local-area networks spanning multiple buildings, where right-of-way was an obstacle to leasing copper lines or fiber-optic cabling. Over the last decade, however, free-space optics has started to move into more mainstream service. Several free space optics companies have begun field trials with telecommunications carriers in the United States, Europe, Asia, South America, and the Middle East. But today the applications of free-space optics are many and varied. To cite just a few:

- Telecommunication and computer networking.
- Point-to-point links.
- Temporary network installation for events or purpose as disaster recovery.
- For communications between spacecraft, including elements of satellite constellation.
- Security applications.
- Military applications (making use of its potential for low electromagnetic emanation when transferring sensitive data for air forces).
- Metro network extensions: carriers can deploy FSO to extend existing metropolitan area fiber rings, to connect new networks, and, in their core infrastructure, to complete SONET rings.
- Enterprise connectivity: the ease with which FSO links can be installed makes them a natural for interconnecting local area network segments that are housed in buildings separated by public streets or other right of-way property.
- Fiber backup: FSO may also be deployed in redundant links to backup fiber in place of a second fiber link.
- Back haul: FSO can be used to carry cellular telephone traffic from antenna towers back to facilities wired into the public switched telephone network.

- Service acceleration: FSO can be also used to provide instant service to fiber-optic customers while their fiber infrastructure is being laid.
- Last-Mile access: In today's cities, more than 95% of the buildings do not have access to the fiber optic infrastructure due to the development of communication systems after the metropolitan areas. FSO technology seems a promising solution to the connection of end users to the service providers or to other existing networks. Moreover, FSO provides high speed connection up to Gbps, which is far more beyond the alternative systems [12, 54].

2.7.2 Safety of FSO

Any laser can present dangers to man, both at an ocular level and a cutaneous level. In this section, we do not mention the cutaneous effects, because the energy levels of FSO equipment do not present a significant risk for the skin. However, the human eye is very sensitive to infrared radiation. The important factors to take into account in order to evaluate the risks are: the signal wavelength, the powers encountered, and the beam form [12].
The majority of the available products are classified as 1 or 1M (see IEC825/EN60825 standards): instructions must accompany the equipment and contain instructions for safe use. It should be noted that the future availability of a standard, specific to free-space digital transmission optical apparatus (IN 60825-12), will allow us to better define and comprehend safety concepts in relation to the use and the environment.

2.7.3 Confidentiality of FSO

The majority of manufacturers use a "one-off" type amplitude modulation for data transmission by laser, the transmission protocol is generally transparent, but the possibility of "hacking" information is limited. Apart from any direct action on the equipment or its accesses, there are only two ways for a person with important technical skills and complex interventions criteria "to recover" the transmitted data.
Information hacking is only possible under the following conditions:

- use of the same FSO equipment, from the same manufacturer, to collect and to decode data.
- intercept a part of the beam for data "collecting" (this is, however, very directional), and "recover" sufficient energy to process them.
- finally, the last difficulty consists of knowing the transmitted protocol, in order to interpret the collected data.

The confidentiality of communication between two communicators is assured if a third person or an unspecified detector cannot collect exchanged information. To achieve this, one can either code information, i.e. use cryptography, or use material techniques to prohibit the information beam from going to specific places.

An optimization model for robust FSO network dimensioning

Introduction

As we described in Chapter 2, FSO is a well established wireless optical transmission technology considered as an alternative to radio communications for example in metropolitan wireless mesh networks. An FSO link is established by means of a laser beam connecting the transmitter and the receiver placed in the line of sight. In these conditions, as explained in the previous chapter, a major disadvantage of FSO links (with respect to fiber links) is their sensitivity to weather conditions such as fog, rain and snow, causing substantial loss of the transmission power over the optical channel due mostly to absorption and scattering. Thus, although the FSO technology allows for fast and low-cost deployment of broadband networks, its operation will be affected by this sensitivity, manifested by substantial losses in links' transmission capacity with respect to the nominal capacity. Therefore, a proper approach to FSO network dimensioning should take such losses into account so that the level of carried traffic is satisfactory under all observed weather conditions. In this chapter we describe such an approach. We introduce a relevant dimensioning problem and present a robust optimization algorithm for such enhanced dimensioning.

1 Problem definition and literature review

The considerations of this chapter are devoted to dimensioning communication networks resilient with respect to multiple partial link degradation. As mentioned above, a big disadvantage of this technology is the vulnerability of the FSO links to weather conditions. This makes the problem of network dimensioning important, and difficult. Typically, a given weather condition affects a subset of the network links and each affected link looses a portion of its nominal capacity. We call such a fraction the link degradation (failure) ratio that can assume some value between 0 (no capacity loss) and 1 (total capacity loss). This discussion motivates the network optimization problem studied in this thesis: how to dimension the network links at the lowest cost and at the same time assure the traffic demand satisfaction at an acceptable level for all observed/predicted weather conditions.

As we will demonstrate, we can make use of robust optimization methods to deal with this problem [4].

The impact of weather conditions on the wireless networks transmission capacity has been studied, and the majority of works have considered failure modeling for a single region failure. In particular, paper [19] discusses three measures of the WMN survivability for a regional failure scenario assuming circular failure areas with random location of failure epicenters. As observed in [19], from the network topology viewpoint, networks with nodes covering a square area in a regular way have a better performance in terms of the total traffic surviving a regional failure. It is also shown that in the case of heavy rain storms, using information on foretasted attenuation of links based on radar measurements allows for periodic updates of the network topology in advance, and thus dealing efficiently with these phenomena. In [20], a mixed-integer programming (MIP) model for network reconfiguration in case of unfavorable weather conditions is presented. The model looks for alternative routes for rerouting some of the disturbed traffic, while reducing the interference between adjacent transmission links. Other studies, such as [12, 21], have considered the relevance and impact of specific weather factors on the FSO links capacity.

As already mentioned, this chapter introduces an optimization model for robust dimensioning of FSO networks in order to achieve resilience with respect to multiple partial link failures. Similar problems have been widely investigated in the literature but for a given list of failure states, see for instance [6] and the list of literature therein. More recently, robust optimization approaches to resilient network dimensioning have been developed in [30, 31, 32] (under traffic demand uncertainty), and in [33] (under signal propagation uncertainty in wireless networks). As majority of work on traffic restoration and resilient network dimensioning has been done for wired networks, multiple partial link failures are virtually not considered despite common appearance of this phenomenon in modern wireless networks that cope with it by means of adjustable modulation and coding schemes (MCS). Multiple partial link failures were addressed in [6] (for the so called Unrestricted Reconfiguration mechanism, commonly called Global Rerouting [34]), and more recently in [35] (for the so called oblivious routing) and in [36] (see below). An optimization approach, based on disjoint path routing, to FSO networks with multiple partial failures is presented in [37].

Paper [36], along with [38], are the starting point for this work. In those two papers the authors have studied a specific traffic protection mechanism, called *Flow Thinning* (FT). The main feature of FT is handling partial failures without any traffic rerouting at all. In FT, each traffic demand is equipped with a set of dedicated routing paths whose flows are thinned accordingly to the current availability of network link capacity (for more details on FT see [36]).

2 Modeling of link availability states

We mentioned that in this thesis we deal with multiple partial degradation of FSO links caused by weather conditions. Hence, we start with a short study of the impact of meteorological phenomena on the transmission capacity of the affected links in order

to build a representative set of failure states corresponding to a recorded list of weather conditions. The particular goal of this part is to describe a convex set of failure states which covers a large part of the failures that could be induced by a given (historic) weather data set. The constructed set will be used as the reference uncertainty set in the robust optimization approach presented below.

Just like radio technology, FSO suffers from the sensitivity of the links transmission capacity to weather conditions. To investigate this issue, our first goal was to estimate link failure degradation ratio (i.e., the fraction of the nominal capacity lost achievable during good weather) in degraded weather conditions. The way we do this is explained in Chapter 2. In case of bad weather conditions, the data transmission quality may be severely affected if no special action is undertaken. A solution is to control the current signal modulation and coding scheme (MCS) applied at the transmitter of the affected FSO link to secure correct data transmission. This, however, results in decreasing effective transmission data rates.

In our considerations we assume four operation modes for each link. The first (basic) mode realizes the nominal link capacity, and is applied in normal (good) weather conditions using the 16-QAM (quadrature-amplitude modulation, see [63]) MCS. The second mode corresponds to weather conditions worse than normal when the scheme is switched to 4-QAM – this assures approximately 50% of the nominal link capacity (degradation ratio 0.5). When the weather conditions are even more degraded, the third mode is applied by switching to the BPSK scheme (binary phase-shift keying, see [64]) scheme, losing approximately 75% of the nominal link capacity (degradation ratio 0.75). The last mode corresponds to harsh weather conditions that make correct data transmission impossible (degradation ratio 1). By using appropriate formula (for more details about link margins and weather data impact, the reader is referred to Chapter 2, Section 2) we can calculate what is the maximum capacity attained in good weather conditions, and the reduction in capacity caused by change of the signal modulation scheme for each weather state.

In order to consider link capacity degradation in optimization modeling, we need to estimate the link failure ratios for various weather conditions that can occur during the network lifetime. Having distinguished the four operation modes, we can determine what is the proper operation mode for each FSO link in a given weather state (note that in general different links see different weather conditions in a given weather state). To do this we apply the formulae given in [65] and deduce the vector of the link failure ratios for each of the considered weather states. The set of all such (different) vectors constitutes the *reference failure set* denoted by $\mathcal{S}$. In our state modeling methodology we analyse the weather records observed over a time period, typically over one year. For each hourly period (out of $365 \times 24 = 8760$ periods) we translate the observed weather conditions into the link failure ratios – in effect each of the hourly period is assigned its link failure ratio vector. That is, when at a given hourly period some geographical area is affected by bad weather, the corresponding (link availability) state is characterized by assigning appropriate failure ratios to the links in this area, for example the ratios equal to 0.5 or 0.75, depending on the degree of degradation the affected links experience. Next, we identify the subset of periods with different link failure ratio vectors to form the so called reference failure set (denoted with $\mathcal{S}$ below). The so formed reference failure sets are used in the numerical study presented in Chapter 4.

In this chapter we also consider a special kind of virtual failure sets, called K-sets (see Section 4.3), parameterized by an integer value K, where K is less than or equal to the number of all links in the network. For a given K, the K-set contains all states corresponding to all combinations of K, or less, simultaneously affected links. It is additionally assumed that when a link is affected, it is always affected with the same failure ratio. For example, the set of single link failure states frequently considered in the literature is a specific case of K-set, where $K = 1$ and the link failure ratio is set to 1 for all links. In our optimization approach the K-sets are used as an approximation of the reference failure set $\mathcal{S}$. The approach consists in using K-sets (for a set of selected values of parameter K) as an input (instead of the true reference failure set) to the robust network dimensioning problem formulated in Section 3, and then testing the so obtained optimal link capacities (called the robust solution) on the true reference failure state. Clearly, the larger the K value, the more severe failure states the K-set contains, resulting in general in more robust (and at the same time likely more costly) solutions.

3 Problem formulation

3.1 Notation

The considered network is modeled using a directed graph $\mathcal{G} = (\mathcal{V}, \mathcal{E})$ composed of the set of nodes $\mathcal{V}$ and the set of links $\mathcal{E}$. In the sequel the number of nodes $|\mathcal{V}|$ and the number of links $|\mathcal{E}|$ will be denoted by V and E, respectively. Each link $e \in \mathcal{E}$ represents an arc, i.e., an ordered pair (v, w) of nodes for some $v, w \in \mathcal{V}, v \neq w$. If $e = (v, w)$ then $a(e) := v$ and $b(e) := w$ denote the origin and destination of arc $e \in \mathcal{E}$, respectively. Furthermore, we define $\delta^+(v) := \{e \in \mathcal{E} : a(e) = v\}$ (the set of links outgoing from node v) and $\delta^-(v) := \{e \in \mathcal{E} : b(e) = v\}$ (the set of links incoming to node v). To each link $e \in \mathcal{E}$ there corresponds a non-negative unit capacity cost $\xi(e)$ (a parameter), and capacity denoted by y_e (when link capacity is an optimization variable) or $c(e)$ (when capacity is fixed). The total cost of the network is thus given by $\sum_{e\in\mathcal{E}} \xi(e)y_e$ or $\sum_{e\in\mathcal{E}} \xi(e)c(e)$ (where $y := (y_e,\ e \in \mathcal{E})$, $c := (c(e),\ e \in \mathcal{E})$).

Traffic demands are represented by the set $\mathcal{D}$ (the number of demands $|\mathcal{D}|$ will be denoted by D). Each demand $d \in \mathcal{D}$ is represented by an ordered pair of nodes $(o(d), t(d))$ (its origin and termination) and the volume $h(d)$ (a parameter) of the traffic that has to be realized form $o(d)$ to $t(d)$. The demand volumes and link capacities are expressed in the same units.

The set of network links is subject to multiple partial failures where each failing link e loses a portion $\beta(e)$ (where $0 < \beta(e) < 1$ is a given parameter called failure ratio) of its nominal capacity $c(e)$. Consequently, each failure state $s \in \mathcal{S}$, where $\mathcal{S}$ denotes the set of failure states (the number of states $|\mathcal{S}|$ will be denoted by S), is identified with a binary vector $s = (s(e),\ e \in \mathcal{E})$ of failure coefficients interpreted as follows: the available capacity of link $e \in \mathcal{E}$ in state s is equal to $(1 - \beta(e)s(e))c(e)$. Below we assume that the set of states $\mathcal{S}$ is composed of all states s with $\sum_{e\in\mathcal{E}} s(e) \leq K$ for a given fixed integer

parameter K ($1 \leq K \leq E$). Note that the number of states in S grows exponentially with the number of links E.

Finally, we assume that in each failure state $s \in \mathcal{S}$ each demand $d \in \mathcal{D}$ can be routed in a bifurcated way along all possible paths from $o(d)$ to $t(d)$, and the resulting traffic flows in particular states are independent of each other. This means that the network applies the so called *Global Rerouting* or *Unrestricted Reconfiguration* mechanism [6, 34].

The problem considered is formulated in the node-link notation (using the link-flows variables x and capacity variables y) as follows:

Problem P($\mathcal{S}$) (main):

$$C(\mathcal{S}) = \min \sum_{e \in \mathcal{E}} \xi(e) y_e \tag{3.1a}$$

$$\sum_{e \in \delta^+(v)} x^s_{ed} - \sum_{e \in \delta^-(v)} x^s_{ed} = \begin{cases} h(d) & \text{if } v = o(d) \\ -h(d) & \text{if } v = t(d) \\ 0 & \text{otherwise,} \end{cases}$$

$$d \in \mathcal{D}, v \in \mathcal{V}, s \in \mathcal{S} \tag{3.1b}$$

$$\sum_{d \in \mathcal{D}} x^s_{ed} \leq (1 - \beta(e)s(e)) y_e, \quad e \in \mathcal{E},\ s \in \mathcal{S} \tag{3.1c}$$

$$x, y \geq 0 \text{ and continuous.} \tag{3.1d}$$

Above, x^s_{ed} is the flow on link e dedicated to carry the traffic of demand d in state s. The objective of P($\mathcal{S}$), i.e., minimizing the cost of links, is specified in (3.1a). Constraint (3.1b) represents the flow conservation equation for each demand d at each node v in each state s, assuring the realization of $h(d)$ for all d in each state s. Finally, the capacity constraint (3.1c) ensures that the capacity of link e is not exceeded in any state s.

In the present study we focus on specific features of the FSO networks such as full-duplex links. This means that a link represents a set of parallel FSO transmission systems. If not stated explicitly otherwise, the systems are assumed to be full duplex, so that a system between node v and node w is composed of two pairs of transceivers. One such pair provides transmission over a light beam from v to w, and the other over a light beam from w to v. Each such light beam carries the data with a given nominal bit-rate of M Gbps, which is typically of the order of 1–20 Gbps [3, 66]. The quantity M is called *link capacity module*. All these, brings the necessity to do some modifications in our notations and the main problem 3.1.

Instead of a directed graph, now we consider a network that is modeled by means of a bi-directed graph $\mathcal{G} = (\mathcal{V}, \mathcal{A}, \mathcal{E})$ composed of the set of nodes $\mathcal{V}$, the set of (directed) arcs $\mathcal{A} \subseteq \mathcal{V}^2 \setminus \{(v, v) : v \in \mathcal{V}\}$, and the set of (bi-directed) links $\mathcal{E} \subseteq \mathcal{V}^{|2|}$ (where $\mathcal{V}^{|2|}$ denotes the family of all 2-element subsets of the set of nodes $\mathcal{V}$). Since the graph is bi-directed, each arc $a = (v, w) \in \mathcal{A}$ has its oppositely directed counterpart $a' = (w, v) \in \mathcal{A}$. For a given arc $a = (v, w)$, its originating node v will be denoted by $o(a)$ and its terminating

node by $t(a)$, i.e., $o(a) = v$ and $t(a) = w$. Furthermore, for each node $v \in \mathcal{V}$ we define $\delta^+(v) := \{a \in \mathcal{A} : o(a) = v\}$ (the set of arcs outgoing from node v) and $\delta^-(v) := \{a \in \mathcal{A} : t(a) = v\}$ (the set of links incoming to node v). In the sequel, the number of nodes $|\mathcal{V}|$ and the number of arcs $|\mathcal{A}|$ will be denoted by V and A, respectively.

To each pair of two oppositely directed arcs $a = (v, w), a' = (w, v)$ there corresponds a bi-directed link $e = \{v, w\} \in \mathcal{E}$ denoted by $e(a)$ (or $e(a')$). Thus, the set of links is defined as $\mathcal{E} := \{e(a) : a \in \mathcal{A}\}$. The two oppositely directed arcs corresponding to link e will be denoted by $a(e)$ and $a'(e)$, hence for $e = \{v, w\}$, $a(e) = (v, w)$ and $a'(e) = (w, v)$. Clearly, the number of links $E = |\mathcal{E}|$ is two times less than the number of arcs: $A = 2E$.

Capacity of links is modular and each module provides the bit-rate of M Gbps separately for each of the two oppositely directed arcs related to the link – this assumption corresponds to full duplex transmission. The capacity of a link is composed of several modules. When the link capacity is optimized, the number of modules installed on link $e \in \mathcal{E}$ is denoted by y_e. Thus, y_e is a non-negative integer variable whose value specifies the link capacity equal to My_e. When the link capacity is fixed, it is denoted by $c(e)$, where $c(e) = Mn(e)$ for some fixed non-negative integer $n(e)$. As a consequence, each of the two oppositely directed arcs of link e has capacity My_e or $Mn(e)$. To each link $e \in \mathcal{E}$ there corresponds a non-negative module cost $\xi(e)$ (a parameter). Hence, the total cost of the network is given by $\sum_{e\in\mathcal{E}} \xi(e)y_e$ or $\sum_{e\in\mathcal{E}} \xi(e)n(e)$. In the sequel, notation $y := (y_e,\, e \in \mathcal{E})$ and $c := (c(e),\, e \in \mathcal{E})$ will be used.

As mentioned above, the set of network links is subject to multiple partial failures (link degradations). A particular configuration of such degradations is referred to a network degradation state, and the set of degradation states is denoted $\mathcal{S}$ (the number of states $|\mathcal{S}|$ is denoted by S). When a link is degraded then it loses a fraction of its capacity specified by a degradation ratio (between 0 and 1) from a given set of possible degradations ratios $\mathcal{R}$, for example $\mathcal{R} = \{0, 0.5, 0.75, 1\}$. In consequence, each degradation state $s \in \mathcal{S}$ can be identified with a vector of the link degradation ratios $\beta(s) = (\beta(e, s),\, e \in \mathcal{E})$, where $\beta(e, s) \in \mathcal{R}$ is the fraction of capacity lost on link e in state s. Thus, in state $s \in \mathcal{S}$ the available capacity of link $e \in \mathcal{E}$ is equal to $\big(1 - \beta(e, s)\big)My_e$ (or $\big(1 - \beta(e, s)\big)c(e)$).

3.2 Problem formulation

Note that in this thesis we use the following convention for vector notation. When a represents a vector of given parameters, then $a = (a(1), a(2), \ldots, a(n))$ (so that a denotes an n-element vector, and $a(i)$ is one of its elements). Yet, when a denotes a vector of variables, then $a = (a_1, a_2, \ldots, a_n)$. Alternatively, when the set of indices is represented by $\mathcal{N}$ (i.e., $\mathcal{N} = \{1, 2, \ldots, n\}$), then we write $a = (a(i),\, i \in \mathcal{N})$ or $a = (a_i,\, i \in \mathcal{N})$, respectively.

The formulation of the the optimization problem in question is as follows:

Problem P($\mathcal{S}$) (main problem in node-arc formulation):

$$C(\mathcal{S}) = \min \sum_{e\in\mathcal{E}} \xi(e) y_e \tag{3.2a}$$

$$\sum_{a\in\delta^+(v)} x^s_{ad} - \sum_{a\in\delta^-(v)} x^s_{ad} = \begin{cases} h(d) & \text{if } v = o(d) \\ -h(d) & \text{if } v = t(d), \\ 0 & \text{otherwise} \end{cases} \quad d \in \mathcal{D}, v \in \mathcal{V}, s \in \mathcal{S} \tag{3.2b}$$

$$\sum_{d\in\mathcal{D}} x^s_{ad} \le \big(1 - \beta(e(a), s)\big) M y_{e(a)}, \quad a \in \mathcal{A},\ s \in \mathcal{S} \tag{3.2c}$$

$$x \ge 0 \text{ and continuous; } y \ge 0 \text{ and integer.} \tag{3.2d}$$

We explained above that, x^s_{ad} is the flow on arc a dedicated to carry the traffic of demand d in state s. The objective of P($\mathcal{S}$), i.e., minimizing the cost of links, is specified in (3.2a). Constraint (3.2b) represents the flow conservation equation for each demand d at each node v in each state s, assuring the realization of $h(d)$ for all d in each state s. Finally, the capacity constraint (3.2c) ensures that the capacity of link e is not exceeded in any state s.

Because of modular links, problem P($\mathcal{S}$) is $\mathcal{NP}$-hard even for a polynomial number of states in set $\mathcal{S}$ (see [6]). Moreover, the direct approach to P($\mathcal{S}$) requires solving linear programs involving a large number of arc-flow variables x (linear relaxations of (3.2) assuming continuous y) during the branch-and-bound process performed by the MIP solver. For this reason, we have developed a more efficient approach to P($\mathcal{S}$). The approach, based on Benders' decomposition [8], is presented next.

4 Solving P($\mathcal{S}$) by cut generation

4.1 Feasibility testing

Let $\mathcal{Y}$ denote the set of all capacity vectors feasible for (3.2) and suppose we wish to test whether a given capacity vector $c = (c(e),\ e \in \mathcal{E})$ is in $\mathcal{Y}$. Because the demand routing in a particular degradation state is independent of the demand routing in the remaining states, we can perform the *feasibility test* in question by checking the feasibility separately for each state by means of the following linear program:

Problem F(c,s) (feasibility of c in state s):

$$O(c,s) = \min \textstyle\sum_{e\in\mathcal{E}} z_e \tag{3.3a}$$

$$[\lambda_d^v] \quad \textstyle\sum_{a\in\delta^+(v)} x_{ad} - \sum_{a\in\delta^-(v)} x_{ad} = \begin{cases} h(d) & \text{if } v = o(d) \\ -h(d) & \text{if } v = t(d), \\ 0 & \text{otherwise} \end{cases} \quad d\in\mathcal{D}, v\in\mathcal{V} \tag{3.3b}$$

$$[\pi_a \geq 0] \quad \textstyle\sum_{d\in\mathcal{D}} x_{ad} \leq \big(1-\beta(e(a),s)\big)c(e(a)) + z_{e(a)}, \quad a\in\mathcal{A} \tag{3.3c}$$

$$x, z \geq 0 \text{ and continuous,} \tag{3.3d}$$

where $O(c,s)$ expresses the minimum of the sum of links' overloads measured by the components of the vector $z := (z_e,\ e\in\mathcal{E})$. The test is valid since c is feasible for s if, and only if, $O(c,s) = 0$. If the result of the test is negative (i.e., $O(c,s) > 0$) we need to find an inequality that separates c from $\mathcal{Y}$. This can be done by considering the dual to (3.3) (whose variables $\lambda := (\lambda_d^v,\ v\in\mathcal{V}, d\in\mathcal{D})$ and $\pi := (\pi_a,\ a\in\mathcal{A})$ correspond to the primal constraints (3.3b) and (3.3c), respectively):

Problem D(c,s) (dual to F(c,s)):

$$W(c,s) = \max\Big\{ \textstyle\sum_{d\in\mathcal{D}} \lambda_d^{t(d)} h(d) - \sum_{e\in\mathcal{E}} (\pi_{a(e)} + \pi_{a'(e)})\big(1-\beta(e,s)\big)c(e) \Big\} \tag{3.4a}$$

$$\pi_{a(e)} + \pi_{a'(e)} \leq 1,\ e\in\mathcal{E}; \qquad \lambda_d^{o(d)} = 0,\ d\in\mathcal{D} \tag{3.4b}$$

$$\lambda_d^{t(a)} - \lambda_d^{o(a)} \leq \pi_a, \quad a\in\mathcal{A}, d\in\mathcal{D} \tag{3.4c}$$

$$\pi \geq 0 \text{ and continuous, } \lambda \text{ continuous.} \tag{3.4d}$$

Let λ^*, π^* be an optimal solution of problem D(c,s). Since $W(c,s) = O(c,s)$ (where $O(c,s)$ is defined by (3.3a)), the inequality that separates c from $\mathcal{Y}$ (provided $W(c,s) > 0$) is as follows:

$$\textstyle\sum_{e\in\mathcal{E}} (\pi^*_{a(e)} + \pi^*_{a'(e)})\big(1-\beta(e,s)\big)My_e \geq \sum_{d\in\mathcal{D}} \lambda_d^{t(d)^*} h(d). \tag{3.5}$$

Since $\sum_{e\in\mathcal{E}} (\pi^*_{a(e)} + \pi^*_{a'(e)})\big(1-\beta(e,s)\big)c(e) = \sum_{d\in\mathcal{D}} \lambda_d^{t(d)^*} h(d) - W(c,s)$ (and $W(c,s) > 0$), $My = c$ does not fulfil (3.5).

Note that to make sure that $c\in\mathcal{Y}$, we in general need to perform the feasibility test (3.4) individually for all states s in $\mathcal{S}$.

4.2 A cut generation algorithm for a given explicit list of states $\mathcal{S}$

The iterative algorithm for solving problem (3.2) for an arbitrary (but given) explicit list of states $\mathcal{S}$ is presented below. It results from application of the classical Bender's decomposition method [8] to P$(\mathcal{S})$ (this particular application can be found in [6]). In each iteration the master problem involving only the capacity variables y is solved and

then its optimal solution y^* is tested for feasibility with respect to P(S). If the test is positive, the algorithm is stopped and y^* is optimal for (3.2). If not, new inequalities deduced from the feasibility tests are added to the master problem and the algorithm is reiterated. (Below, the notation $y \in \Omega$ means that y fulfills all inequalities in the set of inequalities Ω.)

Algorithm 1: cut generation algorithm for an explicit list of states $\mathcal{S}$

Step 0: $\Omega := \{y \geq 0\}$.

Step 1: Solve the master problem:

$$\text{minimize} \quad \sum_{e\in\mathcal{E}} \xi(e) y_e \tag{3.6a}$$

$$\text{subject to} \quad y \in \Omega \quad \text{and integer}, \tag{3.6b}$$

and put $c = (My^*_e, e \in \mathcal{E})$.

Step 2: For each $s \in \mathcal{S}$ solve the feasibility test (3.4) and if $W(c, s) > 0$, then add inequality (3.5) to Ω.

Step 3: If no inequalities have been added to Ω in Step 2, then stop (c is the capacity vector optimal for problem (3.2)). Otherwise go to Step 1.

To solve a given instance of problem P($\mathcal{S}$) we use a modified (two-phase) version of the above algorithm. First, in Phase 1, we apply Algorithm 1 to the linear relaxation of P($\mathcal{S}$), i.e., we assume continuous instead of integer y in (3.6b) which makes the master problem (3.6) a linear program. When Phase 1 is completed, we start Phase 2: we bring back the integrality requirement on y to (3.6b) in the master problem and continue.

4.3 Feasibility testing for K-sets

It is important to observe that Algorithm 1 can become ineffective when the set $\mathcal{S}$ contains a large number of states, as this leads to an excessive number of feasibility tests to be performed in each iteration. A way to deal with issue is proposed below.

Let us consider a special case of the family of state sets denoted by $\mathcal{F}$. A set $\mathcal{S}$ belongs to $\mathcal{F}$ when each link $e \in \mathcal{E}$ is degraded (if at all) with the same degradation rate $\beta(e)$, in all states s in $\mathcal{S}$: $\beta(e, s) \in \{\beta(e), 0\}$, $s \in \mathcal{S}$. A particular example of such a set is the state set $\mathcal{S}(K)$ determined by the so called *K-set*. A K-set, denoted with $\mathcal{U}(K)$, is defined, for any integer $K = 1, 2, \ldots, E$, as the set of binary vectors $\mathcal{U}(K) := \{u = (u(e), e \in \mathcal{E}) : \sum_{e\in\mathcal{E}} u(e) \leq K, u(e) \in \{0, 1\}, e \in \mathcal{E}\}$. Each $u \in \mathcal{U}(K)$ determines a state $s(u) \in \mathcal{S}(K)$ by putting $\beta(e, s(u)) := \beta(e)u(e)$, $e \in \mathcal{E}$. Thus, the support of u determines the set of links failing in $s(u)$, wherein each such link fails with ratio $\beta(e)$. Note that from the viewpoint of problem P($\mathcal{S}$) formulated in (3.2), every set S in $\mathcal{F}$ is dominated by the set $\mathcal{S}(K)$ induced by the K-set with $K = \max\{|supp(\beta(s))| : s \in \mathcal{S}\}$, where

$|supp(\beta(s))|$ denotes the number of non-zero elements in the failure ratio vector $\beta(s)$. The domination in question means that each feasible solution of $\mathrm{P}(\mathcal{S}(K))$ is feasible for $\mathrm{P}(\mathcal{S})$. Thus the optimal solution of $\mathrm{P}(\mathcal{S}(K))$ will be resilient with respect to all states in $\mathcal{S}$. For convenience, the optimization problem (3.3) corresponding to a K-set $\mathcal{U}(K)$ will be from now on denoted by $\mathrm{P}(K)$ instead of $\mathrm{P}(\mathcal{S}(K))$.

Note that the number $U(K) := \sum_{k=0}^{K} \binom{E}{k}$ of the states in $\mathcal{U}(K)$ grows exponentially with the number of links E, provided K increases linearly with E, for example when $K = \lfloor \frac{E}{2} \rfloor$. Thus, although problem $\mathrm{P}(K)$ is linear, it is in general non-compact as the number of variables and constraints is proportional to $U(K)$ and hence exponential with E. Therefore, the direct approach to $\mathrm{P}(K)$ by means of an LP solver is not applicable for large networks, and neither is the Benders' decomposition applied in Algorithm 1 presented in the previous section (to make sure that $c \in \mathcal{Y}$, Algorithm 1 needs to perform test (3.4) individually for all states s in $\mathcal{S}$). For this reason, we have developed a more efficient approach to $\mathrm{P}(K)$. The approach is similar to Benders' decomposition used in Algorithm 1. The difference is that for the state set $\mathcal{S}(K)$ determined by a K-set (for some fixed K), the feasibility test can be made efficient by finding the maximum $W(c) := \max_{s \in \mathcal{S}(K)} W(c,s)$. The adjusted test makes use of binary variables $u := (u_e,\, e \in \mathcal{E})$ that correspond to the vectors $u = (u(e),\, e \in \mathcal{E}) \in \mathcal{U}(K)$, and is as follows:

Problem G(c) (maximum violation):

$$W(c) = \tag{3.7a}$$

$$= \max \Big\{ \sum_{d \in \mathcal{D}} \lambda_d^{t(d)} h(d) - \sum_{e \in \mathcal{E}} (\pi_{a(e)} + \pi_{a'(e)}) c(e) + \sum_{e \in \mathcal{E}} \beta(e) c(e) (\pi_{a(e)} + \pi_{a'(e)}) u_e \Big\}$$

$$\pi_{a(e)} + \pi_{a'(e)} \le 1,\ e \in \mathcal{E}; \qquad \lambda_d^{o(d)} = 0,\ d \in \mathcal{D} \tag{3.7b}$$

$$\lambda_d^{t(a)} - \lambda_d^{o(a)} \le \pi_a, \quad a \in \mathcal{A}, d \in \mathcal{D} \tag{3.7c}$$

$$\sum_{e \in \mathcal{E}} u_e \le K, \tag{3.7d}$$

$$\pi \ge 0 \text{ and continuous};\ \lambda \text{ continuous}; u \text{ binary}. \tag{3.7e}$$

Above, any vector of binary variables $u := (u_e,\, e \in \mathcal{E})$ fulfilling constraints (3.7d) defines a state $s(u) \in \mathcal{S}(K)$ with the failure ratio vector $(\beta(e, s(u)) = \beta(e) u_e,\, e \in \mathcal{E})$. Moreover, for any fixed feasible u the value of the objective function maximized over λ, π is equal to $W(c,s)$ for the so defined $s(u)$. Since in (3.7) we are maximizing also over u, we finally observe that $W(c) = \max_{s \in \mathcal{S}(K)} W(c,s)$, as required.

Note that if we define the set $\widetilde{\mathcal{U}}(K) := \{u = (u(e),\, e \in \mathcal{E}) : \sum_{e \in \mathcal{E}} u(e) \le K, 0 \le u(e) \le 1,\, e \in \mathcal{E}\}$ (i.e., the convex hull of $\mathcal{U}(K)$, called the *uncertainty polytope* [**?**]), then any given capacity vector c is feasible for $\mathrm{P}(K)$ if, and only if, it is feasible for the state set $\bar{\mathcal{S}}(K) := \{s(u) :\ u \in \bar{\mathcal{U}}(K)\}$ characterized by the following vectors of failure ratios:

$$\beta(s(u)) := (\beta(e) u(e),\, e \in \mathcal{E}),\ u \in \widetilde{\mathcal{U}}(K).$$

This follows from the fact that the version of $\mathrm{G}(c)$ with λ and π fixed and u relaxed, i.e., with $0 \le u_e \le 1$ instead of $u_e \in \{0,1\}$, $e \in \mathcal{E}$, is an LP problem with a totally unimodular matrix of coefficients (recall that K is a positive integer).

Certainly, to obtain a proper mixed-integer programming formulation we need to take care of bi-linearities in (3.7) induced by multiplications of variables $(\pi_{a(e)} + \pi_{a'(e)}) \cdot u_e$, $e \in \mathcal{E}$, with u_e binary and the value of $(\pi_{a(e)} + \pi_{a'(e)})$ between 0 and 1. To get rid of these bi-linearities we introduce additional (continuous) variables U_e, $e \in \mathcal{E}$, that in the optimal solution will be equal to $(\pi_{a(e)} + \pi_{a'(e)}) \cdot u_e$. This is done in the next formulation:

Problem GMIP(c) (MIP version of G(c)):

$$W(c) = \max \{ \textstyle\sum_{d\in\mathcal{D}} \lambda_d^{t(d)} h(d) - \sum_{e\in\mathcal{E}} (\pi_{a(e)} + \pi_{a'(e)}) c(e) + \sum_{e\in\mathcal{E}} \beta(e) c(e) U_e \} \tag{3.8a}$$

$$\pi_{a(e)} + \pi_{a'(e)} \le 1,\ e \in \mathcal{E}; \qquad \lambda_d^{o(d)} = 0,\ d \in \mathcal{D} \tag{3.8b}$$

$$\lambda_d^{t(a)} - \lambda_d^{o(a)} \le \pi_a,\ \ a \in \mathcal{A}, d \in \mathcal{D} \tag{3.8c}$$

$$\textstyle\sum_{e\in\mathcal{E}} u_e \le K, \tag{3.8d}$$

$$U_e \le \pi_{a(e)} + \pi_{a'(e)},\ U_e \le u_e,\ \ e \in \mathcal{E} \tag{3.8e}$$

$$\pi \ge 0 \text{ and continuous};\ \lambda, U \text{ continuous};\ u \text{ binary}. \tag{3.8f}$$

Note that the (otherwise necessary) condition $U_e \ge \pi_{a(e)} + \pi_{a'(e)} + u_e - 1$ is omitted in formulation (3.8) since the values U_e in the vector $U := (U_e,\ e \in \mathcal{E})$ are maximized by objective (3.8a). Now let λ^*, π^*, U^* (and u^*) be an optimal solution of (3.8). If $W(c) > 0$ then the capacity vector c is infeasible for the main problem P(K) formulated in (3.17), and the following (Benders) inequality (written in variables y)

$$\textstyle\sum_{e\in\mathcal{E}} (\pi^*_{a(e)} + \pi^*_{a'(e)})(1 - \beta(e) u^*_e) M y_e - \sum_{d\in\mathcal{D}} {\lambda_d^{t(d)}}^* h(d) \ge 0 \tag{3.9}$$

separates c from the set of capacity vectors feasible for P(K). Note that c breaks the above inequality by $W(c) = \max_{s\in\mathcal{S}(K)} O(c, s)$, i.e., by the sum of the link overloads (minimized over the demand routing) in the "worst state" $s \in \mathcal{S}(K)$.

4.4 A cut generation algorithm for $\mathcal{S}(K)$

The iterative algorithm for solving problem (3.2) for link availability states specified through a given K-set is presented below. As for Algorithm 1 for a fixed list of states discussed in Section 4.2, in each iteration the master problem involving only the capacity variables y is solved and then its optimal solution y^* is tested for feasibility with respect to P(K). If the test is positive, the algorithm is stopped and y^* is optimal for (3.2). If not, a new inequality deduced from the feasibility test is added to the master problem and the algorithm is reiterated. (Recall that notation $y \in \Omega$ means that y fulfills all inequalities in the set of inequalities Ω.)

Algorithm 2: cut generation algorithm for the set of states $\mathcal{S}(K)$

Step 0: $\Omega := \{y \ge 0\}$.

Step 1: Solve the master problem:

$$\text{minimize} \quad \sum_{e\in\mathcal{E}} \xi(e) y_e \tag{3.10a}$$

$$\text{subject to} \quad y \in \Omega \quad \text{and integer}, \tag{3.10b}$$

and put $c = (My_e^*, e \in \mathcal{E})$.

Step 2: Solve the feasibility test (3.8). If $W(c) \leq 0$, then stop (c is the capacity vector optimal for problem (3.2)).

Step 3: Otherwise, add inequality (3.9) to Ω and go to Step 1.

As with Algorithm 1, in the computations we apply the two-phase version of Algorithm 2.

4.5 Computational complexity of P($\mathcal{K}$)

The analysis of computational complexity of our problem was proposed by M. Poss and an extended version is published in [9].

When the set of states $\mathcal{S}$ is characterized by means K-sets, i.e., when $\mathcal{S} = \mathcal{S}(K)$, already the linear relaxation of the problem studied in this chapter (i.e., linear relaxation of P($\mathcal{K}$)) becomes difficult. This is suggested by co$\mathcal{NP}$-completeness of the decision version of the feasibility test (3.7). (For a presentation of computational complexity theory, and the notion of co$\mathcal{NP}$-completeness in particular, see [67].) This issue is discussed below.

For a given network graph $\mathcal{G} = (\mathcal{V}, \mathcal{A}, \mathcal{E})$, parameter K ($1 \leq K \leq |\mathcal{E}|$) and vectors $h = (h(d),\ d \in \mathcal{D})$ and $\beta = (\beta(e),\ e \in \mathcal{E})$, let $\mathcal{C}(\mathcal{S}(K))$ be the set (a polyhedron) of all link capacity vectors c, not necessarily modular, that are feasible for all states $s \in \mathcal{S}(K)$, i.e., for which $O(c, s) = 0$ for all $s \in \mathcal{S}(K)$ (see (3.3a)). The separation problem for polyhedron $\mathcal{C}(\mathcal{S}(K))$, corresponding to the feasibility test (3.7) and referred to as DSPS/in, is defined as the following decision problem:

DSPS/in: does a given link capacity vector c belong to polyhedron $\mathcal{C}(\mathcal{S}(K))$?

Note that DSCP/in is in class co$\mathcal{NP}$ (of decision problems) since its complement, i.e., the separation problem of the form

DSPS/out: is a given link capacity vector c outside polyhedron $\mathcal{C}(\mathcal{S}(K))$?

is in class $\mathcal{NP}$. This statement is true because if c is a YES instance of DSPS/out, then any state $s \in \mathcal{S}(K)$ for which c is infeasible can be used as a certificate for verifying this in polynomial time.

Now let us consider a decision problem similar to DSCP/in for a network graph $\mathcal{G} = (\mathcal{V}, \mathcal{A}, \mathcal{E})$ with a set of single source demands $\mathcal{D}$ having their origins in a fixed vertex

$w \in \mathcal{V}$, i.e., $o(d) = w$, $t(d) \in \mathcal{V} \setminus \{w\}$, $d \in \mathcal{D}$. For a given parameter K ($1 \leq K \leq |\mathcal{D}|$), let $\mathcal{H}(K)$ be the set of demand volume vectors h defined as:

$$\mathcal{H}(K) := \{h = (h(d),\, d \in \mathcal{D}) :\ \textstyle\sum_{d\in\mathcal{D}} h(d) \leq K,\ h(d) \in \{0,1\},\ d \in \mathcal{D}\}.$$

Further, let $\mathcal{C}(\mathcal{H}(K))$ be a polyhedron of all link capacity vectors c that are feasible for demand volume vectors $h \in \mathcal{H}(K)$. (Note that each vector h can be realized by means of its individual routing, just like each state s can be realized by its individual routing, see (3.2b).) Finally, define the following (decision) separation problem referred to as DSPH/in:

DSPH/in: does a given link capacity vector c belong to polyhedron $\mathcal{C}(\mathcal{H}(K))$?

(Note that in this setting the link capacities are not affected.) It is shown in Section 2 of [68] that DSPH/in is co$\mathcal{NP}$-complete, provided the *unique games conjecture* holds. (The conjecture has already been used to prove hardness for different problems that have resisted previous attempts, see [69] for an introduction to the conjecture). We will make use of this fact to show that DSCP/in is co$\mathcal{NP}$-complete (provided the unique games conjecture holds) by constructing a polynomial transformation of the instances of DSPH/in to instances of DSPS/in.

Proposition 1: DSPH polynomially transforms to DSPS.

Proof. Consider an instance of problem DSPH/in for a given link capacity vector $c = (c(e),\, e \in \mathcal{E})$ and a bi-directed graph $\mathcal{G} = (\mathcal{V}, \mathcal{A}, \mathcal{E})$ with the set $\mathcal{D}$ of single-source demands and (uncertain) demand volumes described by the set $\mathcal{H}(K)$. Our transformation considers the following augmented (with respect to $\mathcal{G}$) bi-directed graph $\mathcal{G}' = (\mathcal{V}, \mathcal{A}', \mathcal{E}')$, where $\mathcal{E}' = \mathcal{E} \cup \mathcal{E}''$ and $\mathcal{E}'' := \bigcup_{d\in\mathcal{D}} \big\{\{w, t(d)\}\big\}$, and the definition of $\mathcal{A}'$ follows from considering the two oppositely directed arcs corresponding to each (undirected) edge $e \in \mathcal{E}'$. We assume that the sets $\mathcal{E}''$ and $\mathcal{E}$ are disjoint – this means that for each link of the form $\{w, t(d)\}$ that already exists in the original set of links $\mathcal{E}$, a new parallel link is created. Next, we assume $\mathcal{D}' := \mathcal{D}$ (the origins and destinations of the demands are unchanged), and $h(d) = 1$ for each $d \in \mathcal{D}'$. Finally, we define $\beta(e) = 0$, $e \in \mathcal{E}$, $\beta(e) = 1$, $e \in \mathcal{E}''$, and $c'(e) = c(e)$, $e \in \mathcal{E}$, $c'(e) = 1$, $e \in \mathcal{E}''$.

We claim that c' in graph $\mathcal{G}'$ is feasible for all states s in $\mathcal{S}(K)$ if, and only if, c is feasible for all demand volume vectors h in $\mathcal{H}(K)$. To prove this claim we first note that assumption $\beta(e) = 0$, $e \in \mathcal{E}$, implies that c' is feasible for all states induced by $\mathcal{U}(K)$ (i.e, the K-set considered for $\mathcal{G}'$; the definition of $\mathcal{U})K)$ is given in Section 4.3) if, and only if, c' is feasible for all states induced by the set $\widehat{\mathcal{U}}(K) := \{u \in \mathcal{U}(K) :\ u(e) = 0,\, e \in \mathcal{E}\}$. Next we define the bijection $\varphi : \widehat{\mathcal{U}}(K) \mapsto \mathcal{H}(K)$, where, for each $e = \{w, t(d)\} \in \mathcal{E}''$, $\varphi(u)(d) = 1$ if, and only if, $u(e) = 1$. What is more, routing of demands with $h(d) = 1$ for each $d \in \mathcal{D}'$ using the capacity implied by u in graph $\mathcal{G}'$ is equivalent to routing the demands $h(d) = \varphi(u)(d)$, $e = \{w, t(d)\} \in \mathcal{E}''$ in graph $\mathcal{G}$. This holds because if $u(e) = 1$ for a link $e \in \mathcal{E}''$ of the form $\{w, t(d)\}$, the current capacity of e equals 0, and therefore the demand $d \in \mathcal{D}$ must be routed through network $\mathcal{G}$ using capacity c; if $u(e) = 0$ for a link

$e \in \mathcal{E}''$ of the form $\{w, t(d)\}$, the demand d can be entirely routed along this particular link, not using the capacity c of the links in $\mathcal{G}$. □

Corollary: If the unique games conjecture is true, the feasibility test based on formulation (3.7) (used in Algorithm 2) is $\mathcal{NP}$-hard.

Proof. Assume that the unique games conjecture is true. Then, Proposition 1 implies that DSPC/in is co$\mathcal{NP}$-complete since the decision problem DSPH/in (with co$\mathcal{NP}$-completeness proven, under the unique games conjecture, in [68]) can be polynomially transformed to DSPC/in. Thus, DSPC/out, as the complement of DSPC/in, is $\mathcal{NP}$-complete (see Theorem 15.31 in [67]). Thus, the problem formulated in (3.7), as an optimization version of DSPC/out, is $\mathcal{NP}$-hard. □

Finally we note that $\mathcal{NP}$-hardness of the test (3.7) does not necessarily mean that the problem represented by the linear relaxation of formulation P(K) is $\mathcal{NP}$-hard. In fact, it only means, by equivalence of separation and optimization (see Section 3 of Chapter I.6 in [70]), that the family of linear programming problems defined on polyhedron $\mathcal{C}(\mathcal{S}(K))$ (linear relaxation of the master problem (3.10) with $\Omega = \mathcal{C}(\mathcal{S}(K))$ is a member of this family) contains $\mathcal{NP}$-hard linear programming problems. Yet, in general, there can be polynomial problems in the considered family as well. (For a discussion of this issue in network optimization context see [71].) Nevertheless, $\mathcal{NP}$-hardness of (3.7) makes $\mathcal{NP}$-hardness of P(K) quite likely.

5 Modifications and improvements

5.1 Modifications of the optimization model

As shown below, the node-arc formulation (3.2) of P($\mathcal{S}$) can be easily modified in order to capture other types of network graphs besides the so far considered case assuming the bi-directed graph with full-duplex link capacity. Also, the aggregated node-arc formulations (see [6]) can be applied to (3.2) and all the modifications discussed in Sections 5.1.1 and 5.1.2. Such formulations use aggregated arc-flows of the form x^s_{av} (related to the ordinary arc-flows through equality $x^s_{ad} = \sum_{d \in \mathcal{D}, t(d)=v} x^s_{ad}$, $a \in \mathcal{A}, v \in \mathcal{V}, s \in \mathcal{S}$) expressing the total flow of traffic destined to node v on arc a in state s. Finally, link-path formulations can be used, as shown in Section 5.1.3

5.1.1 Directed links

In this case the network graph $\mathcal{G} = (\mathcal{V}, \mathcal{A})$ is directed (rather than bi-directed) so it is not necessary that each arc has its oppositely directed counterpart. Besides, the link

capacity is directed so each arc has its individual capacity y_a (or $n(a)$). To consider this, the objective (3.2a) and constraint (3.2c) are (respectively) modified as follows:

$$C(\mathcal{S}) = \min \sum_{a\in\mathcal{E}} \xi(a)y_a, \qquad \sum_{d\in\mathcal{D}} x^s_{ad} \le \big(1-\beta(a,s)\big)My_a, \;\; a\in\mathcal{A},\; s\in\mathcal{S},$$

where $\xi(a)$ and $\beta(a,s)$ are module costs and failure ratios, respectively, defined for individual arcs (although if two oppositely directed arcs connect the same pair of nodes it is natural to assume that in all states in $\mathcal{S}$ they have equal failure ratios).

Formulations of the feasibility test, its dual, and the maximum violation problem corresponding to the so modified formulation of (3.2) are obtained in essentially the same as formulations (3.3), (3.4), and (3.7), respectively.

5.1.2 Undirected links

In this case the network graph $\mathcal{G} = (\mathcal{V}, \mathcal{E})$ is composed of the set of nodes $\mathcal{V}$ and the set of (undirected) links $\mathcal{E} \subseteq \mathcal{V}^{|2|}$. The extension of (3.2) is is obtained by substituting each undirected edge $e = \{v, w\} \in \mathcal{E}$ by two oppositely directed arcs $a(e) = (v, w)$ and $a'(e) = (w, v)$ (that specify an auxiliary bi-directed graph used to route the arc-flows) and defining the load of edge $\{v, w\}$ as the sum of the loads of arcs (v, w) and (w, v). This is expressed by substituting constraint (3.2c) with

$$\sum_{d\in\mathcal{D}}(x^s_{a(e)d} + x^s_{a'(e)d}) \le \big(1-\beta(e,s)\big)My_e, \;\; e\in\mathcal{E},\; s\in\mathcal{S}.$$

The so adjusted formulation of P($\mathcal{S}$) works for directed demands (as assumed in Section 3.1) as well for undirected demands. In the latter case, each demand $d \in \mathcal{D}$, connecting nodes v and w, say, should be made directed through selecting one of v, w for the originating node $o(d)$ and the other for the terminating node $t(d)$.

As before, formulations of the feasibility test, its dual, and the maximum violation problem for the so modified formulation are essentially the same as for (3.2).

5.1.3 Link-path formulations

All the cases of problem P($\mathcal{S}$) considered in this thesis can be also treated by means of link-path formulations involving path-flows (for a given list of predefined allowable routing paths) instead of arc-flows. The link-path formulation corresponding to node-arc formulation (3.2) is as follows.

Problem P($\mathcal{S}$) (main problem in link-path formulation):

$$C(\mathcal{S}) = \min \sum_{e\in\mathcal{E}} \xi(e) y_e \tag{3.12a}$$

$$\sum_{p\in\mathcal{P}(d)} x^s_{dp} = h(d), \quad d \in \mathcal{D},\ s \in \mathcal{S} \tag{3.12b}$$

$$\sum_{d\in\mathcal{D}} \sum_{p\in\mathcal{P}(d)} \delta(a,d,p) x^s_{dp} \le \big(1 - \beta(e(a),s)\big) M y_{e(a)}, \quad a \in \mathcal{A},\ s \in \mathcal{S} \tag{3.12c}$$

$$x \ge 0 \text{ and continuous; } y \ge 0 \text{ and integer.} \tag{3.12d}$$

Above, x^s_{dp} is the flow on path $p \in \mathcal{P}(d)$ dedicated to carry the traffic of demand $d \in \mathcal{D}$ in state $s \in \mathcal{S}$, where $\mathcal{P}(d)$ is a predefined list of elementary directed paths in graph $\mathcal{G} = (\mathcal{V}, \mathcal{A})$ from node $o(d)$ (origin of demand d) to node $t(d)$ (termination of d). (Recall that an elementary path does not traverse any node more than once.) The left-hand side of the capacity constraint (3.12c) expresses the load of arc a using the given binary arc-path incidence coefficients $\delta(a,d,p)$ ($\delta(a,d,p) = 1$ if, and only if, arc a belongs to path $p \in \mathcal{P}(d)$). Clearly, the arc-flow x^s_{ad} induced by a given set of path-flows realizing demand d is equal to $\sum_{p\in\mathcal{P}(d)} \delta(a,d,p) x^s_{dp}$. The inverse relationship cannot be unambiguously specified, as a given set of arc-flows may induce different sets of path-flows. Yet, a set of path-flows corresponding to a given set of arc-flows can be easily obtained (see [67]).

Although the link-path formulation leads to a dual polytope different from (3.4b)-(3.4d), the dual function (3.4a) used for testing feasibility of the link capacity vector c remains essentially the same. The link-path formulation is valid for both bi-directed, directed and undirected networks, but requires path generation for finding the lists of allowable paths necessary to find the optimal solution when all possible paths are considered.

5.2 Valid inequalities

In fact, the Benders cutting plane approach may need a large number of Benders' inequalities to converge to optimum. This may pose an efficiency issue since test (3.8) (called also the separation problem) performed in Step 2 of our algorithm contains binary variables. One way to deal with this issue is to try to speed up the convergence of the algorithm by using additional valid inequalities on top of the Benders cuts in the master problem solved in Step 1 of the algorithm.

A valid inequality can be obtained by substituting the last sum in (3.7a) by the quantity $K \cdot B$, where $B := \frac{\sum_{e\in\mathcal{E}} \beta(e)c(e)(\pi_{a(e)}+\pi_{a'(e)})}{E}$ is the average value of the terms $\beta(e)c(e)(\pi_{a(e)} + \pi_{a'(e)})$, $e \in \mathcal{E}$. The corresponding test would thus be as follows:

$$\max \Big\{ \sum_{d\in\mathcal{D}} \lambda_d^{t(d)} h(d) - \sum_{e\in\mathcal{E}} (\pi_{a(e)} + \pi_{a'(e)}) c(e) + \tfrac{K}{E} \sum_{e\in\mathcal{E}} \beta(e)c(e)(\pi_{a(e)} + \pi_{a'(e)}) \Big\} \tag{3.13a}$$

$$\pi_{a(e)} + \pi_{a'(e)} \le 1, \quad e \in \mathcal{E} \qquad \lambda_d^{o(d)} = 0, \quad d \in \mathcal{D} \tag{3.13b}$$

$$\lambda_d^{t(a)} - \lambda_d^{o(a)} \le \pi_a, \quad a \in \mathcal{E}, d \in \mathcal{D} \tag{3.13c}$$

$$\pi \ge 0 \text{ and continuous, } \lambda \text{ continuous.} \tag{3.13d}$$

When the resulting maximum is positive, the following valid inequality

$$\sum_{d\in\mathcal{D}} \lambda_d^{t(d)^*} h(d) - \sum_{e\in\mathcal{E}} (\pi^*_{a(e)} + \pi^*_{a'(e)}) y_e + \frac{K}{E} \sum_{e\in\mathcal{E}} (\pi^*_{a(e)} + \pi^*_{a'(e)}) \beta(e) y_e \leq 0 \qquad (3.14)$$

is obtained. Note that (3.13) is a linear programming problem while formulation (3.8) requires binary variables.

Similar valid inequalities can be obtained for subsets $\mathcal{E}'$ of links with $k := |\mathcal{E}'| \leq K$. In the corresponding feasibility test the objective is as follows:

$$\begin{aligned} \max \Big\{ & \sum_{d\in\mathcal{D}} \lambda_d^{t(d)} h(d) - \sum_{e\in\mathcal{E}} (\pi_{a(e)} + \pi_{a'(e)}) c(e) + \\ & + \frac{K-k}{E-k} \sum_{e\in\mathcal{E}\setminus\mathcal{E}'} \beta(e) c(e) (\pi_{a(e)} + \pi_{a'(e)}) + \sum_{e\in\mathcal{E}'} \beta(e) c(e) (\pi_{a(e)} + \pi_{a'(e)}) \Big\}. \end{aligned} \qquad (3.15a)$$

Another useful class of valid inequalities are the cutset inequalities, first introduced in the robust context in [32]. Given a partition $\mathcal{V} = \mathcal{V}_1 \cup \mathcal{V}_2$ of the nodes, the cutset inequality associated with the partition states that the amount of capacity installed on the arcs going from $\mathcal{V}_1$ to $\mathcal{V}_2$ should not be less than the sum of the volumes of the demands from $\mathcal{V}_1$ to $\mathcal{V}_2$. Defining $\mathcal{E}(\mathcal{V}_1, \mathcal{V}_2) = \{a \in \mathcal{A} : o(a) \in \mathcal{V}_1 \wedge t(a) \in \mathcal{V}_2\}$ and $\mathcal{D}(\mathcal{V}_1, \mathcal{V}_2) = \{d \in \mathcal{D} : o(d) \in \mathcal{V}_1 \wedge t(d) \in \mathcal{V}_2\}$, the inequality is formally defined as:

$$\min_{s\in\mathcal{S}} \sum_{a\in\mathcal{E}(\mathcal{V}_1,\mathcal{V}_2)} \big(1 - \beta(e(a), s)\big) c(e(a)) \geq \sum_{d\in\mathcal{D}(\mathcal{V}_1,\mathcal{V}_2)} h(d) \qquad (3.16)$$

While the exact separation of (3.16) requires solving mixed-integer programs, this can also be done heuristically. For instance, in [?] the nodes are randomly partitioned into two subsets and then a local search is performed, picking up one node and moving it to the other subset until there is no more improvement in the violation. If no violated inequality has been found, another initial partition is considered up to a maximum of 5 iterations.

5.3 K-set extension

The model presented and tested in the current chapter takes into account one (but link-dependent) failure ratio level $\beta(e)$ for each link $e \in \mathcal{E}$. In reality, however, links may be affected with different levels of failure ratios, depending on the modulation and coding scheme applied in response to current weather conditions. As mentioned in Section 2, these ratios can for example be equal to 0, 0.5, 0.75, and 1.

To admit such multiple failure ratio levels we can assume that there are K different levels $0 \leq \beta(k) \leq 1$, $k \in \mathcal{K} = \{1, 2, \ldots, K\}$, and that in any considered state s at most $N(k)$ links can experience failure ratio $\beta(k)$, where $1 \leq N(k) \leq E$, $k \in \mathcal{K}$. The corresponding polytope is specified as follows.

$$\sum_{k\in\mathcal{K}} u_e^k = 1, \quad e \in \mathcal{E}, \quad \sum_{e\in\mathcal{E}} u_e^k \leq N(k), \; k \in \mathcal{K},$$

where the binary variable $u_e^k = 1$ if, and only if, link e is degraded with the failure ratio $\beta(k)$.

The so obtained state characterization can be used to solve the problem analogous to P(K) by appropriately modifying formulations (3.7) and (3.8). In fact, an even more general version of the K-set (referred to as the uncertainty polytope) was considered in [36].

6 A compact model for hybrid FSO/fiber networks

This section deals with wireless networks composed of FSO (free space optics) links supported by terrestrial optical fiber connections in order to increase resilience to adverse weather conditions. FSO networks have some noteworthy properties such as transmission range of several kilometers, high transmission bandwidth, low cost (as compared with the fiber optical technology), immunity to electromagnetic interference, etc. However, a major disadvantage of FSO links is vulnerability to weather conditions. When the transmission power received at the end node of an FSO link is decreased, the signal modulation and coding scheme (MCS) at the transmitter should be adjusted accordingly; in effect, an FSO link can be kept operational, but with decreased capacity, even if the channel is affected.

Yet, since in severe weather conditions some FSO links may not be able to realize any reliable transmission at all (whichever MSC is used), when the network is not equipped with resilience mechanisms for ensuring and maintaining an acceptable level of service, these weather degradation may lead to significant data losses and sometimes even to network disconnection [9]. In these extreme cases link degradation ratio on some links may become equal to 1 leading to network disconnection (such disconnections can be observed for $10 - 15\%$ of the weather states during a one year period). Therefore, it is reasonable to consider using fibers instead of free space light beams since weather insensitive (and high capacity) fibers installed on the key links will ensure network connectivity in all weather states(see [39] and [72]). Certainly, the so obtained connectivity does not come for free because of the high cost of the optical fiber connections as compared to the FSO systems and hence the number of fibers should be kept at minimum. Thus, for designing hybrid FSO/fiber networks we need an optimization model for finding cheapest configurations of links (and their capacities) that will be able to carry the demanded traffic on acceptable level in all weather states foreseen in network operation. This is not a simple task as it requires not only robust network optimization methods but also a tractable way of characterizing possible weather states (which are not known in advance) and their influence on FSO link capacity. In the continuation of this chapter we present an approach to the so described task and illustrate its effectiveness by means of numerical studies.

Evidently , the combination of the two above described network mechanisms, i.e., MCS control and the use of optical fibers, will assure network resilience only when network links are properly dimensioned. This simply means that in all the foreseen weather conditions the current capacity available on the links (both FSO and fiber) is sufficient to carry the demanded traffic on an acceptable level. Introducing and studying a particular optimization model that takes the above requirement into account and at the same time minimizes the total cost of network links (note that this will limit the use of fibers which

are more expensive to install/hire than the FSO links) is the main goal and motivation of this second part of Chapter 3.

6.1 Problem formulation

We will continue to use the same notation as in Section 3.1. As already mentioned, we are considering hybrid optical networks with two types of links, FSO (free space) links and fiber (terrestrial) links. We assume that the cost of installing a fiber link between two given nodes is substantially higher as compared to an FSO link, but it guarantees high (full duplex) transmission rate of L Gbps on each of the two oppositely directed arcs composing the link. The capacity of an FSO link is modular and each module provides (full duplex) transmission rate equal to M Gbps on each of the two oppositely directed arcs of the link. Note that the fiber link transmission capacity L is typically provided by means of an optical transmission system (such as a DWDM full duplex system with bit-rate of the order of 10 Tbps) while the FSO link transmission capacity is achieved by means of parallel full duplex FSO systems between several transceiver pairs installed at the end nodes of the link. Typically, each such system can provide bit-rate M of the order of 10 Gbps.

The capacity of a link is thus provided either by several FSO modules or of just one but very large fiber module (L is 1-3 orders of magnitude greater than M). When the link capacity is optimized, the number of FSO modules installed on link $e \in \mathcal{E}$ is expressed by a variable y_e while the presence of a fiber on link e is determined by a variable q_e. That is, y_e is a non-negative integer variable determining the FSO link capacity equal to $M \cdot y_e$ while q_e is a binary variable indicating the presence ($q_e = 1$) or lack ($q_e = 0$) of a fiber on link e. In consequence, each of the two oppositely directed arcs of link e has capacity $My_e + Lq_e$. To each link $e \in \mathcal{E}$ there corresponds a non-negative cost $\xi(e)$ for the FSO module, and $\kappa(e)$ for the fiber module; it is assumed that $\kappa(e) >> \xi(e)$). Hence, the total cost of the network is given by $\sum_{e\in\mathcal{E}}(\xi(e)y_e+\kappa(e)q_e)$. When link capacities in the network are given and fixed, then, for each link $e \in \mathcal{E}$, $c(e)$ will denote its FSO capacity (equal to 0 or to a multiple of M), and $c'(e)$ its fiber capacity (0 or L). Hence, the total capacity of e is equal to $c(e) + c'(e)$; note that actually one of these quantities will be equal to 0. In the following we will use the vectors $y := (y_e,\, e \in \mathcal{E})$, $q := (q_e,\, e \in \mathcal{E})$, $c := (c(e),\, e \in \mathcal{E})$, and $c' := (c'(e),\, e \in \mathcal{E})$ to denote the capacity variables or parameters.

When a link, link e, say, is degraded in a particular state $s \in \mathcal{S}$, all FSO systems realized on e lose the same fraction of their capacity that is specified by a (link) degradation ratio denoted by $\beta(e, s)$ from a given set of degradation ratio values $\mathcal{R}$, for example $\mathcal{R} = \{0, 0.5, 0.75, 1\}$. In consequence, each degradation state $s \in \mathcal{S}$ can be identified with a vector of link degradation ratios, which represents the fraction of capacity of link e *not available* in state s. Since the fiber link, if provided, is always fully available ($\beta(e, s) = 0$ for a fiber link e), the capacity of link $e \in \mathcal{E}$ available in state $s \in \mathcal{S}$ is equal to $\big(1 - \beta(e, s)\big)My_e + Lq_e$. Note that if link e is selected to be the fiber link ($q_e = 1$) then there is no use to provide any FSO transmission systems on it ($y_e = 0$) because e is always available and its capacity is assumed sufficient to carry any traffic load induced by the traffic matrix and the demand routing used.

6.2 Problem formulation

The basic problem of hybrid FSO/fiber network we consider can be formulated as a mixed-integer program (MIP) in the node-arc notation (using the arc-flows variables $x := (x^s_{ad},\, a \in \mathcal{A}, d \in \mathcal{D}, s \in \mathcal{S})$ and the link capacity variables $y = (y_e,\, e \in \mathcal{E})$, $q = (q_e\,, e \in \mathcal{E})$.) Formulation of the optimization problem in question is as follows:

Problem P($\mathcal{S}$) (main problem in node-arc formulation):

$$C(\mathcal{S}) = \min \textstyle\sum_{e\in\mathcal{E}}(\xi(e)y_e + \kappa(e)q_e) \tag{3.17a}$$

$$\textstyle\sum_{a\in\delta^+(v)} x^s_{ad} - \sum_{a\in\delta^-(v)} x^s_{ad} = \begin{cases} h(d) & \text{if } v = o(d) \\ -h(d) & \text{if } v = t(d), \\ 0, & \text{otherwise} \end{cases} \quad d \in \mathcal{D}, v \in \mathcal{V}, s \in \mathcal{S} \tag{3.17b}$$

$$\textstyle\sum_{d\in\mathcal{D}} x^s_{ad} \le \big(1 - \beta(e(a), s)\big) M y_{e(a)} + L q_{e(a)}, \quad a \in \mathcal{A},\ s \in \mathcal{S} \tag{3.17c}$$

$$x \ge 0 \text{ continuous};\ y \ge 0 \text{ integer};\ q \text{ binary}. \tag{3.17d}$$

Above, x^s_{ad} is the flow on arc a dedicated to carry the traffic of demand d in state s. The objective of P($\mathcal{S}$), i.e., minimizing the cost of links, is specified in (3.17a). Constraints (3.17b) are the flow conservation equations for each demand d at each node v in each state s, assuring the realization of $h(d)$ for each d in each state s. Finally, the capacity constraint (3.17c) ensures that the capacity of link e is not exceeded in any state s.

Note that because of high costs $\kappa(e)$ of the fiber links (that by assumption are significantly larger than costs $\xi(e)$ of the FSO links), the optimal solution of problem P($\mathcal{S}$) will, first of all, minimize the total cost (equal to $\sum_{e\in\mathcal{E}} \kappa(e)q_e$) of those fiber links that are necessary to make the network (demand-wise) connected in all states in $\mathcal{S}$.

6.2.1 A cut generation algorithm for an explicit state set $\mathcal{S}$

An iterative algorithm for solving (3.17) is given below. It results from applying Benders' decomposition [8] to P($\mathcal{S}$) (this particular application can be found in [6]). In each iteration, first the master problem involving only the capacity variables y, q is solved, and then its optimal solution (y^*, q^*) is tested for feasibility with respect to P($\mathcal{S}$). If the test is positive, the algorithm is stopped and solution (y^*, q^*) is optimal for P($\mathcal{S}$). If not, new inequalities deduced from the feasibility tests are added to the master problem and the algorithm is reiterated. (Below, the notation $(y, q) \in \Omega$ means that variables y and q fulfill all inequalities in the set of inequalities Ω.)

A1: cut generation algorithm for state set $\mathcal{S}$
Input: *network topology (nodes/links), traffic demands matrix, set of degradation states*

S.
Output: *number of FSO modules for each link, location of terrestrial fibers.*

Step 0: $\Omega := \{y \geq 0\}$.

Step 1: Solve the master problem:

$$\text{minimize} \quad \sum_{e\in\mathcal{E}} \left(\xi(e)y_e + \kappa(e)q_e\right) \tag{3.18a}$$

$$\text{subject to} \quad (y,q) \in \Omega \tag{3.18b}$$

$$y \text{ integer}, \; q \text{ binary}$$

and put $c(e) = My_e^*$, $c'(e) = Lq_e^*$, $e \in \mathcal{E}$, where (y^*, q^*) is an optimal solution of (3.18).

Step 2: For each $s \in \mathcal{S}$ solve the feasibility test (3.4) and if $W(c, c', s) > 0$, then add inequality (3.5) to Ω.

Step 3: If no inequalities have been added to Ω in Step 2, then stop: (y^*, q^*) is an optimal solution for problem (3.17). Otherwise go to Step 1.

6.3 Network optimization procedure

When it comes to applying the above described algorithms, computational effectiveness should be considered. It turns out that keeping both vectors of decision variables (y and q) in the master problem (3.18) would lead to excessive computation times when applying A1 and A2 directly to the network instances of the sizes considered in the numerical study presented in Chapter 5. Therefore in the actual implementation used in the study, we took advantage of two assumptions: (i) the cost of the fiber link (equipped with an optical transmission system) is much higher than the cost of an FSO system, i.e., $\kappa(e) >> \xi(e), e \in \mathcal{E}$, and (ii) the capacity L of the fiber is virtually infinite since an optical fiber transmission system would be sufficient to carry even the sum of all demand volumes, i.e., $\sum_{d\in\mathcal{D}} h(d)$. Thus, in practice we will install only a few fibers (at most $V-1$), just to ensure full demand connectivity (or, at least, high connectivity) in all states in $\mathcal{S}$, where demand connectivity in a given state s means that for each demand there exists a path between the demand's end nodes composed of links with degradation ratios $\beta(e,s)$ strictly less than 1 (in such a case, the state is called *connected*, and *disconnected* otherwise). In fact, in the case when all states are connected, the fibers will not be installed at all because of their high cost. Clearly, when a fiber link is installed then no additional FSO systems are needed to be installed on that link.

Taking the above into account, in our numerical experiments we assume that vector q specifying the assignment of fibers is predefined, i.e., fixed and given, so that only the vector y of FSO link capacities represents the problem variables. More specifically, we run numerical experiments for instances where the subset of fiber links has been fixed, and we do this separately for consecutive subsets with increasing number of (fiber) links, starting

from one-link subsets, and choose the cheapest subset that assures network connectivity. Thus, there is no need for variables to determine the subset of links where the fiber is installed. A detailed explanation of the optimization procedure used for the numerical study is described in Chapter 5.

Network optimization procedure - Phase 1

1. For a given set of states $\mathcal{S}$ (with pairwise different link degradation ratio vectors $\beta(s) := (\beta(e,s),\, e \in \mathcal{E}),\, s \in \mathcal{S}$) we first identify all states that contain disconnected demands assuming that no fiber links are used ($q = 0$). We denote the set of such states with $\mathcal{S}''(0)$ and call it *the set of disconnected states*. The complementary set, denoted with $\mathcal{S}'(0) := \mathcal{S} \setminus \mathcal{S}''$, is called *the set of connected states*.

2. We apply algorithm A1 assuming $q = 0$ for set $\mathcal{S}'(0)$. Let the resulting link capacity vector be denoted by $y(0)$.

3. Assuming $c = y(0)$ and $c' = 0$, for each state $s \in \mathcal{S}''(0)$ we solve the following version of problem $\mathrm{F}(c, c', s)$:

$$Q(c,c',s) = \min \textstyle\sum_{d\in\mathcal{D}} z_d \tag{3.19a}$$

$$\textstyle\sum_{a\in\delta^+(v)} x_{ad} - \sum_{a\in\delta^-(v)} x_{ad} = \\ = \begin{cases} h(d) - z_d & \text{if } v = o(d) \\ -h(d) + z_d & \text{if } v = t(d), \\ 0 & \text{otherwise} \end{cases} \quad d \in \mathcal{D}, v \in \mathcal{V} \tag{3.19b}$$

$$\textstyle\sum_{d\in\mathcal{D}} x_{ad} \le (1 - \beta(e(a),s))c(e(a)) + c'(e(a)), \quad a \in \mathcal{A} \tag{3.19c}$$

$$x, z \ge 0 \text{ and continuous.} \tag{3.19d}$$

   In this way we obtain the values $T(s,0) := Q(c,c',s)$, which express the total *traffic not carried* in the states $s \in \mathcal{S}''(0)$ when no fibers are provided. Next, we compute the quantity $T(0) := \sum_{s\in\mathcal{S}''(0)} n(s) \cdot T(s,0)$ where $n(s)$ denotes the number of real weather states that correspond to the same state s in the reference set $\mathcal{S}$. Using $T(0)$ we compute an important quality measure, namely the *fraction of carried traffic* by the network averaged over all weather states in $\mathcal{W}$ considered in the optimization process. This value is given by the formula $AT(0) := \frac{H-T(0)}{H}$ where $H := \sum_{s\in\mathcal{S}} \sum_{d\in\mathcal{D}} n(s)h(d)$.

4. We look for the best network solution in terms of extending demand connectivity achieved by replacing a selected subset of $m \ge 1$ FSO links by fiber links. We first consider adding only one fiber link ($m = 1$). For that we simply examine each FSO link in $\mathcal{E}$ one by one. For a given fixed fiber link e, we update the sets $\mathcal{S}'$ and $\mathcal{S}''$, and apply algorithm A1 as above but assuming $q = 0$ except for $q_e = 1$. Then for the so obtained $y(1)$ we compute $T(1)$ in the same way as $T(0)$. After doing that for all links we finally select the link e^* with the smallest $T(1)$, i.e., the smallest amount of

traffic lost, and select the so defined network configuration for the optimal solution. The fraction of carried traffic is then defined as $AT(1) := \frac{H-T(1)}{H}$.

5. We repeat the above calculations for $m = 2$, i.e., for every pair of $(e, e') \in \mathcal{E}^{|2|}$, and find the best placement of a pair of fiber links (e^*, e'^*) that results in the smallest amount $T(2)$ of traffic lost. The fraction of carried traffic $AT(2)$ is defined analogously to $AT(1)$, using $T(2)$ instead of $T(1)$.

6. For $m \geq 3$ we apply a simplified approach: the choice of the m-th fiber is done by adding the best choice fiber link to the set of $m-1$ fiber links already found for the $m-1$ case. The values of $AT(m)$ are calculated as before, using appropriate $T(m)$ values. Clearly, once $T(m)$ becomes equal to 0, Phase 1 is terminated and the so obtained selection of fiber links is used in Phase 2.

Network optimization procedure - Phase 2

7. We optimize the network for selected cases of link K-sets, fixing the sets of $m = 0, 1, \ldots$ fiber links found in Phase 1. Since in all cases we assume that for all FSO links the link degradation ratio $\beta(e)$ is below 0.5, we use a different formula for $\beta(e, s(u))$ when $u_{v(e)} = u_{w(e)} = 1$ namely $\beta(e, s(u)) = 2\beta(e)$ (instead of $\beta(e, s(u)) = 2\beta(e) - \beta(e)^2$). Thanks to that we can reduce the computation time of the feasibility test whose objective function is now modified as follows:

$$W(c, c') = \max\Big\{ \sum_{d\in\mathcal{D}} \lambda_d^{t(d)} h(d) - \sum_{e\in\mathcal{E}} \Pi_e\big((1 - \beta(e)(u_{v(e)} + u_{w(e)}))c(e) + c'(e)\big)\Big\}. \tag{3.20}$$

8. The vectors y obtained for the considered list of K-sets and the three cases of $m = 0, 1, 2$ fibers (in each case vector q is predefined), are tested for the traffic loss $T(m)$ they induce for the original state set $\mathcal{S}$ in the same way as in Phase 1. Then the fraction of carried traffic $AT(m)$ is calculated as in Phase 1.

7 Concluding remarks

The contribution of our work consists in studying a network dimensioning problem taking into account resilience to multiple partial link degradation. In contrast to related investigations on resilient networks, we deal with the problem involving a very large number of degradation states, described by the so called uncertainty set (an instance of the budgeted uncertainty set formally described in [4]) for which we propose an optimization model together with a cut generation solution algorithm, and use it for a numerical study of a specific case of robust FSO network dimensioning.

In the chapter we have presented a robust optimization approach to modular dimensioning of FSO networks taking into account degradation of link capacities due to weather conditions. Central to the approach is a cut-generation algorithm for minimizing the cost

of links for a network robust to all link failure states (where different link losses different portions of their nominal capacity) described by a given K-set (uncertainty polytope). In order to optimize a realistic network, we first analyze the weather data and produce a representative set of its link failure states (called the reference failure set). Then we dimension the network (using Algorithm 2) assuming uncertainty K-sets for several values of parameter K and check to what extent the states in reference failure set are covered by the K-set based solution.

In the second part of the chapter, we have presented a robust optimization approach to modular dimensioning of hybrid FSO/fiber networks resilient to degradation of link capacities caused by weather conditions. In such networks, FSO wireless links are supported by terrestrial optical fiber connections in order to improve the resilience in question. In our approach, we first optimize link capacity (i.e., we solve the network dimensioning problem) taking into account all weather states for a given year, for which we produce a representative set of the link degradation states (called the reference degradation set). Then we dimension the network assuming a special (uncertainty) set of link degradation states represented by the so-called link K-set. Finally, we examine how good is the traffic satisfaction in question as compared to the satisfaction achieved with the solution obtained when all states in the reference set are considered in optimization explicitly.

Part 2

This second part of this thesis is composed of Chapters 4, 5, 6 and the Conclusion Chapter. In this part we will focus more on the improvements and the generalization of our approach. Chapter 4 tackles the problem of the so-called uncertainty sets (or uncertainty polytopes). We propose to approximate the reference failure set with a special kind of virtual failure set called K-set, parameterized by an integer value K, where K is less than or equal to the number of all links in the network. In Chapter 5 we present extensive numerical studies illustrating the efficiency of our approach to robust FSO network dimensioning. We performed our tests on two network instances corresponding to *polska* and *nobel − germany* that are available at *sndlib.zib.de*. Chapter 6 describes a realistic FSO network instance. We call this instance PMAN (Paris Metropolitan Area network) since it was created using the real data for the Paris metropolitan area. We have performed several tests on this network instance and the results are presented in the last part of the chapter. We conclude this part summarizing the work we have done and we give some possible future directions we will work on.

Model Enhancement

The FSO networks considered in this thesis are characterized by fluctuations of capacity currently available on the links caused by adverse weather conditions. For this reason, optimization of FSO becomes complex as it has to cope with degradation of data transmission on the FSO links at the network design stage. As a continuation of our previous studies, this issue is undertaken below by introducing a new way of characterizing link degradation states for optimization purposes.

In Chapter 3 we have proposed to approximate the reference failure set with a special kind of virtual failure set called K-set, parameterized by an integer value K, where K is less than or equal to the number of all links in the network. For a given K, the K-set contains all states corresponding to all combinations of K, or less, simultaneously affected links. In this chapter we consider simultaneous degradations of K nodes (meaning degradation of all adjacent links), instead of degradation of all possible combinations of K links. This allows achieving more cost-efficient link-dimensioning for the same or even higher traffic satisfaction, as compared to the previous characterization.

Inspired by the hitting set problem a new idea was to find a large number of subsets of two or three affected links and to use all possible combinations (composed of 2 or at most 3 of these subsets) to build a new kind of virtual failure set that covers as much as possible the reference failure set that we got from the study of real weather data records. Next, is this new failure set that will serve as input for our cut-generation algorithm so that we can dimension the network at a minimum cost and for a satisfactory demand realization. Numerical results will illustrate the effectiveness of our findings.

Introduction

In our works on FSO given in the previous chapters, we presented optimization techniques for the problem of fluctuations in link capacities of communication networks caused by adverse circumstances, such as bad weather affecting the received signal strength in wireless networks. This problem is complex since it requires consideration of the state-dependent capacities for all network traffic demands in all possible network states caused by weather degradations. Closely related to that is the issue of preparing the data required to characterize the set of link degradation states for the dimensioning problem. Such data are obtained by translating weather states into network states characterized by link

degradations ratios (presented in Chapter 2). The set of the considered link degradation states, called the reference set of states, typically contains a large number of states. Furthermore, we need to dimension the network to deal with future weather states as well, which motivates the need for a compact characterization of the reference sets. In this chapter we propose a version of uncertainty sets that estimate the original sets of degradation states more accurately. First we consider an enhanced type of a K-set, where instead of link degradations we consider node degradations. The main motivation for this enhancement comes from the nature of degradation caused by the nature of weather conditions. That is, when bad weather hits a given subarea of the network area then it affects the transceivers in all nodes in the subarea and, in consequence, all links incident to the affected nodes are degraded simultaneously. This results in a sort of geographic-aware uncertainty sets, which are expected to cover the set $\mathcal{S}$ more effectively than link K-sets.

Another alternative characterization of the link degradation states that we will explore, captures the incidence of a group of links in several degradation states; more precisely, we find the most frequent subsets of links simultaneously affected by the weather phenomenona. For that we define a special kind of uncertainty set, called a covering K-set, using a generalization of the minimum hitting set problem. This uncertainty set comes as an alternative of former uncertainty sets already proposed and investigated before. The presented considerations are illustrated by a numerical study.

1 New approximation of the set of degradation states

1.1 Optimization problem

In our considerations we assume an undirected network graph $\mathcal{G} = (\mathcal{V}, \mathcal{E})$ composed of the set of nodes $\mathcal{V}$ and the set of undirected links $\mathcal{E} \subseteq \mathcal{V}^{|2|}$, where $\mathcal{V}^{|2|}$ is the set of all 2-element subsets of $\mathcal{V}$, i.e., each link $e \in \mathcal{E}$ represents and unordered pair $\{v, w\}$ of nodes for some $v, w \in \mathcal{V}$ ($v \neq w$). The unit capacity cost on a given link e is denoted by $\xi(e)$. As the network links are exposed to adverse weather conditions, we consider an explicit list of *link degradation states* $\mathcal{S}$ induced by considered set of weather conditions.

In fact, for given link degradation state list $\mathcal{S}$, the considered problem is not too difficult to solve by the commercial solvers (like CPLEX). However, an issue appears here since when the network is to be optimized, the list of states is not known and can only be estimated based on historical weather records for the network area. Such an estimation can be done for, say, a coming year by using the data for the past year but this does not guarantee a reliable estimations due to weather variations and enormous number of possible link degradation states implied by future weather conditions.

To deal with this problem the so called uncertainty sets can be used (we have presented this uncertainty sets in Chapter 3, Section 4.3. Such sets, described in a compact way, can be used instead of the explicit list of link degradation states $\mathcal{S}$, and when properly constructed they can provide solutions that cover most of the real weather conditions with

a reasonable total capacity cost $C(y)$. To apply this approach the problem formulation must be adjusted in order to use an uncertainty set instead of the explicit list $\mathcal{S}$ to characterize link degradation states; such formulations for certain types of uncertainty sets (the so called K-sets), together with a specialized solution algorithm, are given in Chapter 3, Section 4.3. As compared to $\mathcal{S}$, these K-sets contain a limited number of link degradation sets, and are compactly described through a system of inequalities.

1.2 Main problem formulation in node K-set

As we explained, instead of using an uncertainty set including all states, now we use a special kind of "idealized" state sets, called K-sets, parameterized by an integer value K less than or equal to the number E of links in the network. For a given $0 \leq K \leq E$, the K-set contains the states corresponding to all combinations of K, or less, links simultaneously degraded. The proposed approach consists of using K-sets (for a set of selected values of parameter K) as an input (instead of the true state set $\mathcal{S}$) in the resilient network dimensioning problem, and then testing the so obtained optimal link capacities (called the robust solution) on the reference degradation set S.

In the present study we consider an enhanced type of a K-set, where instead of link degradations we consider node degradations. The main motivation for this enhancement comes from the nature of degradation caused by the nature of weather conditions. Such a K-set, denoted with $\mathcal{Q}(K)$, is defined, for any integer $K = 1, 2, \ldots, V$, as the set of binary vectors $\mathcal{Q}(K) := \{u = (u_v,\, v \in \mathcal{V}) : \sum_{v\in\mathcal{V}} u_v \leq K,\, u_v \in \{0,1\}\}$. Each $u \in \mathcal{Q}(K)$ determines a state $s(u)$ by assuming that, for each $e \in \mathcal{E}$, the degradation ratio $\beta(e, s(u))$ is defined through equality $1 - \beta(e, s(u)) = (1 - \beta(e)u_{v(e)})(1 - \beta(e)u_{w(e}$ for a given fixed fraction $\beta(e)$ $(0 < \beta(e) \leq 1)$. It follows that $\beta(e, s(u)) := \beta(e)(u_{v(e)} + u_{w(e)}) - \beta(e)^2 u_{v(e)}u_{w(e)}$, $e \in \mathcal{E}$. We mention here that the new $\beta(e, s(u))$ is an enhancement to the previous version of $\beta(e)$. Thus, the support of vector u, i.e., $\{e \in \mathcal{E} : \beta(e, s(u)) > 0\}$ determines the set of links degraded in state $s(u)$, where each such link is degraded with ratio $\beta(e)$ (when only one of its end nodes is degraded) or $2\beta(e) - \beta(e)^2$ (when both end nodes of e are degraded). The set $\{s(u) : u \in \mathcal{Q}(K)\}$ of the states determined by K-polytope $\mathcal{Q}(K)$ will be denoted by $\mathcal{S}(K)$. In Chapter 5, the so described K-set will be called *node K-set* and denoted by "node(K)".

The solution approach for the problem involving the state set $\mathcal{S}(K)$ is based on algorithm A1 formulated in 3, Section 6.2.1. The difference is that now a modified feasibility test to generate the cuts is used: instead of feasibility tests (3.4) executed for each state s on

the explicit list of states $\mathcal{S}$, only one test is considered:

$$W(c,c') = \max\Big\{ \sum_{d\in\mathcal{D}} \lambda_d^{t(d)} h(d) - \sum_{e\in\mathcal{E}} \Pi_e (c(e)+c'(e)) + \\ + \sum_{e\in\mathcal{E}} \Pi_e \beta(e) c(e) (u_{v(e)} + u_{w(e)}) - \sum_{e\in\mathcal{E}} \Pi_e \beta(e)^2 c(e) u_{v(e)} u_{w(e)} \Big\} \tag{4.1a}$$

$$\Pi_e = \pi_{a(e)} + \pi_{a'(e)}, \quad e \in \mathcal{E} \tag{4.1b}$$

$$\Pi_e \le 1, \quad e \in \mathcal{E} \tag{4.1c}$$

$$\lambda_d^{o(d)} = 0, \quad d \in \mathcal{D} \tag{4.1d}$$

$$\lambda_d^{t(a)} - \lambda_d^{o(a)} \le \pi_a, \quad a \in \mathcal{A}, d \in \mathcal{D} \tag{4.1e}$$

$$\sum_{v\in\mathcal{V}} u_v \le K \tag{4.1f}$$

$$\Pi, \pi \ge 0 \text{ continuous; } \lambda \text{ continuous; } u \text{ binary.} \tag{4.1g}$$

Certainly, to obtain a proper mixed-integer programming formulation we need to eliminate non-linearities in (4.1a) induced by products $\Pi_e \cdot u_{v(e)}$, $\Pi_e \cdot u_{w(e)}$ and $\Pi_e \cdot u_{v(e)} \cdot u_{w(e)}$, where $u_{v(e)}, u_{w(e)}$ are binary and Π_e is between 0 and 1. This can be easily done by introducing, for each such product, a continuous non-negative variable X'_e, X''_e and Y_e, respectively, together with additional constraints $X'_e \le \Pi_e, X'_e \le u_{v(e)}, X'_e \ge \Pi_e + u_{v(e)} - 1$, $X''_e \le \Pi_e, X''_e \le u_{w(e)}, X''_e \ge \Pi_e + u_{w(e)} - 1$, $Y_e \le \Pi_e, Y_e \le u_{v(e)}, Y_e \le u_{w(e)}, Y_e \ge \Pi_e + u_{v(e)} + u_{w(e)} - 2$ that imply $X'_e = \Pi_e u_{(v(e)}$, $X''_e = \Pi_e u_{(w(e)}$ and $Y_e = \Pi_e u_{v(e)} u_{w(e)}$. Note that for any fixed feasible u the value of the objective function defined by the right-hand side of (4.1a) maximized over λ, π, Π is equal to $W(c,c',s)$ (see (3.4a)) for $s = s(u)$. Since in (4.1) we are maximizing also over u, we finally observe that $W(c,c') = \max_{s\in\mathcal{S}(K)} W(c,c',s)$, as required.

Now assume that $W(c,c') > 0$. Then, the Benders inequality induced by the optimal solution $\lambda^*, \pi^*, \Pi^*, u^*$ of (4.1) is as follows:

$$\sum_{e\in\mathcal{E}} \Pi_e^* \big(1 - \beta(e)(u^*_{v(e)} + u^*_{w(e)}) + \beta(e)^2 u^*_{v(e)} u^*_{w(e)}\big) M y_e + \sum_{e\in\mathcal{E}} \Pi_e^* L q_e \ge \sum_{d\in\mathcal{D}} {\lambda_d^{t(d)}}^* h(d). \tag{4.2}$$

Observe that in general the state set $\mathcal{S}(K)$ does not have to reflect any realistic set of states, in particular the values $\beta(e, s(u))$ need not correspond to real degradation ratios from the set $\mathcal{R}$ defined in Section 3.1. In fact, set $\mathcal{S}(K)$ is meant to be used for network dimensioning so that for properly chosen parameters K and $\beta(e)$, $e \in \mathcal{E}$, the resulting link capacities y, q will be sufficient to carry the demand traffic in a given realistic reference degradation state $\mathcal{S}$ and the cost of y, q will be near to the optimal cost $C(\mathcal{S})$ for problem (3.2). Our aim is to help network control to achieve a carefully designed and operated network. Our concern is not the short-term operational time-horizon, but the long-term planning horizon, and our aim is to elaborate a link dimensioning procedure best suited to most of the expected weather conditions. In this aspect, the proper choice of parameters K and $\beta(e)$ means the best parameter combination giving a low cost and high traffic satisfaction with respect to the reference degradation set composed of link degradation sets induced by weather states recorded during a given time period (what we may call a realistic degradation set). We show in our numerical results that for different values of K

we have different values of traffic satisfaction for different total link cost. This information may be useful to network managers to decide on appropriate link dimensioning according to their economical strategy.

Finally, we note that formulation (4.1) can be extended to handle combinations of both links and nodes degradations in a unique K-set. We recall that the problem in hand is $\mathcal{NP}$-hard and remains hard to solve for large size instances.

1.3 Compact uncertainty sets

Let $\mathcal{F} \subseteq 2^{\mathcal{E}}$ be a given family of subsets of the set of links $\mathcal{E}$ and let $\Delta(e, f)$ denote the binary incidence coefficient equal to 1 if, and only if, $e \in f$ for $f \in \mathcal{F}$. Now, for a given integer parameter $K \geq 1$, consider a set $\mathcal{U}(K, \mathcal{F}) \subset \{0,1\}^{|\mathcal{E}|+|\mathcal{F}|}$ described by the following system of inequalities in binary variables $u = (u_e : e \in \mathcal{E})$ and $y = (y_f : f \in \mathcal{F})$:

$$\sum_{f \in \mathcal{F}} y_f \leq K \tag{4.3a}$$

$$u_e \leq \sum_{f \in \mathcal{F}} \Delta(e, f) y_f, \quad e \in \mathcal{E} \tag{4.3b}$$

$$u_e \in \{0,1\},\ e \in \mathcal{E};\ \ y_f \in \{0,1\},\ f \in \mathcal{F}. \tag{4.3c}$$

The purpose of introducing $\mathcal{U}(K, \mathcal{F})$ is to define the so called *uncertainty set*, which is a set of u vectors $\mathcal{U}'(K, \mathcal{F})$ that describe a list of degradation states. The definition is as follows:

$$\mathcal{U}'(K, \mathcal{F}) := \{u : \exists y \in \{0,1\}^{|\mathcal{F}|},\ (u, y) \in \mathcal{U}(K, \mathcal{F})\}. \tag{4.4}$$

The idea is that each vector $u \in \mathcal{U}'(K, \mathcal{F})$ defines a set $s(u) := \{e \in \mathcal{E} : u_e = 1\}$ of degraded links. Assuming that each link is in all states degraded with the same link degradation ratio $\beta(e)$, we get a full description of the link degradation states determined by a given uncertainty set.

In fact, the so introduced notion of uncertainty set is a generalization of some previously used notions. To illustrate this point let us first consider the family $\mathcal{F} = \{\{e\} : e \in \mathcal{E}\}$. Since in this case we can identify the singletons $\{e\}$ composing family $\mathcal{F}$ with the corresponding links, the set $\mathcal{U}(K, \mathcal{F}) \subset \{0,1\}^{2|\mathcal{E}|}$ is defined by:

$$\sum_{e \in \mathcal{E}} y_{\{e\}} \leq K \tag{4.5a}$$

$$u_e \leq \sum_{e' \in \mathcal{E}} \Delta(e, \{e'\}) y_{\{e'\}}, \quad e \in \mathcal{E} \tag{4.5b}$$

$$u_e \in \{0,1\},\ e \in \mathcal{E};\ \ y_{\{e\}} \in \{0,1\},\ e \in \mathcal{E}. \tag{4.5c}$$

Clearly, the resulting uncertainty set $\mathcal{U}'(K, \mathcal{F})$ is defined simply like this:

$$\sum_{e \in \mathcal{E}} u_e \leq K \tag{4.6a}$$

$$u_e \in \{0,1\},\ e \in \mathcal{E}. \tag{4.6b}$$

The above set describes in a compact way the list of states $s(u)$, $u \in \mathcal{U}'(K, \mathcal{F})$, containing all the states corresponding to simultaneous degradation of a subset of k links (there are $\binom{|\mathcal{E}|}{k}$ of such states) for all $k = 0, 1, \ldots, K$. The so defined uncertainty set corresponds to the notion of *link K-set* presented before.

Another kind of a known uncertainty set is obtained for $\mathcal{F} = \{\delta(v) : v \in \mathcal{V}\}$, where $\delta(v)$ denotes the set all links in $\mathcal{E}$ incident with node $v \in \mathcal{V}$. Then the set is as follows:

$$\sum_{v\in\mathcal{V}} y_{\delta(v)} \leq K \tag{4.7a}$$

$$u_e \leq \sum_{v\in\mathcal{V}} \Delta(e, \delta(v)) y_{\delta(v)}, \quad e \in \mathcal{E} \tag{4.7b}$$

$$u_e \in \{0,1\},\ e \in \mathcal{E};\ \ y_{\delta(v)} \in \{0,1\},\ v \in \mathcal{V}. \tag{4.7c}$$

Simplifying the notation by using variables y_v instead of $y_{\delta(v)}$, we can rewrite (4.7) like this:

$$\sum_{v\in\mathcal{V}} y_v \leq K \tag{4.8a}$$

$$u_{\{v,w\}} \leq y_v + y_w, \quad \{v, w\} \in \mathcal{E} \tag{4.8b}$$

$$u_e \in \{0,1\},\ e \in \mathcal{E};\ \ y_v \in \{0,1\},\ v \in \mathcal{V}. \tag{4.8c}$$

The set $\mathcal{U}'(K, \mathcal{F})$ resulting from (4.8) corresponds to the notion of *node K-set* considered in [39].

1.4 Covering K-sets

Below we will show a way to find families $\mathcal{F}$ for constructing uncertainty sets for a given (possibly very large) state list $\mathcal{S}$.

Let us assume that all states s in $\mathcal{S}$ (each representing a set of simultaneously degraded links) have cardinality greater or equal to a given integer parameter p. Now, let $X^{|p|}$ denote the family of all p-element subsets of a given set X, and consider the following binary programming problem:

$$\min \quad \sum_{f\in\mathcal{E}^{|p|}} x_f \tag{4.9a}$$

$$\sum_{f\in s^{|p|}} x_f \geq K, \quad s \in \mathcal{S} \tag{4.9b}$$

$$x_f \in \{0,1\}, \quad f \in \mathcal{E}^{|p|}. \tag{4.9c}$$

Finally we define the family $\mathcal{F} := \{f \in \mathcal{E}^{|p|} : x^*_f = 1\}$ (where x^* is an optimal solution of (4.9)) and call the so obtained uncertainty set $\mathcal{U}'(K, \mathcal{F})$ the *p-covering K-set* of the list of states $\mathcal{S}$. Note that formulation (4.9) is actually a generalization of *minimum hitting set problem* — a well known NP-hard combinatorial problem [73].

The so obtained family $\mathcal{F}$ may be seen as containing those subsets (of reasonable size p) of links that are frequently simultaneously affected, and we assure protection against link

degradation states that contain all links included in up to K of such subsets.

To illustrate the concept of p-covering K-set, consider a simply network instance with 11 links ($\mathcal{E} = \{e_1, e_2, \ldots, e_{11}\}$) and the set $\mathcal{S} = \{s_1, s_2, \ldots, s_7\}$ composed of 7 states given in Table 4.1.

Table 4.1 – An example of 2-covering K-sets.

state set	composition	$p = 2, K = 1$	$p = 2, K = 2$
s_1	$\{e_2, e_3, e_5, e_7, e_9, e_{11}\}$	$\{e_7, e_9\}$	$\{e_7, e_9\}, \{e_2, e_3\}$
s_2	$\{e_2, e_4, e_6, e_7, e_8\}$	$\{e_2, e_4\}$	$\{e_2, e_4\}, \{e_6, e_8\}$
s_3	$\{e_3, e_5, e_6, e_8, e_{10}, e_{11}\}$	$\{e_6, e_8\}$	$\{e_6, e_8\}, \{e_5, e_{10}\}$
s_4	$\{e_1, e_2, e_4, e_7, e_8, e_9, e_{10}\}$	$\{e_7, e_9\}$	$\{e_7, e_9\}, \{e_2, e_4\}$
s_5	$\{e_2, e_3, e_6, e_7, e_9, e_{10}\}$	$\{e_7, e_9\}$	$\{e_7, e_9\}, \{e_2, e_3\}$
s_6	$\{e_1, e_2, e_4, e_6, e_8, e_{11}\}$	$\{e_2, e_4\}$	$\{e_2, e_4\}, \{e_6, e_8\}$
s_7	$\{e_2, e_4, e_5, e_6, e_9, e_{10}\}$	$\{e_2, e_4\}$	$\{e_2, e_4\}, \{e_5, e_{10}\}$

Solving the binary problem (4.9) for $p = 2, K = 1$, we obtain the following family $\mathcal{F}$ (composed of three 2-link subsets of $\mathcal{E}$) defining the corresponding 2-covering 1-set: $\{\{e_2, e_4\}, \{e_6, e_8\}, \{e_7, e_9\}\}$. For $p = 2$ and $K = 2$, the resulting family defining the 2-covering 2-set has 2 additional subsets: $\{e_2, e_3\}, \{e_5, e_{10}\}$. In the above table, columns 3 and 4 illustrate how the sets in $\mathcal{S}$ are actually covered by the sets from the corresponding families $\mathcal{F}$.

Note that an advantage of using covering K-sets is that they are defined using the information of the actual list of states $\mathcal{S}$ that is to be approximated; this feature is not present when specifying link or node K-sets.

2 Concluding remarks

In the chapter we have presented some new ideas on the robust optimization problem related to FSO network resilient to link capacities degradation caused by weather conditions. Our solution approach optimizes link capacity taking into account all weather states for a given time period, for which we determine a reference set of (link capacity degradation) states. One of the main issues here is the potential (large) size of the reference set, which may make the optimization problem computationally untraceable for large networks.

To handle this, in our previous chapters we used the so called link K-sets (where up to K arbitrary links can be degraded simultaneously). In this chapter we have presented a new uncertainty set that we call node K-sets (where up to K arbitrary nodes can de degraded simultaneously) where K specifies the number of areas (represented by groups of specific links or nodes) that can be simultaneously affected by bad weather.

Furthermore, we have investigated a more general notion of K-set, called p-covering K-set, where the link groups are more appropriate for the reference set approximation, and show how to build such groups of links. In the following chapters, we test these new uncertainty sets for a selected set of values of parameters p and K ($p = 2$ and $K = 2, 3$) and check to

what extent the demand traffic matrix is satisfied by the obtained solution in all states in the reference set of states $\mathcal{S}$, and at what cost.

Numerical Study

1 Introduction

Below we present results of a numerical study illustrating the performance of our optimization approach for various weather scenarios. All numerical calculations were performed on an Intel (R) Core (TM) i7-4610M, 3.0 GHz computer with 16 GB of RAM. The algorithms were coded in Java and the optimization problems were solved with IBM ILOG CPLEX 12.6 (using Concert Technology) running with the default setting.

In our approach, we have assumed global rerouting, that is we are allowed to reroute all traffic, affected or not, for each network state. Then, we solve the link dimensioning problem for various weather scenarios. More precisely, we first optimize link capacity (i.e., we solve the network dimensioning problem) taking into account all weather states for the time horizon, for which we produce the reference set of states. Then we dimension the network assuming a special (uncertainty) set of link degradation states represented by the so-called link, node K-set or p-covering K-set where K specifies the number of areas (represented by network links, nodes or group of links) that can be simultaneously affected by weather conditions. For all the considered K-sets the degradation ratio $\beta(e) = 0.50$ was assumed uniformly for all affected links in the network. This value represents the degradation ratio of more than 80% of affected links all over the degradation states (not considering the normal states, i.e. corresponding to sunny days with no link affected), while two-third of such states contain only links with the same degradation ratio $\beta(e) = 0.50$. We run the optimization approach for a selected set of values of parameter K, checking to what extent the demand traffic matrix is satisfied by the K-set based on solution in all states in the reference degradation set. Finally, we have examined the percentage of carried traffic achieved for different K-sets as compared to carried traffic observed when all states in the reference set are tested for the obtained dimensioned network.

We have tested our optimization approach on three network examples The first two networks are derived from the instance called *nobel-germany* and *polska* that can be found in SNDlib [10]. The third network instance we use for our numerical studies is called PMAN (Paris Metropolitan Area Network) since it was created using the real data for the Paris Metropolitan Area. It should be noted that although all the data used to construct the PMAN instance are real, the instance itself does not exist in reality and was elaborated only for our own purpose. A full characterization of PMAN, together with numerical results, are given in Chapter 6.

2 Different weather scenarios

As indicated above, the weather conditions are determinant for a reliable transmission of data under FSO technology, and as such it is crucial to measure the limits of weather conditions with respect to different geographical areas. To do this, we need first to build a representative weather scenario set. To be as realistic as possible, we will make all our evaluations for European cities. Using the weather records from [74], three different weather scenarios were constructed following the guidelines of the Köppen-Geiger climate classification system [75]: the first scenario, typical for southern Europe (called "Mediterranean climate" scenario), the second, typical for middle Europe (called "moderate continental climate" scenario), and the third, typical for northern Europe (called "cold continental climate" scenario). These scenarios were then used to estimate link degradation state for each hour of a typical year for *nobel-germany*. A detailed description of such an estimation process is given in the next section.

2.0.1 Determining weather scenarios

As mentioned above, weather conditions are a very important factor for reliable transmission when FSO technology is used. Therefore, to do our estimation we have investigated historical weather data for 26 cities in Europe taken from [74, 75], and deduced groups of cities with respect to the aforementioned three categories of weather scenarios, namely Mediterranean climate, Moderate continental climate and Cold continental climate categories. Respectively, in the Mediterranean climate category cities, we have included:

- Valletta
- Marseilles
- Athens
- Lisbon
- Madrid
- Nice
- Monaco
- Tirana
- Barcelona
- Podgorica

In the second group (moderate continental climate) there are included 8 cities:

- Milan

- Paris
- Amsterdam
- Copenhagen
- Birmingham
- Dublin
- Glasgow
- Brussels

In the last one (cold continental climate) we have considered:

- Helsinki
- Oslo
- Stockholm
- Warsaw
- London
- Vienna
- Zurich
- Hamburg

Next, for each group we have deduced the average number of sunny and partially cloudy days, foggy, thick fog, snow and storm snow days for a period of 4 years (2014-2017). Taking into account the average duration of fog, thick fog, snow and storm snow phenomenon's, we have deduced the number of states affected with respectively 0.5, 0.75 and 1.0 or mixes degradation ratio. Selected characteristics of link degradation states for *nobel-germany* corresponding to all $365 \times 24 = 8760$ hours of the year are given in Table 5.1.

Table 5.1 – Distribution of link degradation states

	Mediterranean climate	moderate continental climate	cold continental climate
nominal states	68.46%	47.96%	27.47%
degradation ratio 50%	20.95%	25.48%	30.01%
degradation ratio 75%	3.76%	9.45%	15.18%
degradation ratio 100%	0.6%	4.01%	7.43%
various degradation ratios	6.23%	13.01%	19.91%

The second step for generating the weather scenarios, is deciding the distribution of weather phenomenon's on the different links of the target network, *nobel-germany*. First,

all link states in sunny or partially cloudy days are taken as fully operational. For the other states, we have proceed as follows: we have first created several groups of a fixed number of affected links included in each of them and then we increase in a progressive way the number of affected links. For instance, the first group contains 3 links, the second 5 links, the third has 8 links, and so on until the last one which contains almost all links of the network. For each group we have generated randomly a geographical area and choose the desired number of links in the neighborhood of the area (in our case this is realized by fixing on or some neighbor nodes and choosing among links adjacent to these nodes). In the case of cold continental climate category, we have assumed that states generated for each group of links mentioned above will have the same weight while for the Mediterranean climate and moderate continental climate these weights are taken as decreasing with the number of links included in the group.

The first weather scenario corresponds to Mediterranean climate conditions. In this case, among the 8760 hourly states, 68.46% of them are with no degraded links. For the remaining part, we have 20.95% of link with degradation ratio 0.5, 3.76% with link degradation ratio 0.75 and 0.6% of links totally lost (degradation ratio 1.0). The remaining states, 6.23%, are states where we have in the same time links with degradation 0.5, 0.75 or 1.0.

For the second weather scenario we have considered an average representation of weather conditions. The observed conditions were translated into the multiple partial link degradation states corresponding to all hourly periods in the considered one-year time horizon, which gives 365*24 = 8760 "hourly" states in total. In this set of hourly states there are 47.96% states with no affected links at all (these are the nominal states). In 25.48% of cases we have states with degradation ratio of 0.5, in 13.10% the transmission degradation ratios are 0.5, 0.75 or 1.0. We consider 9.45% of these hourly states with a transmission degradation ratio equal to 0.75. Finally, there is a small number of hourly states with a few links affected in 100% (link degradation ratio 1 = total loss of communication), just 4.01%.

The third weather scenario is called the cold continental climate scenario. To build this scenario we have done some assumptions. First of all when we have in the same time both snow and fog, the snow impact is stronger than the fog's one. For this we take in consideration only snow precipitations. Furthermore, a snow storm can last 3 hours at minimum and is followed from a period of 2-3 hours of dense fog. To calculate this scenario we took in consideration the weather conditions with an average number of snowing days (101 snowing days per year). We found out that nearly 1/3 of snowing days fall in the category of snow storm. So, we have 101 (days)*1/3 (probability of storm)*3 (hour duration of storm) =101 hourly states with snow storm with the link capacity is totally lost. Moreover we have 101 (days)* 2 (hours of dense fog) = 202 hourly states. For the same city we have 188 days of fog per year. Knowing that fog and snow are weather elements that come together and the fact that the fog can be dense (visibility less than 1 km) for a duration of 4 hours, we obtain (188-101)* 4 hours = 348 hourly states with dense fog (in our work we consider this as total link degradation). In summary, we have 101+ 202 + 348= 651 hourly states with total link degradation (or 7.43% of all hourly states).

For the links with a degradation ratio 0.75 we have 101* 1/3*24 + (188-101)* 6 =1330

hourly states or 15.18% of all states. For the remaining states we have 2406 hourly states (or 27.47%) with nominal capacity, 30.01% with transmission loss ratio of 0.5 and 19.91% with transmission loss ratio of 0.5, 0.75 or 1.0. The reader can find the data for these scenarios in [76].

3 Results for test networks

The discussion presented in this section aims at illustrating various aspects of the proposed robust approach based on Algorithm 2 on a reasonable (but actually not real) FSO network example (a slightly different variant of the considered example was studied in [77]). To speed up the calculations we have considered only the linear relaxation of $\mathrm{P}(\mathcal{S})$.

3.1 Polska network

We have tested the proposed algorithm on a network example derived from the instance called *polska* that can be found in SNDlib (available at *sndlib.zib.de*). The original instance from SNDlib connects $V = 12$ nodes (metropolitan areas) and is composed of $E = 18$ undirected links. There are $D = 66$ undirected traffic demands expressed in Mbps. In our study we have examined a bi-directed version of *polska*, i.e., the basic network type considered, with $A = 2E = 36$ arcs and $D = 132$ demands, where each original (undirected) demand d has been split into two oppositely directed demands d', d'' linking the same nodes as d with $h(d') = h(d'') = \frac{h(d)}{2}$. The link module M is assumed to be equal to 1 Mbps, and the cost of one module on each link to 1 (i.e., $\xi(e) = 1$, $e \in \mathcal{E}$).

The reference set of failure states $\mathcal{S}$ for the *polska* study was obtained as described in Chapter 2. We analysed the weather states recorded over a one-year period (from August 16, 2014, to August 15, 2015) available at *www.worldweatheronline.com*. For the sake of simplicity only the weather conditions observed in the 12 metropolitan areas connected by the network were taken into account, assuming that the link connecting two given areas is affected by the worse of the weather condition in the two areas. The observed conditions were translated into the multiple partial link failure states corresponding to all hourly periods in the considered one-year time horizon, which gives $365 \times 24 = 8760$ "hourly" states in total. In this set of hourly states (denoted with $\widetilde{\mathcal{S}}$) there are 60.77% states with no affected links at all (these are the nominal states). It also happens that in the majority of states in $\widetilde{\mathcal{S}}$ the 4-QAM modulation and coding scheme is applied on each affected link instead of 16-QAM (i.e., the MCS used on a link in good weather conditions). This reduces the nominal capacity of the affected links by 50% (link failure ratio 0.5) – there are 39.15% of such states in $\widetilde{\mathcal{S}}$. In the remaining 0.08% of the hourly states, the MCS of some affected links is changed from 16-QAM to BSPK which reduces the nominal capacity by 75% (link failure ratio 0.75). Finally, there is a very small number of hourly states with a few links affected in 100% (link failure ratio 1 – total loss of communication). In terms of the average hourly state there are 89.3% of non-affected links, 10.7% of links with the failure rate 0..50, 0.017% links with the failure rate 0.75, and only 0.003% of

links totally failed (failure ratio 1). Finally, we observed that out of all the 8760 hourly states there are only 159 states that are mutually different – these states constitute the reference failure set $\mathcal{S}$ for *polska*.

In the reported numerical experiments we first solve (using Algorithm 2) the instances of problem P(K) (3.17) for all K-sets ($K = 0, 1, \ldots, 18$) assuming the failure ratio $\beta(e) = 0.25$ for all 18 links when they fail. After that, for each K, we calculate the volume of traffic that cannot be carried in the hourly states in the reference failure states list $\widetilde{\mathcal{S}}$ that are outside the set of states $\mathcal{S}(K)$, i.e., in the hourly states outside the set of states induced by the considered K-set assumed for robust optimization.

Below we present the first set of results computed for network *polska* by means of Algorithm 2, the cut generation-based optimization algorithm for K-sets described in Section 4.4. As already mentioned, we consider the linear relaxation of problem P(K) that assumes continuous link capacities y and hence the algorithm is limited to Phase 1. The results include the minimum cost for P(K) (Figure 5.1), and the number of Benders' cuts (3.9) generated to reach the optimal robust solution together with the total computation time in seconds (Figure 5.2).

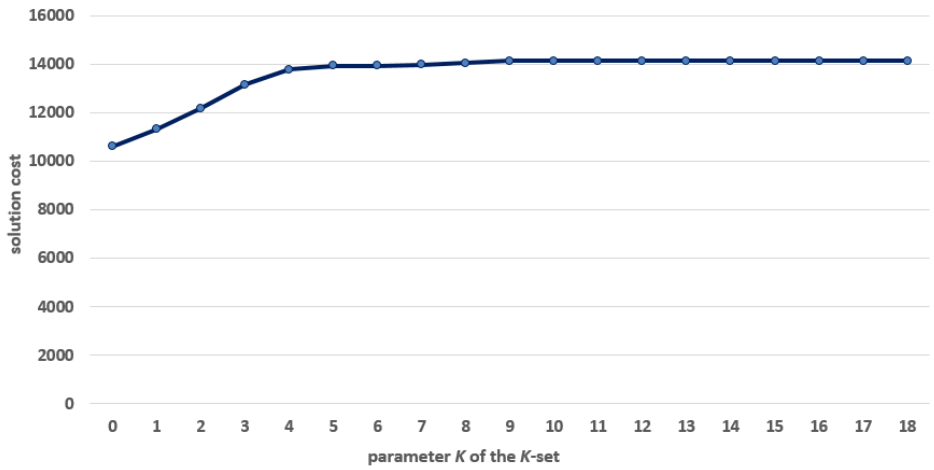

Figure 5.1 – network *polska* – cost for different K-sets obtained with Algorithm 2 for continuous link capacities case (Phase 1).

Figure 5.1 shows that the cost of the network becomes stable (and equal to 14 128 cost units) already for $K = 9$. This means that the additional capacity required to protect the traffic for all possible 9 (or less) simultaneous link failures (with the failure ratio 0.25) is already sufficient for all more severe simultaneous failures of K links where $K > 9$. In fact this additional capacity is equal to exactly 25% of the capacity required for unprotected network (case $K = 0$, with the cost equal to 10 596). This is not surprising since the network protected for the simultaneous failure of all 18 links with the failure ratio 0.25 (case $K = 18$) is obtained from the unprotected network by simply increasing the capacity of each link by 25%.

Concerning the time needed to obtain optimal solutions through the proposed cutting-plane algorithm, we note that the computation time of problem P(K) for all K is reasonable. However, we may expect that for large networks the algorithm, in its

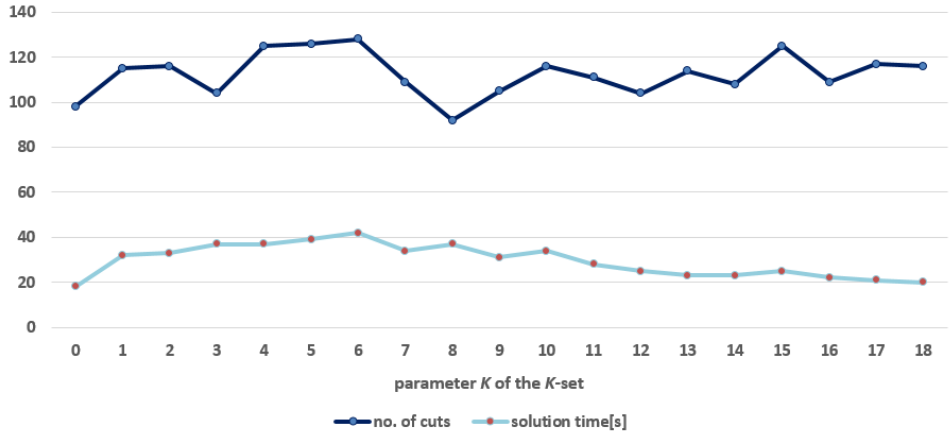

Figure 5.2 – network *polska* – computation time and number of cuts achieved with Algorithm 2 for continuous link capacities case (Phase 1).

current form, can exhibit excessive computation times. Thus, inclusion of additional valid inequalities (like those proposed in Section 5.2) could become important for speeding up the algorithm.

The upper graph shown in Figure 5.2 shows that there is no particular relationship between the number of the generated Benders' cuts (determined by the appropriate number left to the vertical axis) and the value of parameter K. The time required by Algorithm 2 to optimize the network (shown by the lower graph and determined by the numbers left to the vertical axis interpreted as seconds), however, does reveal such a relationship: the solution time is larger for intermediate values of K than for the values of K close to 1 or 18. This is because the separation time, i.e., the time spent in testing, which constitutes majority of time required by Phase 1 of Algorithm 2, is lower where K becomes closer to 0 or 18 as there are less combinations of failing links to be considered in the separation procedure. This phenomenon was also observed in [30] and the references therein.

To end this section, we mention that instead of using Phase 1 of Algorithm 2, for $K = 0$ the linear relaxation of problem (3.17) can be solved directly, just by allocating the whole demand volume $h(d)$ for each $d \in \mathcal{D}$ to its shortest (with respect to the costs $\xi(e)$, $e \in \mathcal{E}$) path. Note that the so obtained optimal link capacity vector y^* will specify an optimal solution also for the case $K = |\mathcal{E}|$ if the individual link capacity y^*_e for each link $e \in \mathcal{E}$ is divided by $1 - \beta(e)$ (provided all $\beta(e) < 1$). Moreover, the optimal demand routing x^* for $K = 0$ is optimal for $K = |\mathcal{E}|$ as well. The computational time required by the so described (shortest path allocation) approach is negligible.

3.1.1 Robustness with respect to the hourly states

Table 5.2 reports, for each K, the results of testing the robustness of the optimal link capacity vector $y^* = (y_e,\, e \in \mathcal{E})$ obtained for $\mathrm{P}(K)$ against all (hourly) states in the set $\widetilde{\mathcal{S}}$ of all 8760 hourly states. Certainly, formulation of $\mathrm{P}(K)$ assures that the optimal capacity vector is sufficient to carry all the traffic demands $h(d)$, $d \in \mathcal{D}$, in each state in $\mathcal{S}(K)$, i.e.,

in each state induced by $\mathcal{U}(K)$. Yet, for the states in the reference failure set $\mathcal{S}$ (recall that there are 159 states in $\mathcal{S}$) outside $\mathcal{S}(K)$)) this is not guaranteed. Hence, for each such state $s \in \mathcal{S} \setminus \mathcal{S}(K)$ we have computed the volume of traffic that cannot be satisfied in this state, using a linear programming formulation similar to (3.3). In the formulation, link capacities are set to $c(e) := \big(1 - \beta(e,s)\big)y^*_e$, $e \in \mathcal{E}$, and the routing is optimized in order to minimize the total traffic loss, i.e., $\sum_{d\in\mathcal{D}} z_d$, where $0 \le z_d \le h(d)$, and $h(d) - z_d$ is the actual total traffic carried for demand d is the considered state. In Table 5.2 column "average traffic carried [%]" is the average percentage of total traffic carried (with respect to the total traffic demand) over all of the 8760 states in $\widetilde{\mathcal{S}}$, and "not covered states [%]" is the percentage of the states in $\widetilde{\mathcal{S}}$ for which some part of the offered traffic is not realized.

K	average carried traffic [%]	not covered states [%]
0	97.36	39.23
1	98.86	26.06
2	99.64	9.41
3	99.88	3.08
4	99.96	1.26
5	99.99	0.19
6	99.99	0.21
7	99.99	0.09
8	99.99	0.24
9	99.99	0.09
10	99.99	0.08
11	99.99	0.08
...	...	...
18	99.99	0.08

Table 5.2 – network *polska* – coverage of the states outside $\mathcal{S}(K)$.

The first important observation is that, already for the network dimensioned for $K = 1$, it is possible to guarantee robustness for almost 74% of the hourly states (i.e., only about 26% of the states in $\widetilde{\mathcal{S}}$ experience carried traffic degradation) with the percentage of carried traffic equal to 98.86%. With increasing K, the percentage of the states with no traffic degradation continues to increase until $K = 5$, the case for which our computations reveal the second interesting fact: the network dimensioned for $K = 5$ is already robust against all the states in $\mathcal{S}(18)$, i.e., for the states with all $E = 18$ links or less affected with a failure ratio equal to 0.25 – this effect is clearly seen in Table 5.2. This means that taking into account all $\binom{18}{5}$ states with exactly 5 links affected with the failure ratio 0.25 makes the network robust to all multiple partial link failure states with $\beta(e) \equiv 0.25$. This "saturation effect", for which an intermediate factor of robustness may already offer full protection against all deviations in the input data can be observed also in other (telecommunication) applications of robust optimization (see for example [30] and its list of references). A similar discussion can be found in [78] in the context of demand uncertainty.

Table 5.2 reveals that any K is not sufficient to cover all the states in $\widetilde{\mathcal{S}}$ and at least 0.08% of hourly states cannot be fully covered when the failure ratio in $\mathcal{S}$ is assumed

to be 0.25. This is due to the existence of two "nasty" states in the reference failure set $\mathcal{S}$ that include several links affected with failure ratio 0.50 and even links whose entire capacity is lost. For those states the traffic matrix cannot be realized even for large values of K. As a consequence, protection for these two peculiar states, corresponding to about the 0.08% of all states, can never be granted, even imposing protection against the state with all links failing with failure ratio 0.25. Nevertheless, Table 5.2 gives some evidence that considering K-sets for network dimensioning instead of all the states in the reference failure set $\mathcal{S}$ can be effective in terms of the capability of traffic handling in the states outside those induced by the K-set. This is important, as the list of all possible states is in general not known or difficult to retrieve from available historical data.

3.1.2 A reasonable ad-hoc method

We describe here a reasonable ad-hoc method for estimating the proper value of K to be used in network dimensioning. By the proper value of K we mean the minimum K that ensures the maximum achievable coverage (as $K = 7$ in Table 5.2). We make use of this ad-hoc method for the general model (3.1). We use such a method in order to have an evaluation of the network dimensioning cost without using the direct optimization approach.

To illustrate what is the proper value of using the K-set (for a given K) in robust network dimensioning, we have performed the following calculations for the *polska* network topology with the above described set $\mathcal{S}$ of the degradation states derived from historical data. Consider the network dimensioned for the given K-set and the degradation ratios for the affected links $\beta(e)$=0.25. Differently from before, only for demonstration purposes, in this section we consider a $\beta(e)$=0.25. Thus, the network can carry a given nominal traffic demand matrix in all K simultaneous partial link failures with degradation ratio 0.25. For simplicity assume that the dimensioning results in the same capacity (equal to 1 capacity unit) assigned to all 18 links. Now we wish to (roughly) estimate the average percentage of the traffic carried over all the states in $\mathcal{S}$. Certainly, for the states in $\mathcal{S}$ that are also in the K-set this percentage is equal to 100%. Yet, for the states in $\mathcal{S}$ but not in the K-set, this percentage is in general less than 100%.

For each such state, the percentage in question is computed in the way best explained through the following example. Consider the state characterized by the vector of the link availability ratios (the link availability ratio is defined as 1 minus the link degradation ratio) given as

$$(0.75, 0.75, 0.75, 1, 1, 1, 1, 1, 1, 1, 1, 1, 1, 1, 1, 1, 1, 1).$$

In this state there are 15 links unaffected (i.e., with full capacity equal to 1) and 3 links affected with the 0.25 degradation ratio. Then, for all $K \geq 3$ this state is covered (meaning that the capacity of the affected links can be recovered) while for $K = 2$ there will remain one affected link with the capacity loss not recovered. Hence, in this state the ratio of available link capacity to the total nominal capacity is equal to $\frac{18-0.25}{18} = 0.9861$ (98.61%), and this value is taken as the percentage of traffic carried in the considered state. For a

state with the link availability ratio vector

$$(0.5, 0.75, 0.75, 1, 1, 1, 1, 1, 1, 1, 1, 1, 1, 1, 1, 1, 1, 1)$$

the corresponding percentage for $K = 2$ is equal to $\frac{18-0.5}{18} = 0.9722$ (97.22%) while for $K = 3$ it will be equal to $\frac{18-0.33}{18} = 0.9817$ (98.71%). Note that here we assume that when the failure reduces the available capacity according to the 0.50 degradation ratio (this is the case for the first link), and when the links are dimensioned to recover from the 0.25 degradation ratio (this was our assumption in network dimensioning), the capacity available for the first link should be calculated as $\frac{1}{0.75}0.5 = 0.67$ unit (i.e., as if the link had capacity equal to $\frac{1}{0.75} = 1.33$). Hence, when the link degradation ratio is 0.5, the remaining available capacity will effectively be equal to 0.67 and hence the link will lose only 0.33 of its (unit) capacity. (Observe that when the link availability ratio in a given state is equal to 0.75 then its available capacity is effectively equal to $\frac{1}{0.75}0.75 = 1$.) Along the same line, for the (very rare) cases when the transmission capacity of a link will be totally lost (degradation ratio 1), no fraction of the link capacity can be recovered.

The above described calculation has been done for all the states in $\mathcal{S}$ corresponding to all the hourly periods included in the considered one year time horizon, that is for 365×24 periods. The resulting average carried traffic percentage for all relevant values of parameter K ($1 \leq K \leq 18$) are reported in Table 5.3. Certainly, this calculation gives only a rough estimation of the amount of the expected carried traffic in the case of failures outside the K-sets, and a more precise calculation is needed when dealing with realistic network configurations.

Yet, the results presented in Table 5.3 give some evidence that considering the K-sets for network dimensioning instead of all possible states can be effective in terms of the capability of traffic handling in the states outside the K-set. This is important as the list of all possible states is in general not known or difficult to get.

Table 5.3 – Average percentage of traffic carried vs. K.

K	estimated average capacity covered [%]
1	89,07142857
2	92,73809524
3	95,32142857
4	97,80952381
5	98,09523809
6	98,70833333
7	98,83928571
8	99,15833333
9	99,19642857
10	99,40685238

When we compare Table 5.2 and Table 5.3 we see that the method works for both the directed and undirected cases (see Section 5.1), but not for the bi-directional links case assumed in the above discussed study, and, for that matter, in the study presented below.

3.2 Network nobel-germany

In this section we will discuss results for a moderate-size network example derived from the instance called *nobel-germany* that can be found in SNDlib [10]. The instance is composed of 17 nodes and 26 undirected links, and there are 121 undirected traffic demands (so that only 89% of all $\frac{17\times16}{2} = 136$ undirected pairs of nodes generate demand) expressed in Mbps (detailed data is available at sndlib.zib.de). The cost of one FSO capacity module on each link is 1 but for this particular instance, the FSO capacity module $M = 1$ Mbps (instead of 10 Gbps) is assumed. This is done to match the values of traffic demands (given in SNDLib) which are of the order of several Mbps. Note that if the traffic demands were scaled up by the factor of 1000 (and expressed in Gbps) then the results presented below would be valid for the (realistic) module size $M = 10$ Gbps as well.

Observe that since the links and demands in *nobel-germany* specified in SNDlib are undirected, the formulations of the master problem and the feasibility tests formulated in the previous sections must be (slightly) adjusted. A way to do it is described in Chapter 3.

Using the weather records from [74, 75], we have built up three different weather scenarios: the first scenario is typical for southern Europe (called "Mediterranean climate scenario"), the second one is typical for middle Europe (called "moderate continental climate" scenario), and the third is typical for northern Europe (called "temperate continental climate" scenario). These scenarios were then used to estimate link degradation state for each hour of a typical year for *nobel-germany*.

For each of the above weather scenarios (which in fact correspond to the sets of weather states $\mathcal{W}$) we performed the calculations. The results for *nobel-germany* are reported below and are presented in:

- Table 5.4 and Figure 6.1 for scenario “Mediterranean climate”
- Table 5.5 and Figure 5.4 for scenario “moderate continental climate”
- Table 5.6 and Figure 5.5 for scenario “cold continental climate”.

Table 5.4 – Impact of using K-set node (*nobel-germany*/Mediterranean climate).

	0-fiber case (m=0)		1-fiber case (m=1)		2-fibers case (m=2)	
	$C^*(0)$	$AT(0)$ [%]	$C^*(1)$	$AT(1)$ [%]	$C^*(2)$	$AT(2)$ [%]
set S'	388	99.84	312	99.85	250	99.89
link(2)	144	99.53	133	99.58	123	99.60
link(3)	149	99.58	135	99.64	124	99.65
node(1)	139	99.52	129	99.59	119	99.63
node(2)	152	99.62	140	99.67	130	99.68
link(7)	155	99.59	145	99.62	137	99.65
link(8)	155	99.63	145	99.67	137	99.68
link(9)	156	99.63	146	99.68	137	99.68

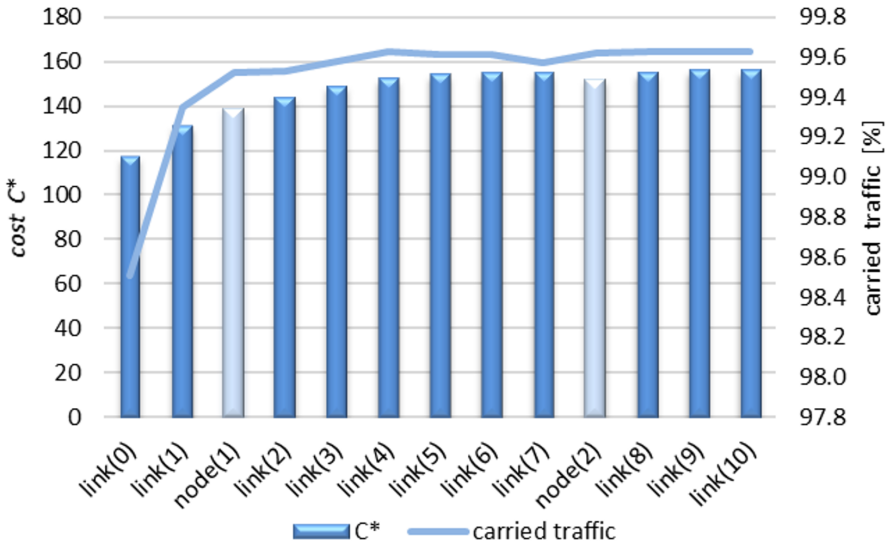

Figure 5.3 – Cost and carried traffic for 0-fiber case (*nobel-germany*/Mediterranean climate).

Table 5.5 – Impact of using K-set node (*nobel-germany*/moderate continental climate).

	0-fiber case (m=0)		1-fiber case (m=1)		2-fibers case (m=2)	
	$C^*(0)$	$AT(0)$ [%]	$C^*(1)$	$AT(1)$ [%]	$C^*(2)$	$AT(2)$ [%]
set S'	419	99.04	401	99.05	319	99.22
link(2)	144	95.01	133	95.26	123	95.68
link(3)	149	95.60	135	95.95	124	96.24
node(1)	139	95.08	129	95.44	119	95.99
node(2)	152	96.06	140	96.35	130	96.73
link(7)	155	95.74	145	96.01	137	96.30
link(8)	155	96.12	145	96.39	137	96.74
link(9)	156	96.13	146	96.42	137	96.78

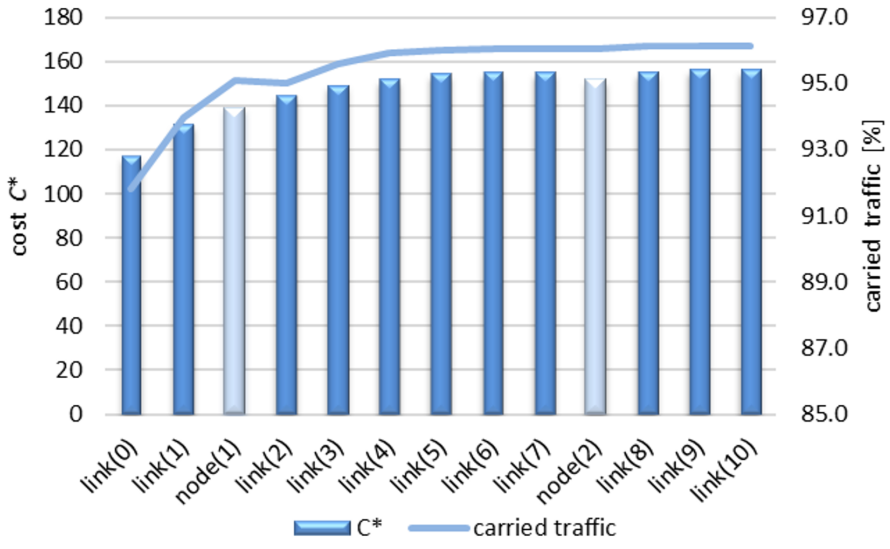

Figure 5.4 – Cost and carried traffic for 0-fiber case (*nobel-germany*/moderate continental climate).

Table 5.6 – Impact of using K-sets (*nobel-germany*/cold continental climate).

	0-fiber case (m=0)		1-fiber case (m=1)		2-fibers case (m=2)	
	$C^*(0)$	$AT(0)$ [%]	$C^*(1)$	$AT(1)$ [%]	$C^*(2)$	$AT(2)$ [%]
set S'	498	98.11	476	98.55	391	98.79
link(2)	144	88.17	133	88.60	123	89.34
link(3)	149	89.24	135	89.88	124	90.61
node(1)	139	88.32	129	88.86	119	89.75
node(2)	152	90.18	140	90.75	130	91.52
link(7)	155	89.89	145	90.41	137	91.07
link(8)	155	90.48	145	91.00	137	91.69
link(9)	156	90.55	146	91.10	137	91.77

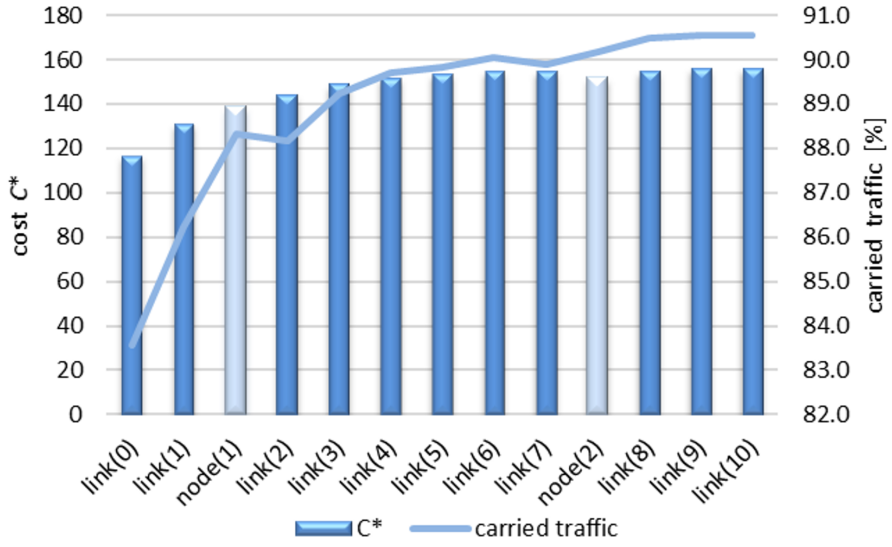

Figure 5.5 – Cost and carried traffic for 0-fiber case (*nobel-germany*/cold continental climate).

Additionally, in Table 5.7 we show how the percentage of disconnected states decreases when one or two fibers are allowed. Regarding the advantages of using K-sets in network

Table 5.7 – Percentage of disconnected states for different network configuration

	mediterranean climate	moderate continental climate	cold continental climate
0-fiber case	0.59%	4.13%	10.97%
1-fiber case	0.52%	4.01%	9.05%
2-fiber case	0.52%	3.90%	8.02%

dimensioning, we first of all notice that the link capacity cost obtained with K-sets decreases, in comparison with the network dimensioned for the explicit state list $\mathcal{S}'$, the FSO link cost (for all $m = 0, 1, 2$) significantly. At the same time the K-sets maintain, but only for "Mediterranean climate" and "moderate continental climate" scenarios, acceptable fractions of carried traffic. For the "cold continental climate" scenario these fractions are

not as good when compared to the explicit state list dimensioning. For *nobel-germany*, the FSO link cost achieved with node(1) is visibly the lowest for all cases. In the columns of the three corresponding tables we can notice that for node(1) we have $C^*(0) = 139$ (cost for $m = 0$), while all other values of $C^*(0)$ are greater or equal to 144. The same phenomenon can be noticed in the columns for $m = 1$ and $m = 2$. Since the fraction of carried traffic for node(1) is acceptable for the "Mediterranean climate" and "moderate continental climate" cases, this particular node K-set can be recommended. For the "cold continental climate" case, however, when these fractions are considered under expectations of the network operator, node(2) or link(8) are a better option.

If we now use the p-covering K-sets approach, we will have the following results.

Table 5.8 – Mediterranean climate.

uncertainty set	cost $C^*(K)$	carried traffic $AT(K)$[%]	computational time [s]
link(1)	149	99.07	75.41
node(1)	179	99.57	66.21
link(2)	188	99.64	73.61
set(2)	207	99.72	152.31
link(3)	208	99.76	102.38
link(4)	221	99.79	95.45
node(2)	221	99.81	692.24
set(3)	223	99.79	171.06
link(5)	228	99.76	112.56
link(6)	229	99.82	114.34
link(7)	230	99.82	134.05
link(8)	230	99.82	163.04
link(9)	231	99.82	137.26
link(10)	231	99.82	108.76

Table 5.9 – Temperate continental climate.

uncertainty. set	cost $C^*(K)$	carried traffic $AT(K)$ [%]	computational time [s]
link(1)	149	92.11	65.03
node(1)	179	94.50	70.11
link(2)	188	94.51	82.56
set(2)	203	95.41	140.02
link(3)	208	95.87	109.06
set(3)	218	96.71	123.11
node(2)	221	96.90	729.97
link(4)	221	96.67	103.95
link(5)	228	96.47	122.43
link(6)	229	96.94	129.25
link(7)	230	97.03	155.91
link(8)	230	97.02	166.05
link(9)	231	97.02	136.18
link(10)	231	97.15	111.53

Tables 5.8, 5.9 and 5.10 show the results for different types of uncertainly sets (link K-sets, node K-sets) compared to p-covering K-sets approach described above (for $p = 2$).

Table 5.10 – Cold continental climate.

uncertainty. set	cost $C^*(K)$	carried traffic $AT(K)[\%]$	computational time [s]
$link(1)$	149	81.06	68.58
$node(1)$	179	84.82	72.38
$link(2)$	188	84.83	80.61
$set(2)$	190	85.22	96.95
$set(3)$	205	87.35	120.74
$link(3)$	208	87.19	110.31
$link(4)$	221	88.85	110.68
$node(2)$	221	89.46	742.51
$link(5)$	228	88.79	118.61
$link(6)$	229	89.73	122.52
$link(7)$	230	89.97	150.59
$link(8)$	230	89.92	168.46
$link(9)$	231	90.07	135.62
$link(10)$	231	90.08	103.61

Such sets have been computed in advance with respect to the reference set of states. Typically, we have used formulation (4.9) with $p = 2$ and $K \in \{2, 3\}$ to compute such subsets. Although the problem is NP-hard, the computation time for the considered instances does not exceed 3 minutes. The number of subsets are for $K = 2$ and $K = 3$ respectively 18 and 20 for "cold continental climate" scenario, 45 and 60 for "temperate continental climate" scenario, and finally 67 and 113 for "Mediterranean climate" scenario. In each table, the uncertainty set used is pointed in the first column where $link(K)$ represents a link K-set, $node(K)$ a node K-set, and $set(K)$ a covering K-set. The second column gives the optimal capacity cost $C^*(K)$. The third column represents the average carried traffic $AT(K)$. The last column shows the computation time in [s]. For our results we have considered only the states where the network is connected. (It happens that in 10-15% of the time the weather conditions are extremely bad so that can cause the disconnection of the network.)

When comparing the total capacity cost and the average carried traffic percentage for different types of uncertainty sets, namely for link K-sets, node K-sets, and 2-covering K-sets, we observe that in all tables, using 2-covering K-sets is competitive as compared to using link K-sets. In particular, consider the results for 2-covering 3-set given in Tables V and VI. (Recall that using this set, i.e., $set(3)$, protects the traffic against all combinations of simultaneous link degradation in three sets of two links each; these sets compose the family obtained in the construction of this set, see Section 1.4.) For this set we achieve costs (218, 205) carried traffic percentages (96.71%, 87.35%). Considering results for $link(4)$ in Table V and for $link(3)$ in Table VI, we observe higher costs (221, 208) and lower carried traffic percentage (96.67%, 87.19%). Yet, although not always comparable, in some cases (as in Table IV), node K-sets perform better than the other two K-set types approaches; for instance see the $node(2)$ result and compare it with $set(3)$ and $link(4)$). Note that as compared to node K-sets, 2-covering 3-sets ($set(3)$) solutions are cheaper for temperate and cold continental climate at the same time achieving competitive percentages of carried traffic.

4 Concluding remarks

In this chapter we have presented some numerical results on a robust optimization problem related to FSO network dimensioning resilient to link capacities degradation caused by weather conditions. Our solution approach optimizes link capacity taking into account all weather states for a given time period, for which we determine a reference set of (link capacity degradation) states. One of the main issues here is potential (large) size of the reference set, which may make the optimization problem computationally untractable for large networks. Furthermore, we need to construct such a reference set of states using historical weather data records, which may not fit the future states for which the network is being optimized. We have shown in the previous chapter how to approximate the reference set, where in this chapter we have provided a set of numerical results run on some moderate-size network instances and for three different weather scenarios. The numerical results show that using p-covering K-sets for state modeling gives encouraging results when compared to the previously considered link and node K-set uncertainty sets.

A realistic network instance

1 Paris Metropolitan Area Network

In this Chapter we present results of applying our robust optimization approach to a realistic FSO network instance. We call this instance PMAN (Paris Metropolitan Area network) since it was created using the real data for the Paris metropolitan area (summarized in the following sections). However, although all the data used to design the PMAN instance are real, the instance itself is not real, and has been elaborated only for the purpose of this paper. This time, as we consider a realistic network instance, we consider the MIP version of problem P($\mathcal{S}$) with modular links (i.e., integer y). Because of that the optimization process involves both phases of Algorithm 2 presented in Chapter 3.

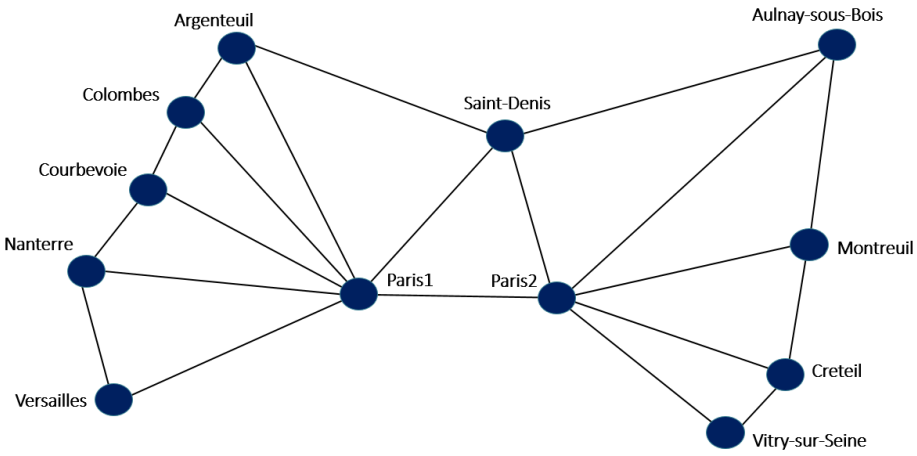

Figure 6.1 – Paris Metropolitan Area Network.

1.1 Paris Metropolitan Area network – data used in the study

In the PMAN case study we have considered the FSO transport system equipment provided by LightPointe Company [3], and more precisely the LightPointe's AireLink 80 10Gig system. The system requires one radio at each side of the FSO link and achieves 10 Gbps full duplex data transmission rate, which implies the link capacity module M equal to 10 Gbps (in each direction). As the considered system allows for the maximum

distance of 15 km between two antennas linked by a light beam under clear weather conditions, the 15 km link range is assumed as well. As for *polska*, the cost of one (10 Gbps) module on each link is equal to 1 (i.e., $\xi(e) = 1$, $e \in \mathcal{E}$). This means that the cost of the network defined in (3.17a) expresses the total number of capacity modules (i.e., FSO systems) installed in the network.

The topology of PMAN is depicted in Figure 6.1. The network is composed of $V = 12$ (core) nodes and covers an area of around 250 km^2. Two nodes (Paris1 and Paris2) are located in the inner Paris area, and the remaining 10 nodes represent autonomous cities around it. The set of links is composed of all possible links whose end nodes are within 15 km in the line of sight (the distances between node/cities are given in Table 6.1), resulting in $E = 21$ links (and $A = 42$ arcs) in total. The traffic matrix for PMAN includes all $D = V(V-1) = 132$ directed traffic demands (expressed in [Gbps]) and is given in Table 6.3

cities	(1)	(2)	(3)	(4)	(5)	(6)	(7)	(8)	(9)	(10)	(11)	(12)
(1) Paris1	–	10.0	8.8	10.0	10.2	8.2	9.0	12.4	13.2	16.0	11.6	18.9
(2) Paris2	10.0	–	8.8	15.0	15.2	13.2	16.3	22.4	8.2	8.0	6.6	9.0
(3) Saint Denis	8.8	8.8	–	8.1	7.7	8.7	12.1	22.4	16.7	18.3	10.2	10.7
(4) Argenteuil	10.0	15.0	8.1	–	2.8	5.9	6.9	18.4	20.7	23.6	17.0	18.5
(5) Colombes	10.2	15.2	7.7	2.8	–	3.6	4.8	16.2	18.1	21.2	15.2	18.0
(6) Courbevoie	8.2	13.2	8.7	5.9	3.6	–	3.6	13.9	15.6	19.0	14.1	18.3
(7) Nanterre	9.0	16.3	12.1	6.9	4.8	3.6	–	11.5	17.8	21.6	17.5	21.9
(8) Versailles	12.4	22.5	22.4	18.4	16.2	13.9	11.5	–	19.5	23.9	23.9	30.9
(9) Vitry-Sur-Seine	13.2	8.2	16.7	20.7	18.1	15.6	17.9	19.5	–	4.4	9.1	18.1
(10) Creteil	16.0	8.0	18.3	23.6	21.2	19.0	21.6	23.9	4.4	–	8.9	17.2
(11) Montreuil	11.6	6.6	10.2	17.0	15.2	14.1	17.5	23.9	9.1	8.9	–	9.1
(12) Aulnay-Sous-Bois	18.9	9.0	10.4	18.5	18.0	18.3	21.9	30.9	18.1	17.2	9.1	–

Table 6.1 – Distances between cities [km].

Table 6.1 gives the line-of-sight distance (measured on the map) between all the pairs of the 12 cities composing PMAN. Clearly, the matrix is symmetric and its entries imply the set of 21 potential (undirected) links of PAM that is depicted in Figure 6.1: a link between a pair of cities can be provided if the distance between its end nodes does not exceed 15 km.

The traffic matrix was calculated using formula (6.1) discussed in below. The next table (Table 6.2) contains the data necessary to prepare the traffic matrix for PMAN. The second column of this table gives the population in the areas served by each node (*http://population.city/france*). Assuming that the average family consists of 4 persons (actually, according to [79], the real figure is 3.85), we calculated the number of families in each area (column 3). Next, we took the estimations of the average rate of the traffic downloaded (DL, column 4) and uploaded (UL, column 4) from/to the Internet per family in each area (using the data available at [80]), and finally computed the aggregated DL (column 6) and UL (column 7) traffic rate from/to the Internet per the whole areas. In the calculations we considered only the residential traffic, as for instance VoIP and

peer-to-peer traffic, assuming that (i) the considered traffic is equal to 10% of the whole generated traffic, and (ii) only 10% of population is served by this network.

cities Ile-de-France	population 2016	number of families	DL traffic per family [Mbps]	UL traffic per family [Mbps]	aggregated DL traffic [Gbps]	aggregated UL traffic [Gbps]
Paris1	1 099 921	274 980.25	28.71	21.65	7893.31	5954.70
Paris2	1 099 921	274 980.25	28.71	21.65	7893.31	5954.70
Saint-Denis	116 302	29 075.50	19.14	10.23	556.42	297.36
Argenteuil	107 408	26 852.00	11.71	4.75	314.46	127.55
Colombes	88 257	22 064.25	30.60	25.04	675.14	522.58
Courbevoie	88 776	22 194.00	30.60	25.04	879.11	555.83
Nanterre	92 607	23 151.75	30.60	25.04	708.42	579.81
Versailles	83 879	20 974.25	30.50	13.16	639.78	275.98
Vitry-Sur-Seine	92 791	23 197.75	32.50	13.16	753.53	305.24
Creteil	90 282	22 570.50	32.50	13.16	733.16	296.98
Montreuil	104 963	26 240.75	19.14	10.23	502.17	268.36
Aulnay-Sous-Bois	82 513	20 628.25	19.14	10.23	394.76	210.97

Table 6.2 – Demographic data and traffic estimates.

Using the data from Table 6.2, we calculated the (directed) traffic matrix $T = [T(i,j)]_{i,j=1}^{12}$ for PMAN applying the following formula for all directed pairs (i,j), $i,j = 1,2,\ldots,12$, $i \neq j$:

$$T(i,j) = UL(i) \cdot \frac{P(j)}{\sum_{k=1}^{12} P(k) - P(i)} + DL(j) \cdot \frac{P(i)}{\sum_{k=1}^{12} P(k) - P(j)}. \tag{6.1}$$

In the formula, $P(k)$, $DL(i)$ and $UL(i)$ denote the entries in columns 2, 6 and 7, respectively, of Table 6.2. The formula is based on the assumption that the (directed) traffic demand from city i to city j is estimated as the sum of a fraction of the upload (UL) traffic generated at city i (this fraction is proportional to the share of the population of the area j in the total population of PMAN outside the area of i), and a fraction of the download (DL) traffic received at city j (this fraction is proportional to the share of the population of the area of i in the total population of PMAN outside the area of j).

We considered the weather conditions observed during all hours in a one year period, this time from January 1, 2016 until December 31, 2016 available at *www.worldweatheronline.com*. As for *polska*, the observed conditions were translated into the corresponding failure states. In effect, we obtained the set of all $366 \times 24 = 8784$ hourly failure states (2016 was a leap-year) – this full set of hourly states will be denoted by $\widetilde{\mathcal{S}}$. It happens that among these 8784 states, there are 1253 (14.26%) of the so called *disconnected states*. Each such state contains a set of links with failure ratio equal to 1 (i.e., totally failing) that is a cut that splits the network into separate (connected) components so that some of the demands cannot be realized at all.

Besides, in the study we will consider a subset of $\widetilde{\mathcal{S}}$, namely the set $\widetilde{\mathcal{S}}'$ of all $8784 - 1253 = 7531$ *connected states* obtained by deleting the disconnected states from $\widetilde{\mathcal{S}}$. Among the

cities	(1)	(2)	(3)	(4)	(5)	(6)	(7)	(8)	(9)	(10)	(11)	(12)
(1) Paris1	–	74.38	5.40	4.26	4.99	5.02	5.24	4.74	5.41	5.26	4.87	3.82
(2) Paris2	74.38	–	5.40	4.26	4.99	5.02	5.24	4.74	5.41	5.26	4.87	3.82
(3) Saint-Denis	5.56	5.56	–	0.23	0.34	0.35	0.36	0.33	0.38	0.37	0.29	0.23
(4) Argenteuil	4.60	4.60	0.25	–	0.27	0.28	0.29	0.26	0.30	0.30	0.22	0.01
(5) Colombes	5.39	5.39	0.37	0.29	–	0.36	0.37	0.34	0.39	0.37	0.34	0.26
(6) Courbevoie	5.42	5.42	0.37	0.29	0.36	–	0.37	0.34	0.39	0.38	0.34	0.26
(7) Nanterre	5.66	5.66	0.39	0.30	0.37	0.37	–	0.34	0.40	0.39	0.35	0.28
(8) Versailles	4.22	4.22	0.26	0.18	0.26	0.27	0.28	–	0.29	0.28	0.23	0.18
(9) Vitry-Sur-Seine	4.68	0.13	0.29	0.20	0.29	0.29	0.31	0.28	–	0.31	0.26	0.20
(10) Creteil	4.55	4.55	0.28	0.20	0.28	0.29	0.30	0.27	0.31	–	0.25	0.20
(11) Montreuil	5.02	5.02	0.30	0.20	0.31	0.31	0.33	0.29	0.34	0.33	–	0.21
(12) Aulnay-Sous-Bois	3.94	3.94	0.23	0.16	0.24	0.24	0.26	0.23	0.27	0.26	0.21	–

Table 6.3 – Traffic matrix [Gbps].

7531 connected hourly states in the reduced set $\widetilde{\mathcal{S}}'$, 68.46% are nominal states with no degraded links. As for *polska*, the majority of the remaining states are characterized only by the 16-QAM to 4-QAM change in MCS that reduces the nominal capacity of the affected links by 25% (link failure ratio 0.25) – there are 20.95% of such states in $\widetilde{\mathcal{S}}'$. In the remaining 10.59% of states there are links degraded by the failure ratio 0.5 and/or 1.

As far as the average connected hourly state in $\widetilde{\mathcal{S}}'$ is concerned, there are 94.7% of non-affected links, 4.3% of links with the failure ratio 0.25, 0.5% of links with the failure ratio 0.5, and 0.5% of totally failed links (failure ratio 1). Finally, we observed that out of all the 7531 connected hourly states there are only 206 states that are mutually different – these states constitute the reference failure set $\mathcal{S}$ for PMAN.

1.2 Algorithm efficiency

Table 6.4 presents numerical results illustrating the efficiency of Algorithm 2 for PMAN. The results are analogous to those for *polska* – the main difference is that for PMAN the modular links are considered, while for *polska* the link capacities were assumed to be continuous. This is reflected in Table 6.4 where the group of three columns under the common name "Phase 1" describe the optimal solutions (for the K-sets with $K = 0, 1, \ldots, 21$) of the linear relaxation of the considered MIP problem (3.17), obtained by means of Phase 1 of Algorithm 2. The column "Phase 1 + 2" shown in the Table, in turn, describes the computational time for modular solutions for PMAN obtained through applying Phase 2 after Phase 1 in Algorithm 2.

The solutions of the linear relaxation of $\mathrm{P}(K)$ obtained with Phase 1 behave similarly as the solutions for *polska*. The cost becomes stable already for $K \geq 6$, and the computation time, after initial increase and achieving maximum for $K = 11$, starts to decrease (with some exceptions).

K	Phase 1			Phase 1+2		
	C^*	no. of cuts	time [s]	C^*	no. of cuts	time [s]
0	25.2	92	13.0	32	2213	1398.1
1	30.5	101	20.3	35	106	21.9
2	32.2	116	23.6	36	140	28.7
3	33.1	143	35.0	37	143	36.5
4	33.4	133	31.0	37	135	31.5
5	33.5	134	31.0	37	135	32.0
6	33.6	148	35.0	37	150	35.4
7	33.6	147	36.0	37	148	36.6
8	33.6	153	37.0	37	157	38.8
9	33.6	154	37.0	37	159	39.0
10	33.6	147	34.0	37	163	37.0
11	33.6	166	41.0	37	185	45.0
12	33.6	152	35.0	37	172	39.0
13	33.6	156	31.0	37	262	54.0
14	33.6	172	34.0	37	248	47.1
15	33.6	174	31.2	37	256	48.0
16	33.6	150	26.0	37	242	42.0
17	33.6	168	29.0	37	315	62.0
18	33.6	171	28.0	37	260	43.0
19	33.6	170	27.0	37	257	45.0
20	33.6	174	27.0	37	251	42.0
21	33.6	167	24.2	37	236	36.5

Table 6.4 – PMAN – results of robust optimization.

As far as the results for the modular links case are concerned, we first note that for $K = 0$ (only the nominal state considered) the number of additional cuts (added in Phase 2) and the computation time become substantial. This is implied by a particular nature of the polyhedron of all feasible y vectors, different than that of the corresponding polyhedra for $K \geq 1$. In the modular case the behavior of the solutions for $K \geq 1$ is basically similar to that of the linear relaxation assumed in Phase 1. In this case the cost stabilizes at $K = 3$ while the maximum computation time is observed for $K = 17$.

We have also optimized the modular case for $K = 0$ and $K = 1$ directly, by applying the CPLEX MIP solver to formulation (3.17) with an explicit list of states. Clearly, for $K = 0$ such a list contains only the nominal state while for $K = 1$ it contains all single link degradation states with only one link degraded at a time (with the failure ratio 0.25). In the first case it took only 5 seconds to reach the optimal solution with $C^* = 32$ while in the second case it took as much as 1313 seconds reach the optimal solution with $C^* = 35$. This illustrates the fact that for $K \geq 1$ the cut-based method of Algorithm 2 is superior to the direct approach.

Finally, let us note that most of the algorithm's execution time (roughly 90%) has been spent in the cut generation subproblem, i.e., in the feasibility test solved in Step 2 of

Algorithm 2. This confirms the remark at the beginning of Section **??** stating that extra valid inequalities are worth considering to speed-up the convergence of the algorithm.

1.2.1 Robustness with respect to the hourly states

Figures 6.2 and 6.3 show to what extent the network with modular links dimensioned for the consecutive K-sets (with the number of modules given in column 5 of Table 6.4) is able to cover all 8784 hourly states (labelled with "all states", i.e., the states in $\widetilde{\mathcal{S}}$), and for all connected hourly states (labeled with "connected states", i.e., the states in $\widetilde{\mathcal{S}}'$). The figures for "average carried traffic [%]" and "not covered states [%]" were obtained in the same way as for *polska* (see Section 4.3). The figures reveal that the coverage for the connected states case is very good already for $K = 0$ (this is due to links' modularity since, typically, not all modules are fully utilized), and becomes stable for $K \geq 5$. These results are quite promising, as we may expect that the network dimensioned for a K-set even with a small value of K will cover, to a reasonable extent, also the states that were not observed in the historical data or are difficult to extract from such data.

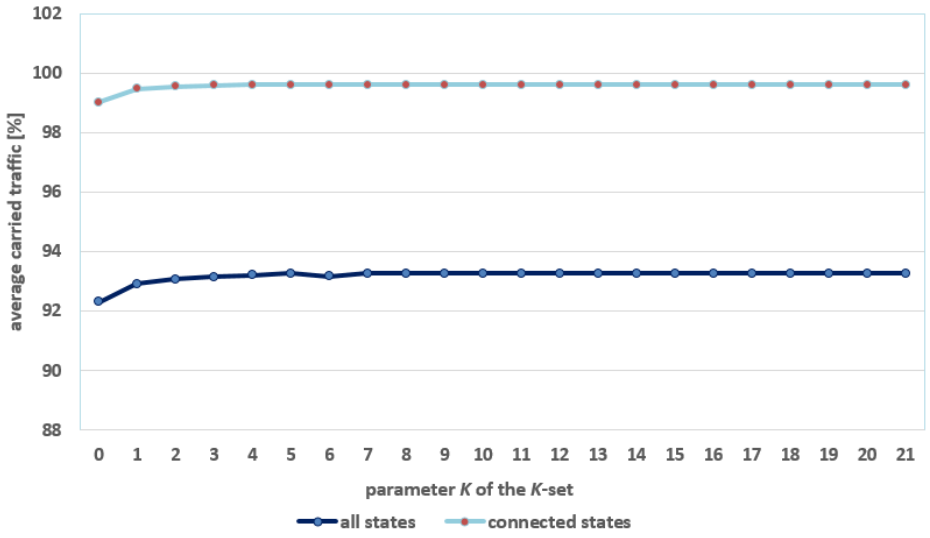

Figure 6.2 – PMAN – results of robust optimization obtained with Algorithm 2.

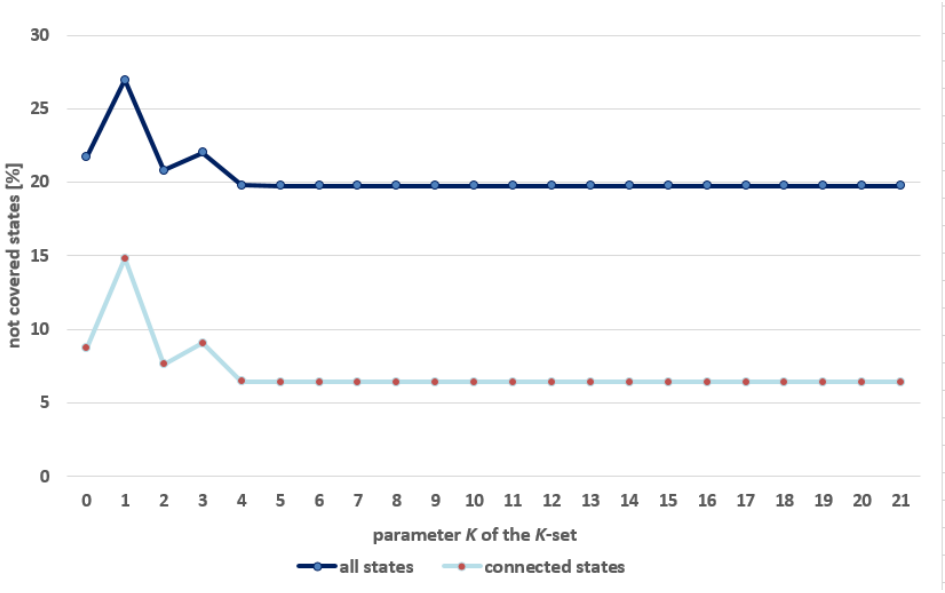

Figure 6.3 – PMAN – states that are not covered with Algorithm 2.

1.2.2 An exact solution

For PMAN we have also computed the exact solution covering the whole states in the reference failure set $\mathcal{S}$ (with 206 distinct states). We have achieved that by solving the MIP formulation (3.2) of $\mathrm{P}(S)$ directly, and not using Algorithm 1. Such an optimal solution, obtained in 407 seconds, has the minimum cost equal 145 (recall that the assumed module costs $\xi(e) = 1$, $e \in \mathcal{E}$, imply that this cost is equal to the total number of modules installed on the links). This is a large difference as compared to the cost equal to 37 obtained for the K-sets with $K \geq 3$ that cover 99.60% of traffic and 19.75% of states. In fact, this is mainly due to the large amount of traffic traversing the link between Paris1 and Paris2 that is relatively often affected, sometimes totally. To restore the traffic lost on this link, a substantial additional (protection) capacity is necessary not only on this link but also on the routes around it. This effect is shown in Figure 6.4, where the pair of figures (one in brackets) next to a given link specifies its capacity expressed as the number of 10 Gbps modules. The first figure (not in brackets) is the link capacity when all links are the FSO links, while the second (in brackets) is the link capacity when Paris1-Paris2 is a fiber link and the remaining links are FSO links.

The above result shows that building a 100% robust FSO network can be very costly. A natural remedium for this issue (considered for example in [37]) would be to use a terrestrial fiber technology for some selected (bottleneck) links instead of the wireless FSO technology since the fiber links are not sensitive to weather conditions and thus can be assumed to be never degraded in our model (failure ratio always equal to 0). For example, assuming that the Paris1-Paris2 link is realized on a fiber (and the rest 20 links are FSO links), the optimum solution of $\mathrm{P}(S)$ requires 56 modules instead of 145, that is, as much as 91 modules less than required in the pure FSO network.

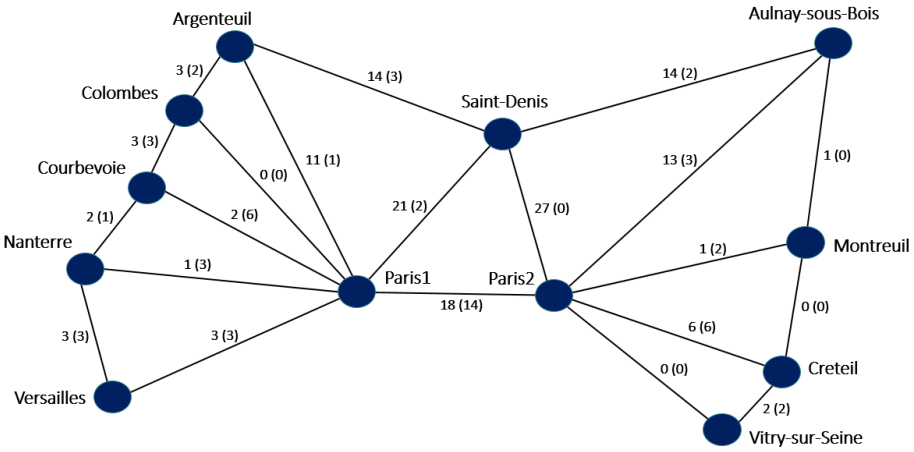

Figure 6.4 – PMAN – link capacity.

1.2.3 Results for hybrid FSO/fiber PMAN network

In this section we discuss the results for the hybrid network model presented in Chapter 3. Table 6.5 shows the influence of using fiber links on the FSO link cost $C^*(m)$ (where $C^*(m) := \sum_{e \in \mathcal{E}} y_e^*$ and y^* is the vector of optimal sizes of FSO links when m fibers selected in Phase 1 are installed), and on the fraction of the average carried traffic $AT(m)$, $m = 1, 2, \ldots, 11$. The consecutive rows depict, for each m, the values of $C^*(m)$ and $AT(m)$, and, additionally, the percentage of disconnected states in $\mathcal{W}$ and the total computational time. To obtain these results we dimensioned the network applying Phase 1 of the optimization procedure described in Section 6.3 for appropriate sets of connected states $\mathcal{S}'$ and sets of disconnected states $\mathcal{S}''$. Since it happens that the first choice fiber link e^* is placed between Paris 1 and Paris 2, the FSO link cost for $m = 1$ is drastically decreased with respect to the case with no fibers ($m = 0$). This is because the cost of the fiber links is not counted in $C^*(m)$ and the fiber links do not suffer from capacity degradation. In effect, when the fiber between Paris 1 and Paris 2 is provided, the large traffic demand between these nodes (plus some other traffic) is carried with no cost.

Adding consecutive fibers keeps on decreasing the FSO cost until all demands become connected in all states in $\mathcal{S}$ (using only the fiber links), which happens for $m = 11$. Next we observe that the carried traffic grows by 2 percentage points when the first fiber is added (from 95.19% to 97.16%), and the percentage of disconnected states in $\mathcal{W}$ drops by 4.4 percentage points. When m is increased beyond 1, the carried traffic grows monotonically (but slowly) to 100% while the percentage of disconnected states decreases gradually but not monotonically to 0%. This happens because in Phase 1 of the optimization procedure we do not control the number of disconnected states, as we do it only for the carried traffic. The computation time ranges from 227 to 12650 seconds, and in general tends to grow with m.

As a conclusion we may state that adding only one or two fibers to PMAN would be beneficial as this will non-negligibly increase the carried traffic (and connectivity) and at the same significantly decrease the number of installed FSO systems. Installing more fibers could of course be considered but benefit from it would be low.

Table 6.5 – Impact of fiber links, PMAN dimensioned for $\mathcal{S}'(0)$.

number of fibers m	FSO cost $C^*(m)$	carried traffic $AT(m)$ [%]	disconnected states [%]	time [s]
m=0	145	95.19	19.75	227.1
m=1	42	97.16	14.36	1251.8
m=2	36	97.61	10.83	1859.3
m=3	26	97.75	12.91	1726.1
m=4	21	98.26	11.67	1000.9
m=5	20	98.47	12.01	2269.9
m=6	18	98.60	10.85	6109.8
m=7	14	98.89	10.59	3380.4
m=8	13	98.99	7.10	6518.7
m=9	12	99.15	5.92	12650.3
m=10	4	99.71	4.06	4999.7
m=11	0	100.00	0.00	5593.1

Table 6.6 illustrates efficiency of using node (and link) K-sets assuming link degradation ratio $\beta(e)$ equal to 0.25 uniformly for all links. Three cases are considered: 0-fiber ($m = 0$: no fibers added), 1-fiber ($m = 1$: one fiber added) and 2-fibers ($m = 2$: two fibers added). For each case, the cost, fraction of carried traffic, and computation time are given in the consecutive rows of the table. The results for the explicit state list $\mathcal{S}'$ are taken from the rows $m = 0, 1, 2$) in Table 6.5. The results for the node K-sets (namely node(1), node(2)) were calculated by means of Phase 2 of the optimization procedure, while the results for the link K-sets (link(3), link(4), link(6), link(7)) were computed by an algorithm analogous to A2.

Table 6.6 – Impact of K-sets, PMAN.

	0-fiber case (m=0)			1-fiber case (m=1)			2-fibers case (m=2)		
	$C^*(0)$	$AT(0)$ [%]	time [s]	$C^*(1)$	$AT(1)$ [%]	time [s]	$C^*(2)$	$AT(2)$ [%]	time [s]
set S'	145	95.19	227.1	42	97.16	1251.8	36	97.61	1859.3
link(3)	37	93.15	41.1	21	96.19	39.8	19	96.72	40.1
link(4)	37	93.21	35.5	21	96.29	36.3	19	97.05	38.2
node(1)	36	93.19	36.9	20	96.19	37.4	18	96.85	37.2
node(2)	37	93.25	42.4	21	96.30	44.6	20	97.10	44.8
link(6)	37	93.16	37.5	21	96.26	37.7	20	97.03	37.5
link(7)	37	93.26	39.3	22	96.94	40.3	20	97.51	39.8

The results of Table 6.6 for the 0-fiber case ($m = 0$) are shown in a graphical form in Figure 6.5. For completeness, Figure 6.5 contains additional results (for link(0), link(1), link(2), link (5), link(8), link(9)). Note that link(0) corresponds to the case when only one state is considered, namely the nominal state (all links fully available), so that its cost $C^* = 32$ is the lower bound for the cost for all other cases.

We recall that $AT(k)$ gives the average carried traffic in percentage. Table 6.6 reveals that in fact all the considered K-sets (except for link(0)) give virtually the same fraction of carried traffic for all three values of m ($m = 0, 1, 2$), which are (around) 93.1%, 96.2%, and 97%, respectively. These values are less than the corresponding values for the explicit state list case (in the row named set $\mathcal{S}'$) by, respectively, 2, 1, and 0.5 percentage points. These are acceptable values from the quality of traffic handling viewpoint. Moreover, the costs

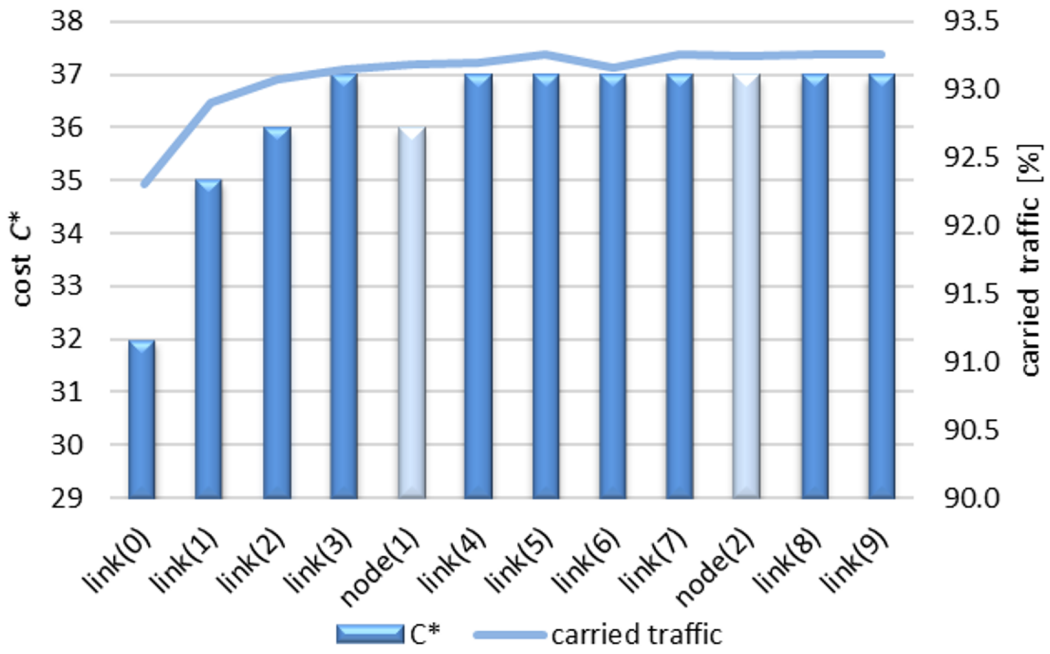

Figure 6.5 – FSO link cost C^* and carried traffic, PMAN.

C^* for the K-sets (except for link(0)) are almost the same, and substantially smaller than for the case of the explicit list $\mathcal{S}'$. Taking this into account, and the fact that the K-set approach requires substantially shorter (of at least one order of magnitude) computation times as compared to the explicit state list approach, the former approach is a reasonable alternative to the latter, especially when the weather state set $\mathcal{W}$, and thus the reference state set $\mathcal{S}$ are not available and/or hard to forecast. Examining Figure 6.5 we also note that the node K-set node(1) should be recommended for PMAN dimensioning because of its low cost $C^* = 36$ which gives the gain equal to $\frac{37-36}{37-32} = 20\%$ with respect to other K-sets whose cost is equal to 37 (except for link(1)). The case link(1) (with cost $C^* = 35$) could also be considered for the dimensioning with cost gain $\frac{37-35}{37-32} = 40\%$ but at the expense of a slightly decreased fraction of carried traffic. Moreover, for the 1-fiber and 2-fiber cases the use of node(1) becomes even more beneficial cost-wise.

1.2.4 Results for p-covering K-sets PMAN network

As before we have tested our optimization approach for a $\beta(e) = 0.5$ (link degradation ratio), for the three uncertainty sets on PMAN as shown in Table 6.7, Comparing to *nobel-germany* instances, the results for PMAN pleads clearly in favor of the new uncertainty set proposed in this study. One may note that $set(2)$ has a lower cost compared to $link(3)$ or $node(1)$ while giving one of the highest traffic satisfaction for all uncertainty scenarios. We can observe that in some cases the obtained results don't exhibit the expected relation between the cost and the traffic satisfaction, that is, for the same uncertainty set type, higher is the cost higher the traffic satisfaction should be. The reason for that stands in the fact that these criteria are optimized separately. In our optimization approach we

build a link cost-efficient network for some given uncertainty set and we measure what is the highest traffic satisfaction this network can provide for each state of the reference set. Hence, it may happen that one network instance with a given dimensioning distribution performs better than another instance with a higher dimensioning cost but with a different distribution of capacities. This may be observed in Table 6.7 for cases $link(3)$ and $link(5)$ or $set(2)$ and $set(3)$.

Table 6.7 – PMAN network.

uncertainty set	cost $C^*(K)$	carried traffic $AT(K)$[%]	computational time [s]
$link(1)$	45	93.39	31.76
$link(2)$	48	93.63	39.76
$set(2)$	50	93.70	93.47
$link(3)$	51	93.67	47.24
$set(3)$	51	93.64	86.51
$node(1)$	52	93.51	87.23
$link(4)$	54	93.71	50.06
$node(2)$	54	93.48	435.24
$link(5)$	54	93.45	49.01
$link(6)$	54	93.54	52.74
$link(7)$	54	93.45	51.41
$link(8)$	54	93.47	72.86
$link(9)$	54	93.47	77.84
$link(10)$	54	93.47	72.50

Conclusions and future works

In today's optical and wireless network communication world, Free Space Optics communication system is a topics of a major interest. The advantages it has and the promising future it presents, make this technology one of the most investigated from both academics and industry. Despite the numerous advantages it has, FSO suffers from a big disadvantage: vulnerability of the FSO links to weather conditions. In this framework, the main purpose of this thesis was to introduce an optimization model for robust dimensioning of FSO networks in order to achieve resilience with respect to multiple partial link degradations. We took a closer look to the problem and the first issue we investigated was to find a representative mathematical model that allows us to translate the weather conditions into FSO link capacities availability. In Chapter 2 we gave such a model and all the technical elements we have to take into account when working with FSO networks.

In Chapter 3 we presented a robust optimization approach to modular dimensioning of FSO networks taking into account degradation of link capacities due to weather conditions. We started by a general case and then we focus on a specific features of FSO networks such as full-duplex links. This means that a link represents a set of parallel FSO transmission systems. For this reason, we modified our first model and we considered a network that is modeled by means of a bi-directed graph. Central to our approach was a cut-generation algorithm for minimizing the cost of links for a network robust to all link failure states. In this scenario, different link losses different portions of their nominal capacity. In order to optimize a realistic network, we first analyzed the weather data and produced a representative set of its link failure states (called the reference failure set). Then we dimensioned the network assuming uncertainty K-sets for several values of parameter K and checked to what extent the states in reference failure set were covered by the K-set based solution.

Sometimes the weather can be very bad and since the FSO links are directly affected by weather conditions, this means that some FSO links may not be able to work properly. In these conditions, the degradation of communication can lead to significant data losses or even to network disconnections. Therefore, it was reasonable to consider the possibility of using fibers instead of free space light beams. In this way (using fibers on the key links) we could ensure network connectivity in all weather scenarios. Given all these, in the continuation of our work we considered a robust optimization problem that was able to deal with dimensioning of hybrid FSO/fiber networks. In our approach, we first optimized link capacity (i.e., we solved the network dimensioning problem) taking into account all weather states for a given year. Then we dimensioned the network assuming a special (uncertainty) set of link degradation states represented by the so-called link K-set, where

K specifies the number of links were simultaneously affected by bad weather. We did this for a selected set of values of parameter K, checking to what extent the demand traffic matrix is satisfied. Finally, we examined how good was the traffic satisfaction in question as compared to the satisfaction achieved with the solution obtained when all states in the reference set were considered in optimization explicitly.

The large-scale failures frequently result in the so-called region failures, i.e., simultaneous failures of network elements located in a specific geographical area. For this, in Chapter 4 we tracked a new approach to our problem. We modified our main model and instead of K simultaneously affected links, we considered K nodes (meaning degradation of all adjacent links). We have tested our approach on a moderate-size network instance (*nobel-germany*) for three different weather scenarios. Also, we studied the effectiveness of our approach on a realistic network instance (based on the Paris Metropolitan Area data). The presented numerical study illustrated the advantage of using node K-sets over the previously used link K-sets.

Finally, inspired by the hitting set problem a new idea was to investigate a more general notion of K-set, called p-covering K-set, where the link groups were more appropriate for the reference set approximation. The main idea was to find a large number of subsets of two or three affected links and to use all possible combinations (composed of 2 or at most 3 of this subsets) to build a new virtual failure set that covers as much as possible the reference failure set that we got from the study of real weather data records. Next, we tested these new uncertainty sets for a selected set of values of parameters p and K ($p = 2$ and $K = 2, 3$) and checked to what extent the demand traffic matrix was satisfied by the obtained solution in all states in the reference set of states $\mathcal{S}$, and at what cost. This investigation was the subject of our last research.

Numerical results illustrated in a convincing way the effectiveness of our findings. They show that we reduce in a significant way the cost of network dimensioning problem when we compare the the direct solution for all states and the solution we have using link K-sets. In the same time the total traffic satisfaction ratio is high and in acceptable levels. As the model evolves, even the results get better. When we compare the results we have for link K-sets and node K-sets, we gain in terms of cost and traffic satisfaction. The cost keeps falling as we move from node K-sets approach to p-covering set model.

Even the work we have done until now is promising, there is still place for improvements. When we first started this thesis, the final idea was to implement our approach and algorithms in a real FSO network and to compare the real life results with the ones that came out of the simulations we did. Unfortunately, this was not possible. Another thing that we regret was the fact that we could have done more numerical tests on different network sizes and typologies, and to see how these results could help us to enhance our model and our solution approach. The time was not promising us to do such a thing. We tested our model and the solution approach on small and medium size networks. When it comes to large networks, we faced the problem of execution time. Our algorithm took to much time to converge to the optimal solution.

During these three years of work, we devoted our efforts in enhancing the model and finding a more representative uncertainty polytope. One thing we regret is the fact of not using the Branch & Bound method. Instead, we have implemented the Benders cutting

plane approach. In fact, the Benders cutting plane approach sometimes needed a large number of Benders' inequalities to converge to optimum. This posed an efficiency issue since test (3.8) (called also the separation problem) performed in Step 2 of our algorithm contained binary variables. One way to deal with this issue was to try to speed up the convergence of the algorithm by using additional valid inequalities on top of the Benders cuts in the master problem solved in Step 1 of the algorithm.

We note here that most of the algorithm's execution time (roughly 90%) has been spent in the cut generation subproblem, i.e., in the feasibility test solved in Step 2 of Algorithm 2. This confirms the remark stating that extra valid inequalities are worth considering to speed-up the convergence of our algorithm.

The model we have presented and tested in this thesis takes into account one level of degradation ratios $\beta(e)$. In practice, however, links may be affected with different levels of degradation ratios depending on the severity of weather conditions and the corresponding modulation and coding scheme. A more general model taking multiple levels of degradation ratios into account could be the subject of a future, more comprehensive study. In this optic, we took into account one level of degradation ratios $\beta(e)$ and we considered the worse case of degradation ratio $\beta(e)$ between the transmitter and the receiver. For example if for link e we have two different degradation ratios $\beta_1(e)$ and $\beta_2(e)$, to characterize the one state degrasation state for this link, we chosed the bigger between them. Maybe this hypothesis we build was very strong and pessimist. An alternative hypothesis will be considering a degradation ratio that is the average of $\beta_1(e)$ and $\beta_2(e)$.

If we come back to the last part of our work, the idea of p-covering set model, when we chose the affected links to build the representative subsets, we don't consider the level of degradation ratio. We just examine if one link is affected or not, but we don't go further to take into account it's degradation ratio. As far as the future work is concerned, we will continue to investigate a natural extension of the above-described p-covering set model admitting multiple link degradation ratios.

Taking into account what we discussed above, the following extensions/enhancements of the presented approach are worth considering in the future.

- Enhancing the optimization procedure by using valid inequalities (see Section 5.2) to speed up the algorithm convergence.
- Developing a heuristic algorithm for (suboptimal) rounding off the continuous link capacity solution to a modular solution. This will speed up the optimization process as Algorithm 2 will be applied only to the linear relaxation of the main problem (through Phase 1 of Algorithm 2).
- Investigate a natural extension of the p-covering set model (see Chapter 4 admitting multiple link degradation ratios.

Bibliography

[1] J. Sterbenz, D. Hutchison, E. Cetinkaya, A. Jabbar, J. Rohrer, M. Scholler, and P. Smith. Resilience and survivability in communication networks: Strategies, principles, and survey of disciplines. *Computer Networks*, 54:1245–1265, 2010.

[2] Wireless Excellence-LTD. `https://www.cablefree.net/`.

[3] LightePointe AireLink 80 10 Gbps 70/80GHz Radios. `https://www.azenn.com/img/cms/Promotions/Lightpointe/Lancement-10Gbps/AireLink_80_10Gig.pdf`.

[4] D. Bertsimas and M. Sim. The Price of Robustness. *Operations Research*, 52(1):35–53, 2004.

[5] W. Ben-Ameur and H. Kerivin. Routing of Uncertain Traffic Demands. *Optimization and Engineering*, 6:283–313, 2005.

[6] M. Pióro and D. Medhi. *Routing, Flow, and Capacity Design in Communication and Computer Networks*. Morgan Kaufmann, 2004.

[7] M. Pióro. Network optimization techniques. In E. Serpedin, T. Chen, and D. Rajan, editors, *Mathematical Foundations for Signal Processing, Communications, and Networking*, chapter 18, pages 627–684. CRC Press, Boca Raton, USA, 2012.

[8] J.F. Benders. Partitioning procedures for solving mixed variable programming problems. *Numerische Mathematik*, 4:238–252, 1962.

[9] D. Nace, M. Pióro, M. Poss, F. D'Andreagiovani, I. Kalesnikau, M. Shehaj, and A. Tomaszewski. An optimization model for robust fso network dimensioning. *Optical Switching and Networking*, 32:25–40, 2019.

[10] S. Orlowski, M. Pióro, A. Tomaszewski, and R. Wessäly. SNDlib 1.0 – Survivable Netwrok Design Library. *Networks*, 55(3):276–285, 2010.

[11] S. Rajbhandari, Z. Ghassemlooy, J. Perez, H. Le Minh, M. Ijaz, E. Leitgeb, G. Kandus, and V. Kvicera. On the study of the fso link performance under controlled turbulence and fog atmospheric conditions. In *Proceedings of the 11th International Conference on Telecommunications*, pages 223–226. Graz, Austria, June 2011.

[12] O. Bouchet, H. Sizun, C. Boisrobert, F. de Fornel, and P. Favennec. *Free-Space Optics: Propagation and Communication.* ISTE Ltd, 2006.

[13] A. Jabeena and S. Srajan. Performance of fso links using various modulation techniques and cloud effect. *International Journal of Engineering Research and General Science*, 3(2), 2015.

[14] R. Goścień, K. Walkowiak, M. Klinkowski, and J. Rak. Protection in Elastic Optical Networks. *IEEE Network*, 29(6):88–96, 2015.

[15] K. Ali, H. X. Nguyen, Q. Vien, and P. Shah. Disaster management communication networks: Challenges and architecture design. In *Proceedings of 2015 IEEE International Conference on Pervasive Computing and Communication Workshops (PerCom Workshops)*, pages 537–542. St. Louis, MO, USA, March 2015.

[16] R. K. Ahuja, Th. L. Magnanti, and J. B. Orlin. *Network Flows, theory, algorithms, and applications.* Prentice-Hall, Inc., 1993.

[17] J. Rack. *Resilient Routing in Communication Networks.* Springer, Cham, 2015.

[18] A. Sen, S. Murthy, and S. Banerjee. A new paradigm for the design of fault-tolerant networks. In *Proc. of the 15th International Conference on High-Performance Switching and Routing (HPSRâĂŹ09)*, pages 1–7, 2009.

[19] J. Rak. Measures of region failure survivability for wireless mesh networks. *Wireless Networks*, 21:673âĂŞ684, 2015.

[20] J. Rak. A new approach to design of weather disruption-tolerant wireless mesh networks. *Telecommunication Systems*, 61:311–323, 2016.

[21] F. Gjata. Measuring the impact of weather factors to FSO transmission. *Intership Report, Information and Systems Technologies, UniversitÃł de Technologie de CompiÃĺgne*, 2016.

[22] S. Kini, S. Ramasubramanian, A. Kvalbein, and A.F. Hansen. Fast Recovery From Dual-Link or Single-Node Failures in IP Networks Using Tunneling. *IEEE/ACM Transactions on Networking*, 18(6):1988–1999, December.

[23] J. Rak, D. Hutchison, E. Calle, T. Gomes, M. Gunkel, P. Smith, J. Tapolcai, S. Verbrugge, and L. Wosinska. Resilient communication services protecting end-user applications from disaster-based failures. pages 1–4, July 2016.

[24] E. Torkildson, B. Ananthasubramaniam, U. Madhow, and M. Rodwell. Millimeter-wave mimo: wireless links at optical speeds. *In Proceedings of 44th Allerton Conference on Communication, Control and Computing*, 2006.

[25] J. Rak. Measures of region failure survivability for wireless mesh networks. *Wireless Networks*, 21(2):673–684, Feb 2015.

[26] J. Rak, J.L. Marzo, and J. SolÃĭ-Pareta. Design of resilient optical networks. *Optical Switching and Networking*, 33:13–14, 2019.

[27] J. Rak. A new approach to design of weather disruption-tolerant wireless mesh networks. *Telecommunication Systems*, 61(2):311–323, Feb 2016.

[28] X. Long, D. Tipper, and T. Gomes. Measuring the survivability of networks to geographic correlated failures. *Optical Switching and Networking*, 14:117 – 133, 2014. Special Issue on RNDM 2013.

[29] J. L. Marzo, S.G. Cosgaya, N. Skorin-Kapov, C. Scoglio, and H. Shakeri. A study of the robustness of optical networks under massive failures. *Optical Switching and Networking*, 31:1–7, January 2019.

[30] T. Bauschert, C. Büsing, F. D'Andreagiovanni, A.M.C.A. Koster, M. Kutschka, and U. Steglich. Network planning under demand uncertainty with robust optimization. *IEEE Commununications Magazine*, 52:178–185, 2014.

[31] F. D'Andreagiovanni, J. Krolikowski, and J. Pulaj. A fast hybrid primal heuristic for multiband robust capacitated network design with multiple time periods. *Appl. Soft Comput.*, 26:497–507, 2015.

[32] A.M.C.A. Koster, M. Kutschka, and C. Raack. Robust Network Design: Formulations, Valid Inequalities, and Computations. *Networks*, 61(2):128–149, 2013.

[33] F. D'Andreagiovanni. Revisiting wireless network jamming by SIR-based considerations and multiband robust optimization. *Optim. Lett.*, 9:1495–1510, 2015.

[34] S. Orlowski and M. Pióro. Complexity of column generation in network design with path-based survivability mechanism. *Networks*, 59(1):132–147, 2012.

[35] G. Classen, D. Coudert, A.M.C.A. Koster, and N. Nepomuceno. A chance-constrained model and cutting planes for fixed broadband wireless networks. In *Proc. INOC 2011*, 2011.

[36] M. Pióro, Y. Fouquet, D. Nace, and M. Poss. Optimizing flow thinning protection in multicommodity networks with variable link capacity. *Operations Research*, 64(2):273–289, 2016.

[37] Y. Li, N. Pappas, V. Angelakis, M. Pióro, and D. Yuan. Optimization of free space optical wireless network for cellular backhauling. *IEEE JSAC*, 33(9):1841–1854, 2015.

[38] Y. Fouquet, D. Nace, M. Pióro, and M. Poss. An optimization framework for traffic restoration in optical wireless networks with partial link failures. *Optical Switching and Networking*, 23, Part 2:108–117, 2017.

[39] M. Shehaj, D. Nace, I. Kalesnikau, and M. Pióro. Dimensioning of hybrid FSO/fiber networks. In *Proceeding of BalkanCom 2018*. Podgorica, Montenegro, June 2018.

[40] Computational Complexity Theory. https://www.cs.yale.edu/homes/aspnes/classes/468/notes.pdf, 2020.

[41] Complexity Theory. https://brilliant.org/wiki/complexity-theory/, 2019.

[42] J. F. Benders. Partitioning procedures for solvig mixed variable programming problems. *Numerische Mathematik*, 4:238–252, 1962.

[43] W. Ben-Ameur and B. Liau. Design a reliable telephone network. In *Proceeding of IFIP Workshop on Traffic Management*. Montreal, 1999.

[44] G. Dahl and M. Stoer. A cutting plane algorithm for multicommodity survivable network design problems. *Journal of Computing*, 10:1–11, 1998.

[45] L. Lasdon. *Optimization Theory for Large Systems*. MacMillan, 1970.

[46] M. Minoux. *Mathematical Programming: Theory and Algorithms*. John Wiley and Sons, 1986.

[47] M. Fischetti, I. Ljubic, and M. Sinnl. Redesigning Benders Decomposition for Large-Scale Facility Location. *Management Science*, 63(7):2146–2162, 2017.

[48] E. Aarts and J. K. Lenstra. *Local Search in Combinatorial Optimization*. John Wiley and Sons, 1997.

[49] A. Kaur and R. Kumar Panchal. Analysis the effect atmosphere turbulence in freespace optical (fso) communication systems. *International Journal of Engineering and Innovative Technology (IJEIT)*, 3(11):2277–3754, 2014.

[50] O. Strobel. *Optical and Microwave technologies fo telecommunication networks*. ISBN: 978-81-265-6502-3, 2016.

[51] W.O. Popoola and Z. Ghassemlooy. Bpsk subcarrier intensity modulated free-space optical communications in atmospheric turbulence. *Lightwave Technology*, 27:967–973, 2009.

[52] T. Kamalakis G. Ntogari and T. Sphicopoulos. Analysis of indoor multiple-input multiple-output coherent optical wireless systems. *Lightwave Technology*, 30:317–324, 2012.

[53] H. A. B. Shamsuddin et al. H. A. Fadhil, A. Amphawan. Optimization of free space optics parameters: an optimum solution for bad weather conditions. *Optic*, 124(19):3969–3973, 2013.

[54] H. A. Willebrand and B. S. Ghuman. Fiber optics without ïňĄber. *IEEE Spectrum*, 38(8):40–45, 2001.

[55] I. I. Kim, J. Koonz, H. Harkakha, P. Adhikari, R. Stieger, C. Moursund, M. Barclay, A. Stanford, R. Ruigork, J. Shuster, and E. Korevaar. Measurement of scintillation and link margin for terralink laser communication system. In *Proceeding of SPIE, no. 3266*, pages 100–118, 1998.

[56] I. I. Kim, B. McArthur, and E. Korevaar. Comparison of laser beam propagation at 785 nm and 1550 nm in fog and haze for optical wireless communications. In *Proceedings of SPIE, no. 4214*, pages 26–37, 2001.

[57] A. Alkholidi and K. S. Altowij. EïňĂect of clear atmospheric turbulence on quality of free space optical communications in western asia. In *Optical Communications Systems*, pages 41–74. Rijeka, Croatia, 2012.

[58] P.W. Kruse, L.D. McGlauchlin, and R.B. McQuistan. Elements of in-frared technology: Generation, transmission and detection. NY, USA,, 1962.

[59] J. Joss, J. C. Thams, and A. Waldvogel. The variation of raindrop size distribution at locarno. In *Proceeding of International Conference on Cloud Physics*, pages 369–373, 1968.

[60] H. A. Willebrand and B. S. Ghuman. Fiber optics without ïňĄber. *IEEE Spectrum*, 38(8):40–45, 2001.

[61] L. Hanzo, S. X. Ng, T. Keller, and W. T. Webb. *Quadrature Amplitude Modulation: From basics to Adaptive Trellis-Coded, Turbo-Equalised and Space-Time Coded OFDM, CDMA and MC-CDMA Systems.* Springer-Verlag, 2004.

[62] J. S. Blogh, P. J. Cherriman, and L. Hanzo. Dynamic channel allocation techniques using adaptive modulation and adaptive antennas. *Proceedings of the IEEE, J. Sel. Areas Communication*, 19(2):312–321, Feb 2001.

[63] A. Svensson. An introduction to adaptive qam modulation schemes for known and predicted channels. *Proceedings of the IEEE*, 95(12):2322–2336, Dec 2007.

[64] J.S. Malhotra, M. Kumar, and A.K. Sharma. Performance Comparison of PS-QPSK and PM-QPSK Modulation Schemes in High Capacity Long Haul DWDM Optical Communication Link. *International Journal of Engineering Sciences*, 2(5):154–159, 2013.

[65] J. Priyanka, S. Bhuperdra, and C. Rashmi. Survey on performance of free space optical communication links under various field parameters. *IOSR Journal of Electrical and Electronics Engineering (IOSR-JEEE)*, 9(2):71–75, 2014.

[66] FSona optical wireless. http://www.fsona.com/product.php.

[67] B.H. Korte and J. Vygen. *Combinatorial Optimization: Theory and Algorithms*. Springer-Verlag, 2012.

[68] C. Chekuri, F.B. Shepherd, G. Oriolo, and M.G. Scutellá. Hardness of robust network design. *Networks*, 50(1):50–54, 2007.

[69] Subhash Khot. On the unique games conjecture (invited survey). In *Proceedings of the 25th Annual IEEE Conference on Computational Complexity, CCC 2010, Cambridge, Massachusetts, USA, June 9-12, 2010*, pages 99–121, 2010.

[70] G.L. Nemhauser and L.A. Wolsey. *Integer and Combinatorial Optimization*. J. Wiley, 1999.

[71] D. Nace, M. Pióro, A. Tomaszewski, and M. Żotkiewicz. Complexity of a classical flow restoration problem. *Networks*, 62(2):149–160, 2013.

[72] T.A. Pham, H.T.T. Pham, H. Le, and N.T. Dang. High-capacity mixed fiber-wireless backhaul networks using mmw radio-over-mcf and mimo. *Optics Communications*, 400:43 – 49, 2017.

[73] M.R. Garey and D.S. Johnson. *Computers and Intractability*. W.H. Freeman, New York, 1979.

[74] World Weather Online. `https://www.worldweatheronline.com`, last access date 30/04/2019.

[75] Köppen-Geiger climate classification. `https://en.wikipedia.org/wiki/Koppen_climate_classification`, last access date 30/04/2019.

[76] Technical report, UTC, 2018. `https://www.hds.utc.fr/~shehajma/dokuwiki/_media/fr/weather-scenarios.zip`, last access date 30/04/2019.

[77] F. D'Andreagiovanni, D. Nace, M. Pióro, M. Poss, M. Shehaj, and A.Tomaszewski. On robust FSO network dimensioning. In *Proc. 9th International Workshop on Resilient Networks Design and Modeling (RNDM 2017)*. Alghero, Italy, September 2017.

[78] M. Poss and C. Raack. Affine recourse for the robust network design problem: Between static and dynamic routing. *Networks*, 61(2):180–198, 2013.

[79] Chiffres clefs de la Famille 2016. http://www.udaf42.org/sites/default/files/Chiffres_cles_2016.pdf.

[80] Key numbers of Ile-de-France region. http://www.cci-paris-idf.fr/etudes/organisation/crocis/chiffres-cles/chiffres-cles-region-ile-de-france-crocis.